Cruise Report
MV1007
R/V Melville

Collaborative, RUI:
Plume-Ridge Interaction in the Northern Galapagos: Understanding mantle-lithosphere dynamics through geochemistry, geophysical mapping, and gravity modeling

May 17 to June 18, 2010

Puerto Caldera, Costa Rica: Start Port
Puerto Ayora, Santa Cruz Island, Galapagos: Intermediate Port (June 3, 4)
Puerto Caldera, Costa Rica: End Port

Karen Harpp[1], Eric Mittelstaedt[2+], Dan Fornari[3], Dennis Geist[4], and Shipboard Scientific Party

1Colgate University, Dept. of Geology, Hamilton, NY 13346
2 Fluides, Automatiques et Systemes Thermiques Laboratoire, CNRS/UPMC/Univ-Paris-Sud, Orsay Cedex, France
+ Woods Hole Oceanographic Institution, Geology & Geophysics Dept., Woods Hole, MA 02543
3 Woods Hole Oceanographic Institution, Geology & Geophysics Dept. Woods Hole, MA 02543
4, University of Idaho, Dept. of Geological Sciences
Moscow, ID 83844

Funded by the National Science Foundation
Ocean Sciences Division, Marine Geology and Geophysics
OCE-0926491

Table of Contents

Appendices:

1. Introduction

a. Conceptual Overview

A number of conflicting geodynamic models have been proposed to explain how mantle flow occurs between a hotspot and a mid-ocean ridge (MOR) axis. The goal of this project is to use new geochemical and geophysical data and high resolution seafloor mapping to develop a multidisciplinary perspective on the Northern Galápagos Province (NGP). The NGP is the interface between the plume-derived central Galápagos Archipelago and the plume-affected Galápagos Spreading Center (GSC). Because of these spatial and genetic relationships, the NGP is one of the premier locales on Earth to study plume-ridge interaction. The NGP is populated by small volcanic islands and seamounts, many of which define lineaments between the hotspot and the GSC (Figure 1.1).

On MV1007 (the FLAMINGO Cruise: Formation of Lineaments and Anomalous Magmatism In the Northern Galápagos Ocean), we achieved all the objectives delineated in the original proposal. They include: a detailed characterization of seafloor in this area, including EM122 multibeam bathymetry, MR1 sidescan sonar imaging, deep-sea camera traverses, ship-based gravity and magnetic surveys, and dredging (Table 1.1). These data will be used to resolve the regional fabric of the seafloor and deduce crustal and upper mantle structure. The multidisciplinary approach will enable us to assess geodynamic models and significantly advance our understanding of plume-ridge interaction.

Geochemical analyses of dredged samples from the widespread volcanic centers in the NGP will be conducted to produce a two-dimensional image of the mantle in the plume-ridge interface region. These data will be used to determine whether plume transport occurs as broad buoyant flow at the base of the lithosphere, channelized flow, or a component of the ridge's deep return flow. Major and trace element compositions of the volcanic centers will provide insights into melt generation depth and the role of the lithosphere in the plume transport process. Calculation and modeling of gravity anomalies will help distinguish between the different hypotheses for distributions of low-density plume material.

The seafloor mapping documents the orientation and extent of numerous tectonic lineaments and the adjacent seafloor structural fabric. These data allow us to assess evidence for fracturing and extension of crust throughout the NGP and compare apparent ages of volcanic activity of the seamounts to those of the surrounding seafloor. Coupled with Ar-Ar geochronology of dredge samples, these observations will permit us to develop new models for lineament generation.

b. Fieldwork Overview

Fieldwork for this project was undertaken using the Scripps Institution of Oceanography's vessel R/V Melville during May-June, 2010, with a scientific party of 26 individuals from a range of institutions in the US, France, and Ecuador (Appendix I). This project represents a fully integrated collaboration between an undergraduate institution (Colgate University) and major research institutions (WHOI, University of

Idaho), and included 9 undergraduate students who will be continuing research efforts post-cruise.

Data acquisition was focused on a region north of the main Galápagos Archipelago, centered on the transform fault in the Galápagos Spreading Center (GSC) at 90.5ºW and bounded on the west by the Wolf-Darwin Lineament (WDL) and Genovesa Island on the east (Figure 1.1). Ship time was divided between two major efforts: a) a multibeam (EM122) and sidescan sonar (MR1) survey (May 20-May 31); and b) dredging across the survey area (47 dredges; May 31-June 2, June 4-June 18; Table 1.1), which included TowCam surveys over selected areas.

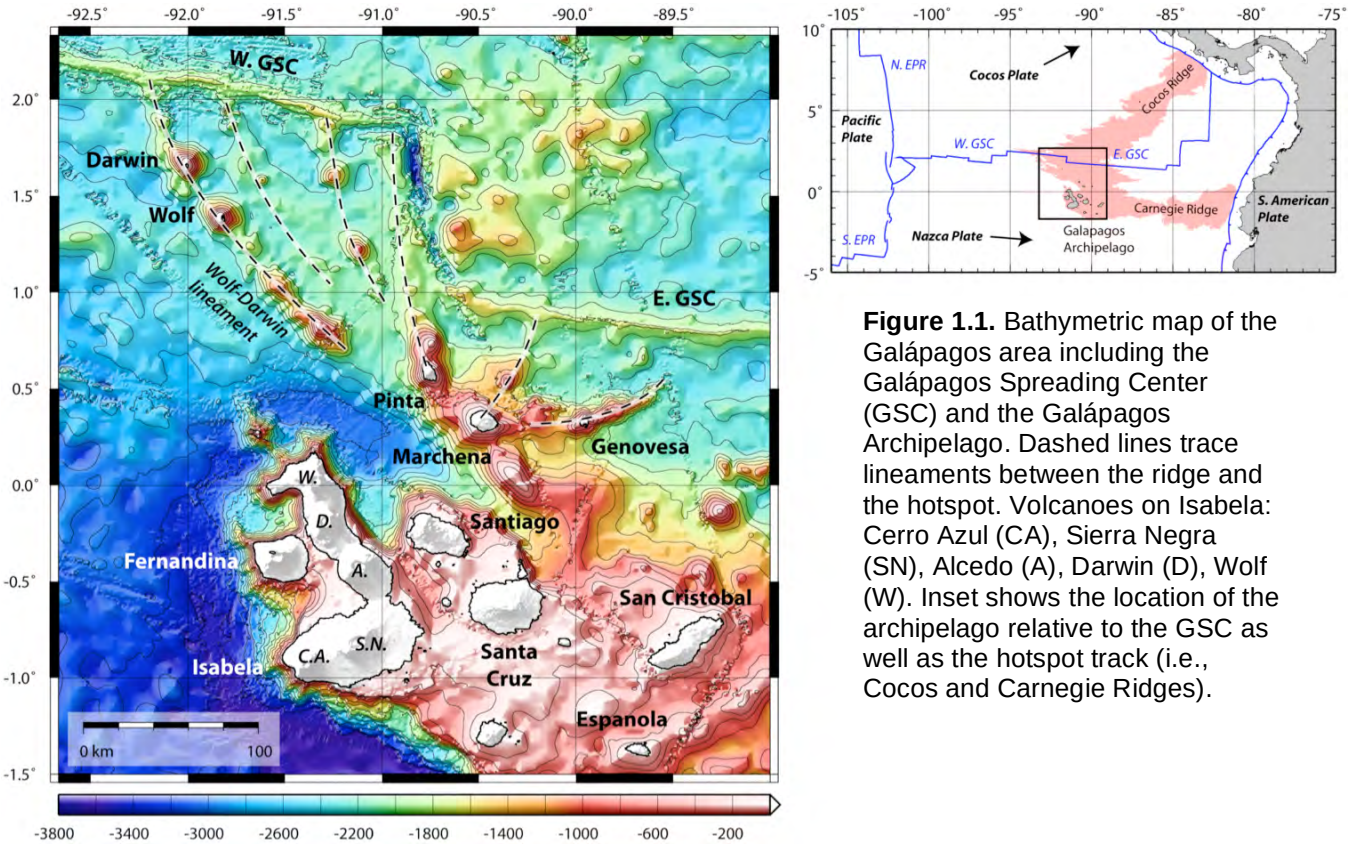

Figure 1.1. Bathymetric map of the Galápagos area including the Galápagos Spreading Center (GSC) and the Galápagos Archipelago. Dashed lines trace lineaments between the ridge and the hotspot. Volcanoes on Isabela: Cerro Azul (CA), Sierra Negra (SN), Alcedo (A), Darwin (D), Wolf (W). Inset shows the location of the archipelago relative to the GSC as well as the hotspot track (i.e., Cocos and Carnegie Ridges).

Sidescan sonar (MR1; Rongstad, 1992) and EM122 multibeam data were collected simultaneously during the survey phase of the cruise, which permitted production of detailed sidescan backscatter and bathymetric maps (Figure 1.2). These data allow us to identify tectonic lineaments and zones of constructive volcanism, as well as contact relationships, and were critical for choosing the best dredge sites to address the project goals.

The sampling program included 47 dredges and 5 sets of wax cores (during TowCam surveys). Primary targets were major volcanic edifices in the study area, regions of recent volcanic activity, and tectonized zones (Figure 1.2). The TowCam system (Fornari, 2003) was used to ground-truth sonar data, study morphological features on volcanic edifices and in tectonized areas, and refine choices of dredge sites.

Table 1.1. MR1007 Cruise Operational Chronology

Date	Event
05/17/10	Underway from Puntarenas, Costa Rica
	Magnetometer deployed
05/19/10	Entered Ecuadorian waters
05/20/10	Deployed MR1
	Magnetometer re-deployed
	start of survey line 1
05/21/10	end of survey line 1; start of survey line 2
05/22/10	end of survey line 2; start of survey line 3
	end of survey line 3; start of survey line 4
05/23/10	end of survey line 4; start of survey line 5
	end of survey line 5; start of survey line 6
05/24/10	end of survey line 6; start of survey line 7
	MR1 down for an hour owing to full hard drive
05/25/10	end of survey line 7; start of survey line 8
	end of survey line 8; start of survey line 9
	end of survey line 9; start of survey line 10
05/26/10	end of survey line 10; start of survey line 11
	end of survey line 11; start of survey line 12
05/27/10	end of survey line 12; start of survey line 13
	end of survey line 13; start of survey line 14
05/28/10	end of survey line 14; start of survey line 15
	end of survey line 15; start of survey line 16
	end of survey line 16; start of survey line 17
05/29/10	end of survey line 17; start of survey line 18
	Magnetometer brought in when line crossed with MR1
05/30/10	end of survey line 18; start of survey line 19
	end of survey line 19; start of survey line 20
	end of survey line 20; start of survey line 21
	end of survey line 21; start of survey line 22
	end of survey line 22; start of survey line 23
	Begin recovery of MR1
05/31/10	MR1 successfully brought in after struggle due to the broken H-link
	end of survey line 23
	start of survey line 24
	end of survey line 24
	start of survey line 25
	end of survey line 25
	start of survey line 26
	end of survey line 26
	start of survey line 27
	end of survey line 27

Date	Event
	start of survey line 28
	end of survey line 28
	start of survey line 29
	Dredge 01 completed
	Dredges 02 and 03 completed
06/01/10	Dredges 04, 05, 06 completed
06/02/10	TowCam 01 completed
	Dredge 07 completed
	Arrival in Puerto Ayora, Galapagos
06/03/10	Departure from Galapagos
06/04/10	Dredges 08, 09, 10, 11 completed
6/5/2010	Wolf Island GPS installation
06/06/10	Dredges 12, 13, 14 completed
	TowCam02 completed
06/07/10	Dredges 15, 16 completed
	Dredges 17, 18 completed
06/08/10	Wolf Island GPS retrieval
	Dredge 19 completed
	Series of variable speed BIST tests of EM122 completed
06/09/10	Dredge 20 completed
	TowCam 03 completed
	Dredges 21, 22, 23 completed
	Dredges 24, 25, 26 completed
06/10/10	Dredges 27, 28, 29, 30 completed
06/11/10	TowCam 04 completed
	Dredges 31, 32, 33, 34, 35 completed
06/12/10	Begin 3.5 kHz Knudsen survey
06/13/10	Magnetometer deployed, Multibeam off
	Dredges 36, 37, 38 completed
	End 3.5 kHz Knudsen survey
06/14/10	Dredges 39, 40, 41, 42, 43 completed
	Dredge 44 completed
06/15/10	TowCam 05 completed
	Dredges 45, 46, 47 completed
	Last survey completed
06/16/10	Magnetometer recovered

Total miles steamed: 75,023.1 nm
Steaming time: 09 days, 44 hours
Station time: 18 days, 38 hours
Detention time: N/A

Figure 1.2 (next page). Map of MV1007 multibeam and HMR1 survey lines and dredge locations. Map also includes dredge sites in the study area from previous cruises (Christie et al., 1992; Harpp and White, 2001; Detrick et al., 2002; Sinton et al., 2003; Cushman et al., 2004; Harpp et al., 2004; Christie et al., 2005).

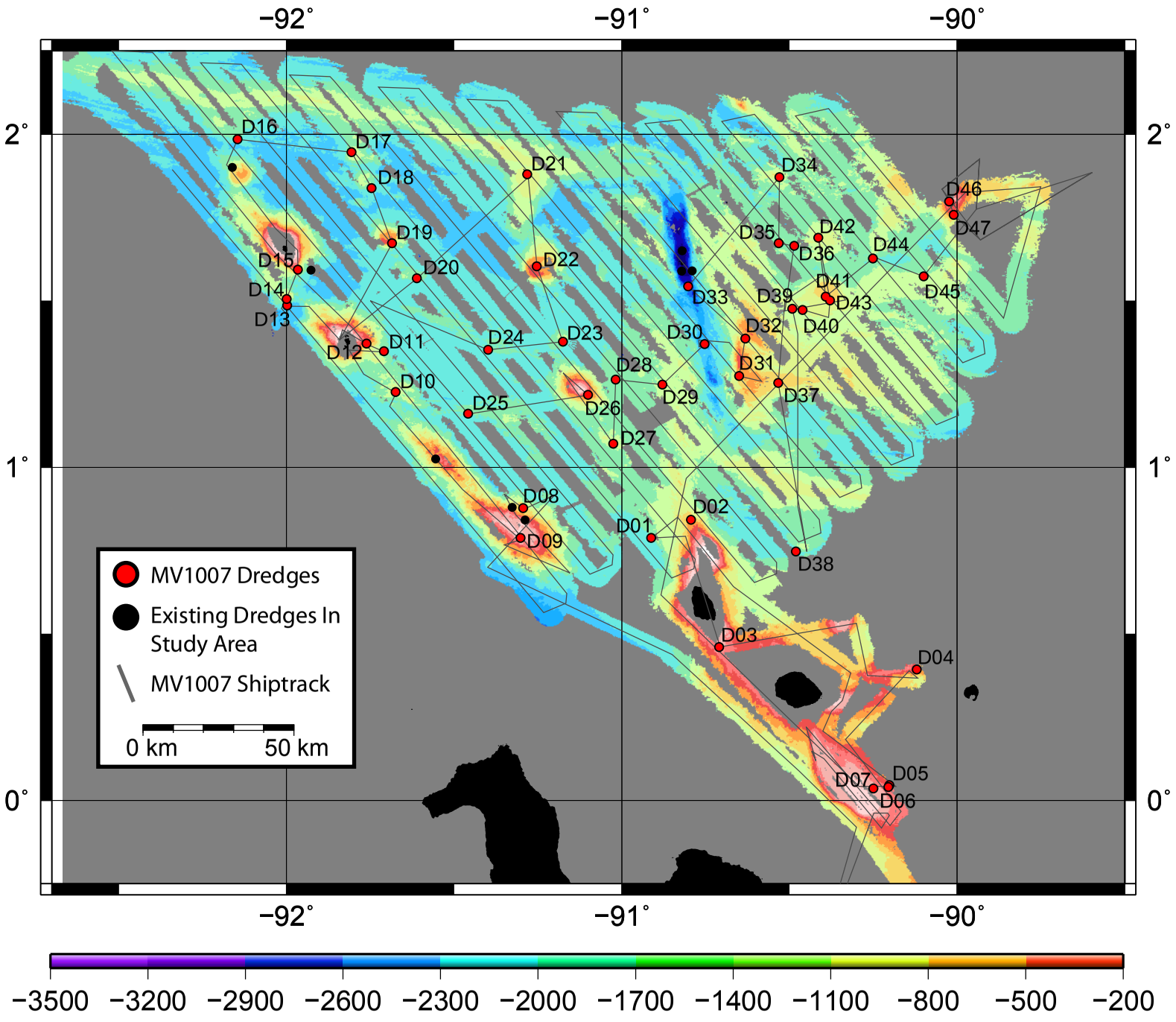
−92°
−91°
−90°
2°
1°
0°
D16
D17
D18
D19
D20
D21
D22
D15
D14
D13
D12
D11
D10
D24
D23
D25
D26
D27
D28
D29
D30
D31
D32
D33
D34
D35
D36
D37
D38
D39
D40
D41
D42
D43
D44
D45
D46
D47
D08
D09
D01
D02
D03
D04
D05
D06
D07
MV1007 Dredges
Existing Dredges In Study Area
MV1007 Shiptrack
0 km
50 km
−3500
−3200
−2900
−2600
−2300
−2000
−1700
−1400
−1100
−800
−500
−200

2. Cruise Objectives

a. Mapping

Compared to the main Galápagos platform and the GSC axis, the submarine geology and bathymetry of the NGP had been poorly documented. Prior to the MV1007 cruise, only three multibeam mapping and dredge sampling programs had been carried out in the northern Galápagos study area. The 1990 PLUME02 cruise on the R/V Thomas Washington (D. Christie, Chief Scientist; Christie, Duncan et al., 1992), which focused on the main Galápagos platform to the south, also carried out SeaBeam mapping of the Wolf-Darwin Lineament (WDL; Figure 1.1), but narrow swath widths severely limit the coverage. The G-PRIME cruise (J. Sinton, Chief Scientist; Sinton, Detrick et al., 2003 had as its objective the Galápagos Spreading Center west of the 90.5ºW transform. The MEGAPRINT cruise was complementary to the G-PRIME cruise (K. Hoernle, Chief Scientist; Christie, Werner et al., 2005), with the primary objective of mapping the transform fault and the eastern GSC near the Galápagos.

The primary mapping objectives of the MV1007 cruise were to survey the NGP, a roughly triangular area centered around the 90.5ºW transform fault and bounded on the west by the Wolf Darwin Lineament, on the north by the GSC, and to the east along a meridian that passes approximately through Genovesa Island (Figure 1.2). This study area includes several submarine lineaments in addition to the WDL, as well as the northern part of the Galápagos platform that extends toward Pinta and Marchena.

b. Previous Rock Sampling

The PLUME02 cruise included 5 dredges along the Wolf Darwin Lineament (Harpp and White, 2001). Major element data are not available for the PLUME02 samples, but trace element and isotopic analyses were summarized by Harpp and White (2001). A more in-depth examination of the WDL was the focus of Harpp and Geist (Harpp and Geist, 2002), and Sinton et al. (Sinton et al., 1996) included Ar-Ar geochronology ages for a limited number of samples from each of the 5 dredges along the lineament (Figure 1.2). The PLUME02 WDL dredge locations as well as results from fieldwork on the five northern Galápagos Islands over the past two decades were taken into account when designing this cruise's sampling of the WDL and areas around Pinta and Marchena Islands and their submarine extensions (Cullen and McBirney, 1987; Vicenzi et al., 1990; Harpp et al., 2002; Harpp et al., 2003; Blair et al., 2002; Reed et al., 2002; Pistiner et al., 2000; Barr et al., 2004).

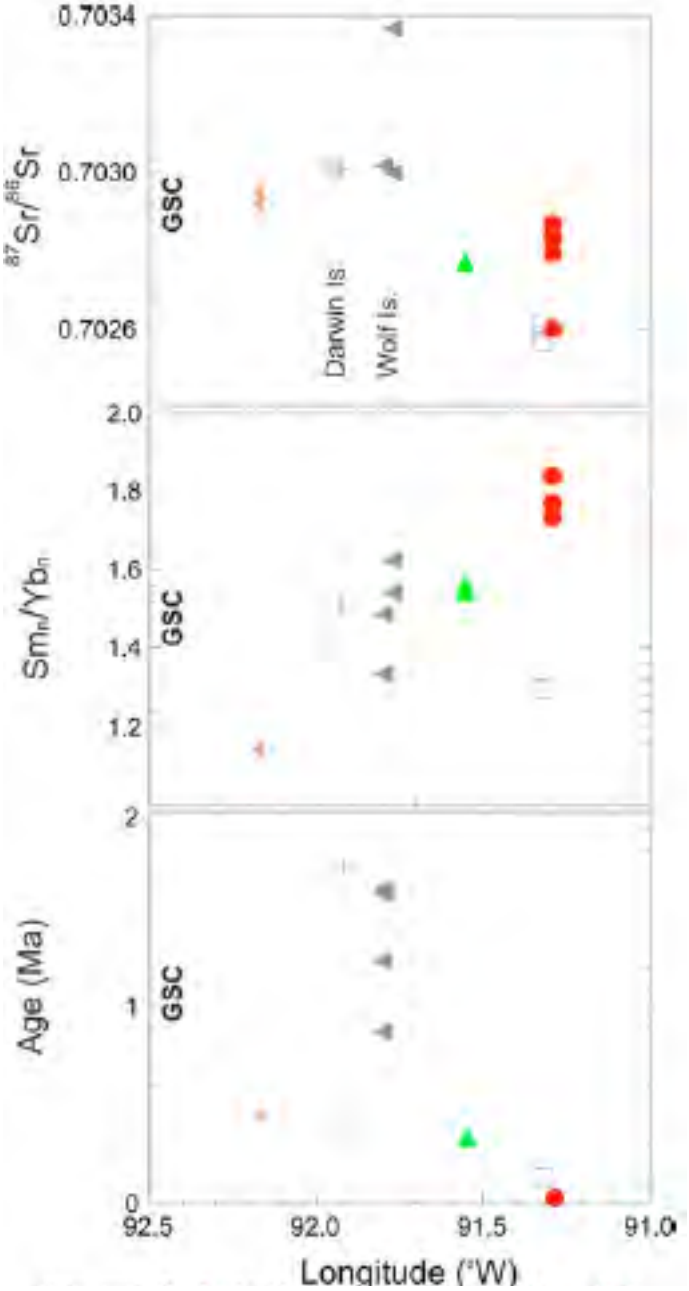

Figure 2.1. Top. Isotopic variations along the WDL; **Middle.** Sm/Yb variations along the WDL (indicator of depth of melting; **Bottom.** Ar-Ar ages aong the WDL (1σ errors 0.1-0.2 Ma). Adapted from Harpp and Geist (2002), Sinton et al. (1996).

Samples from the NGP islands and five PLUME02 dredge sites along the Wolf-Darwin Lineament (Figure 2.1) indicate that NGP volcanism produces a wide range of geochemical compositions, spanning the range defined by lavas from the central archipelago (Harpp and White, 2001; White et al., 1993). Individual volcanoes, however, are nearly compositionally homogeneous (Harpp and Geist, 2002). This suggests that Northern Galápagos volcanic centers sample the mantle on a local (5-10 km) scale, but the mantle is heterogeneous at a longer length scale. In contrast to the systematic geochemical distributions in the central archipelago and along strike of the GSC (White et al., 1993; Harpp and White, 2001; Schilling et al., 2003; Sinton, Detrick et al., 2003; Detrick, Sinton et al., 2002; Cushman, Sinton et al., 2004), the sparse data from the

NGP reveal no clear regional patterns, but hint at some intriguing trends. Among the islands, isotopic signatures (Sr, Nd, Pb) are most enriched at Pinta, but depleted to MOR-levels at Genovesa (Cullen and McBirney, 1987; Vicenzi, McBirney et al., 1990; Harpp, Wirth et al., 2002). Along the WDL, seafloor volcanic centers north of Wolf Island exhibit enriched, plume-like signatures, whereas those to the south are more depleted (Figure 2.1). The intersection between the WDL and the GSC at 92.2ºW is within the most plume-enriched part of the ridge axis (e.g., Detrick et al., 2002; Schilling et al., 1982; Schilling et al., 2003; Sinton et al., 2003). Helium isotopic ratios, in contrast, display typical MOR values along the entire WDL (Graham et al., 1993). These data raise a paradox in the NGP: despite being closer to the plume center, volcanoes like Wolf (Isabela Is.), Genovesa, and the SE WDL are consistently more depleted than any lavas from the GSC in the Galápagos region (Geist et al., 2005; Harpp and Geist, 2002; Harpp et al., 2003). Ages of WDL lavas reach a maximum of ~1 Ma at a seamount north of Wolf and decrease to the north and south (Figure 2.1; Sinton et al., 1996; White et al., 1993).

In their sampling of the GSC axis, the G-PRIME cruise (Sinton et al., 2003; Detrick et al., 2002; Cushman et al., 2004) collected a sample from one area of interest, the 90.5ºW transform fault (Figure 1.2). The MEGAPRINT cruise also dredged in the transform fault in a similar location, as well as a seamount south of the GSC and north of Genovesa Island (Christie et al., 2004; Kokfelt et al., 2005). The PAGANINI cruise (R. Werner, Chief Scientist; Harpp, Wanless et al., 2004; Geldmacher et al., 2003) included one dredge along the eastern transform fault wall as well. All of these samples yielded distinctly depleted, MORB-like signatures (Kokfelt et al., 2005; Cushman et al., 2004). The locations of the PLUME02, G-PRIME, and MEGAPRINT samples were all considered when choosing dredge sites in our study area so as to capitalize on existing data and to avoid duplication of efforts.

3. Cruise Logistics and Operations

a. EM122 Surveying

(D. Fornari, WHOI)

i. EM122 Multibeam Data Acquisition

Data acquisition using the Kongsberg EM122 multibeam system was started outside the EEZ of Costa Rica en route to the study area and continued through most of the cruise (Table 1.1). Multibeam data acquisition during MV1007 was complicated by inadequate documentation in the months prior to our cruise, especially system status, performance, and user-controlled acquisition settings to optimize data collection (the roll-bias test for this system was carried out on a transit leg between Valparaiso and Pt. Montt, Chile in March 2010). During the initial days of the cruise, we struggled to optimize the swath width of the sonar system to match the vendor specifications, that it would produce ~4.5x water depth swaths. This coverage was rarely achieved during the initial surveys. Furthermore, when we arrived at the ship we were informed that significant barnacle growth had occurred on the *Melville's* hull and that this could affect

both ship's speed and perhaps EM122 performance. The barnacle growth unquestionably affected ship speed, but it remains unclear whether growth on the transducers has impacted system performance.

Our sonar acquisition program included the MR1 sidescan, which, because it is also a 12/11 kHz operating frequency sonar, had to be triggered via a slave pulse from the EM122. Hence the ping rate of the MR1 was fundamentally limited by the EM122 ping rate. We had estimated that if the specifications of the system were accurate, we would be able to rely on an average ping rate of ~10 sec (0.1 Hz) over most of the water depths in our survey area, which would yield MR1 swath widths of approximately 11 km full swath. Unfortunately, once we began MR1 surveying in conjunction with EM122 acquisition, several issues with the EM122 became obvious.

First, the system would randomly begin pinging at faster rates (to ~0.16 Hz), despite being in deeper water. We initially had set the system in 'Runtime Parameters' with the following settings:

Angular Coverage: Auto
Beam Spacing: High Density Equidistant
Dual Swath Mode: Dynamic
Ping Mode: Auto
FM Enable: Enabled

It became clear that these settings did not produce either adequate swaths or good (i.e., noise free) data. Prominent artifacts occurred in the data, especially at the transition between the inner and outer arrays. These were manifested as noisy outer swaths as well as a prominent 'railroad track' high along the starboard side (Figure 3.a.1).

Another problem that we experienced with the EM122 system when using the 'Auto' settings and FM-enable in the Runtime Parameters main sounder menu is shown in Figure 3.a.2. When we surveyed areas that have low slopes and sediment cover, the apparently low signal-to-noise ratio significantly impacted the EM122 system's response in that it produced more prominent artifacts, mostly on the starboard side, and reduced the swath width, despite being in deeper water. We continued to experiment with the settings in the early surveys to try to optimize the parameters and it became obvious that using FM-enable only increased artifacts and did not help optimize or expand swath coverage.

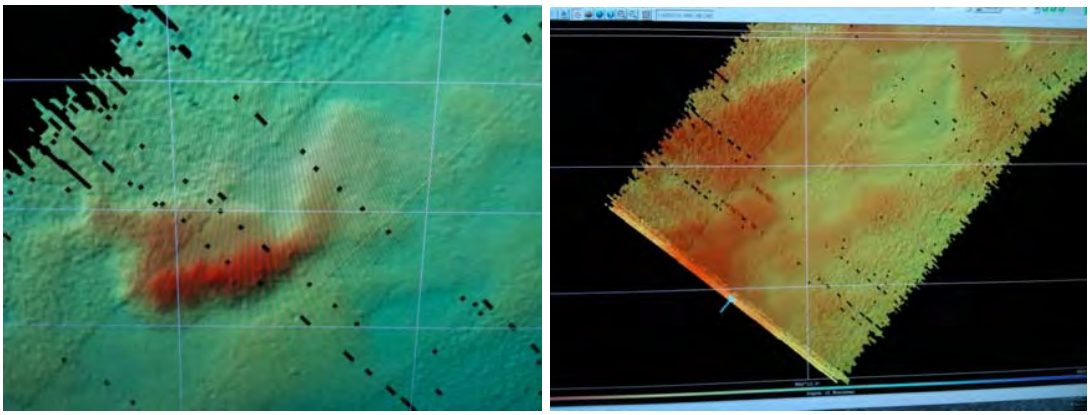

Figure 3.a.1. EM122 data recorded during MV1007 showing noisy outer sectors of the array and the prominent artifact along the starboard mid-section of the swath (upper left in each image).

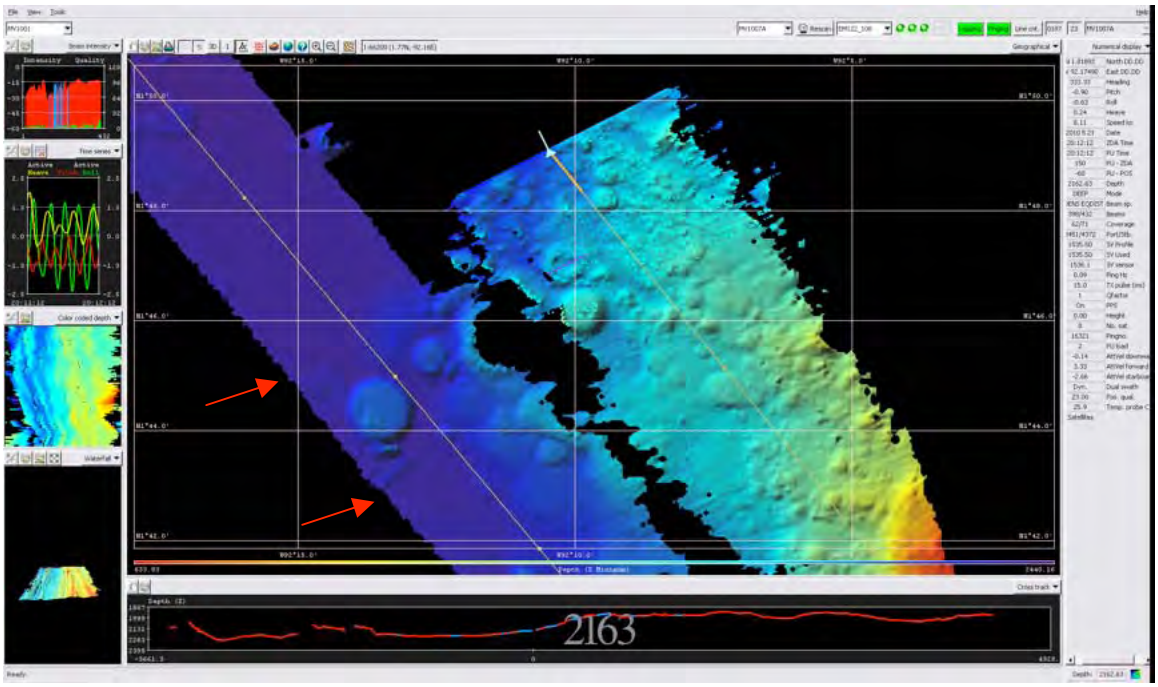

Figure 3.a.2. Screen shot of the SIS screen showing one of our initial lines (left side of image) where we surveyed over flat, sediment-covered seafloor and the swath was narrower, as well as an adjacent swath over rougher terrain with exposed volcanic seafloor where signal-to-noise was higher and the swath expanded considerably despite the mean depth being shallower. Also note that there is a prominent artifact on the starboard side of the left-most swath (line proceeded from upper left to lower right) near the large cone. The FM-enable was turned on for a short period before and after the volcanic cone (red arrows) and one can observe the artifact on the starboard side resulting from this change in the parameter setting.

Based on input from various colleagues, especially Peter Lonsdale at SIO who had used the *Melville's* EM122 to conduct surveys off southern Chile in March 2010, we used a setting sequence for depths greater than 1000 m that was not described in the SIO system logs. This setting was suggested by Lonsdale as a possible solution to by-pass some of the EM122 programmed settings after he had been copied on various emails wherein we detailed the types of problems we were encountering. This set-up involved going into Runtime Parameters, making sure FM-enable was not on, then setting the Angular Coverage to 'Manual', the Ping Mode to 'Deep', and then enabling FM-enable. The changes had to be performed in that precise sequence; otherwise the system would not recognize them and default to an 'automatic' setting. This set of conditions, referenced in our geophysical logs as the 'Lonsdale' setting, was used from about our 4th day onwards (Figure 3.a.3) while conducting simultaneous MR1 sonar and EM122 acquisition. This optimized the multibeam swath width, yielded ping rates that were normally in the 10 sec range except at very shallow depths, and thereby did not force the MR1 swath width to decrease below 10 km full swath. In general when using this setting, we were able to realize 3-4x water-depth swaths without prominent artifacts in the outer swath regions, and with noise levels that were acceptable and able to be minimized in post-processing. One additional factor that may have complicated array performance is that a transmit board for a section of the array was inoperative. This was

not replaced prior to our cruise but was installed in the outermost starboard portion of the array to minimize its impact on the data collection.

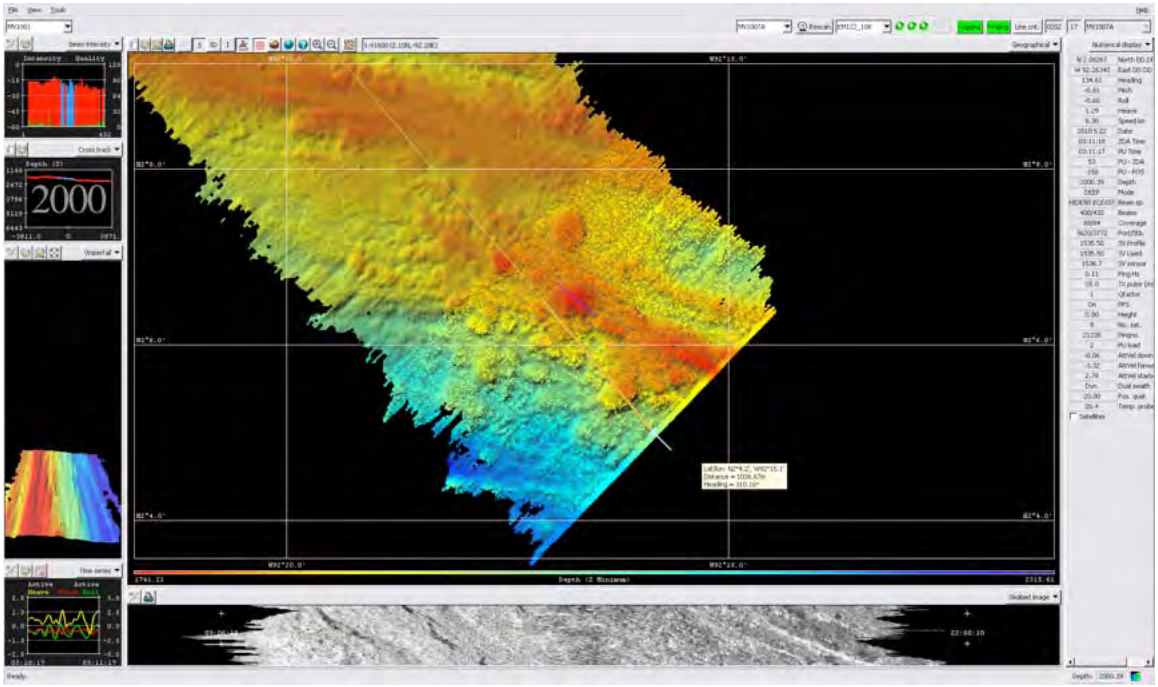

Figure 3.a.3. Swath showing best coverage using the 'Lonsdale' recommended settings.

We communicated numerous technical details to SIO regarding these problems over several weeks during the early part of the cruise with only a few non-technical email responses from the operator despite well-documented emails from us with examples of the problems. SIO indicated they were in contact with Kongsberg about these issues, and had transmitted various BIST and other information to the manufacturer, but as of the writing of this Cruise Report, no formal responses have been forthcoming, either from SIO or Kongsberg regarding both the problems we encountered or suggestions for improvement of system performance. During the 2nd leg of this cruise, we were requested by SIO to perform multiple BIST (system status/noise tests; Table 1.1) at depths greater than 1000 m and speeds from 0 kts to 11 kts, and with engine room equipment off during low speed testing. We carried out these tests and transmitted the data and related environmental information to SIO the same day as the request was received.

In contrast, because of our contacting numerous colleagues in the UNOLS community with experience in multibeam data systems and acquisition (e.g., Peter Lonsdale, SIO; Larry Mayer and Jim Gardner, UNH; Dave Caress, MBARI), and because Paul Johnson, the HMRG leader also had extensive experience with EM122 systems, we were able to get a confirmation that the types of problems we were encountering were not unique to the *Melville's* EM122 installation, and these individuals were very helpful in suggesting alternative settings for the EM122 acquisition (see discussion above). Our experience on this leg points to a need for a common set of practices for how UNOLS operators deal with their multibeam systems, so that all

researchers know how the instruments are performing and how to optimize system settings to produce quality data.

The Kongsberg SIS software and the hardware it is running on are inadequate in terms of computing power. We had to restart SIS and the computers 8 times during our surveys as clearly there are CPU buffer and screen refresh issues that limit how the system displays survey data collected over multiple days and screen gridded at good (i.e., 40 m) resolution so it can be used for real-time interpretation. Improvements to the SIS software, the CPUs, and the operating systems should be a high priority in the near future.

Additionally, we would suggest having an EM122 manual with 'best practices', describing recommended settings for various types of seafloor environments and troubleshooting suggestions. This resource would be highly beneficial to all users and to shipboard technical groups on SIO ships, as well as other ships in the fleet with multibeam sonar systems. The question of noise on each vessel and how this factors into optimizing the system performance and data acquisition must also be a part of this effort, as we now recognize that there are considerable differences in the noise characteristics of each vessel due to hull shape, equipment configuration, noise-reduction of engine room and other equipment, and hull condition. This should be done with input from both engineers and scientists, and there should be a plan to keep it updated on a biannual basis so that the status of each multibeam system in the UNOLS fleet can be monitored.

ii. EM122 Onboard Multibeam Data Processing

Data processing during MV1007 was provided by Ms. Brandi Murphy, from the SIO Shipboard Geophysical Group, UCSD. She was tasked with processing the multibeam data and optimizing the processing to yield cleaned data that could then be gridded at ~50 m data resolution. She started by creating a 30-meter gridded reference surface to identify obvious problem areas and bad data. There were some areas of regular interference, including nearly continuous shallow noise in the beams between 330 and 350. On the port side there was a similar effect but deeper between beams 170 and 190. These artifacts were offset by ~100 m, which was facilitated by using a 5-10 times vertical exaggeration allowing the pings were then removed by hand.

Steep data tags inconsistent with the rest of the seafloor along a swath occur in the outermost beams at the top and bottom of slopes; these were routinely trimmed. The middle sections of these steep slopes appear to be reflecting off real seafloor, which is evidenced when they overlap and cross in the middle; only the tops and bottoms of those artifacts were trimmed.

After we starting using the ‘Manual/Deep/FM-enable’ settings for the EM122 system, it was found that a filter of 4.0° across track angle for the outer beams was needed. When these settings were used, the previous noise in beams 170-190 and 330-320 seemed to disappear. It was still, however, a common area in bad beams. In addition, very deep or shallow beams that did not appear continuous with the seafloor were also removed by hand editing. Once the reference surface looked clean, a surface filter was applied with a standard deviation of 1.7 or 91.08% confidence level and exported as a generic sensor format (GSF) file.

The GSF files were routinely processed during the first leg by Paul Johnson of HMRG who gridded the bathymetric data at 50 m spacing and combined them into the map sets that he was compiling for MR1 sidescan data. In addition, he also made separate bathymetric grid files that included all historical multibeam data for the region. This approach ensured that we had equivalent bathymetric and MR1 sidescan data for all our survey lines, which was essential for real-time decision making in terms of selecting sampling and camera tow sites. The .grd files of bathymetry were compiled into Fledermaus™ .sd visualizations and used onboard to select sample sites and perform preliminary interpretations of seafloor structures in tandem with the MR1 sidescan imagery.

iii. XBT Data Collection, Processing, and Usage During Multibeam Surveying
(E. Mittelstaedt, CNRS)

During the first leg of MV1007, expendable bathythermographs (XBTs) were deployed approximately twice per day. In the second leg of the cruise, a single shallow XBT cast was performed. In total, there were 26 successful XBT casts (Table 3.a.1). Sound speed profiles produced by the XBT temperature data were loaded into the Sonar Information System (SIS) software that controls the EM122 multibeam acquisition. The variable ocean currents in the area of the Galapagos, along with extreme changes in depth associated with the numerous seamounts in the survey area, required sufficiently frequent XBTs to maintain an accurate sound speed profile.

The XBTs measured temperature and produced a sound speed profile to a depth of 1000 m. Normally, the remainder of the profile down to 12,000 m is filled in using the Levitus database, but the archive server aboard the Melville failed and the data were inaccessible. Instead, sound speed profiles were extended by the built-in function in the SIS software. This produced smooth profiles (Figure 3.a.4) that did not vary significantly from Levitus data.

During the first leg of MV1007, XBT-derived sound speed profiles were loaded into the SIS software after each successful cast. During the second leg of MV1007, as the ship neared the location of XBT casts from the first leg, the appropriate sound speed profiles were loaded into the SIS software. This method of collecting and using sound speed profiles allowed for accurate data while conserving the number of XBTs that were consumed during the cruise.

Table 3.a.1: XBT Usage on MV1007

Successful XBT #	GMT date	GMT time	Latitude N	Longitude W	Multibeam centerbeam depth
01	5/18/2010	16:00	7° 35.315	87°16.918	3519
02	5/19/2010	16:00	4° 39.58	89° 59.93	2984
04	5/20/2010	15:00	2° 10.077	92° 38.739	2168
05	5/21/2010	0:30	1° 20.648	91° 52.94	1750
06	5/21/2010	8:15	0° 33.616	91° 11.893	2572
07	5/21/2010	16:30	1° 26.626	91° 49.812	1632
08	5/21/2010	19:30	1° 44.663	92° 6.924	1689
09	5/22/2010	5:15	1° 51.782	92° 4.822	2204
10	5/22/2010	17:15	0° 43.991	91° 1.36	2109
11	5/23/2010	9:00	2° 8.467	92° 4.654	1975
12	5/24/2010	1:15	0° 53.381	90° 55.127	1840
13	5/24/2010	15:00	2° 7.107	91° 49.427	1891
14	5/25/2010	1:30	0° 59.524	90° 53.144	1913
15	5/25/2010	16:30	1° 52.97	91° 30.652	2340
16	5/26/2010	2:45	1° 26.208	91° 1.324	2023
19	5/26/2010	14:54	1° 21.906	90° 50.736	1781
20	5/27/2010	2:35	1° 41.243	90° 59.764	2023
21	5/27/2010	20:04	1° 59.657	91° 8.082	2412
22	5/28/2010	5:15	1° 10.531	90° 20.178	2104
23	5/28/2010	14:23	1° 46.457	90° 43.046	1945
24	5/29/2010	1:45	1° 12.276	90° 7.569	1783
26	5/29/2010	15:40	1° 40.778	90° 17.225	2070
27	5/30/2010	4:50	1° 55.156	90° 1.524	1768
28	5/30/2010	14:20	1° 47.383	90° 1.995	1004
29	5/31/2010	4:40	0° 9.536	90° 28.3	1395
30	6/6/2010	15:08	1° 25.14	91° 50.145	750

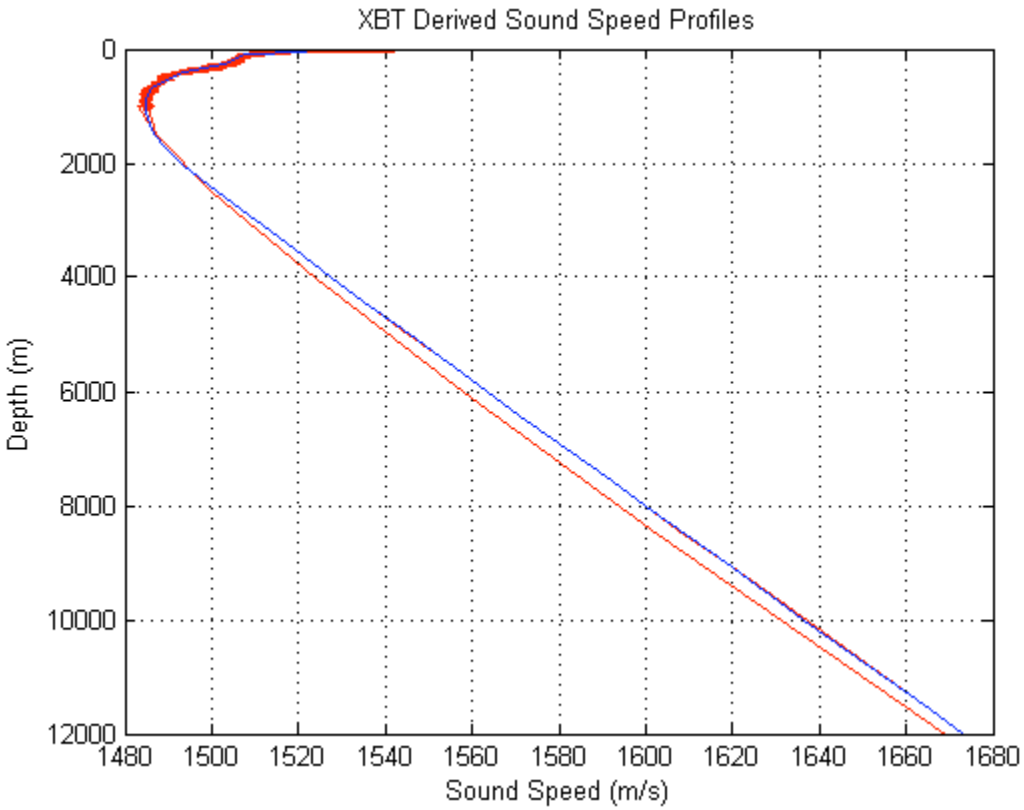

Figure 3.a.4. A compilation of all XBT sound speed profiles extended by the SIS software (red), which are. slightly slower in the last ~11,000 m than the average Levitus profiles from the Galápagos area (blue).

iv. 3.5 kHz Knudsen Sub-Bottom Profiler Operations
(E. Mittelstaedt, CNRS)

The 3.5 kHz Knudsen sub-bottom profiler was utilized twice in the second leg of MV1007. The first instance was a series of north to south survey lines between dredge locations to characterize the ridge-like morphology observed east of the 90.5°W transform fault. The second use of the 3.5kHz profiler was to examine the sediment thickness over the top of a bathymetric high located at 1.5°N 90.3°W. We did not run the 3.5 kHz during the larger EM122 and MR1 surveys because of known noise problems between the subbottom and multibeam systems.

b. Hawaii MR1 Surveying
(P. Johnson, HMRG)

i. Mobilization

The *R/V Melville* arrived in Puerto Caldera, Costa Rica on the morning of May 11th and began demobilization of the MV1006 gear. The HMRG mobilization team arrived at the ship at 2 PM (local), after the ship had installed two steel I-beams welded above the steel plate covering the trawl ramp at the stern of the ship. These beams

were installed to support the MR1 system and launcher, as the ship's architects were concerned about the strength of the steel plate. Initially, the mob team oversaw the unloading of the Launch and Recovery System (LRS), winch, and hydraulic power pack from their 40' container, while the previous leg continued their demobilization. With delays in the unloading of the MV1006 components, it was decided to load all of the components of the MR1 system, as well as a 20' Spares and Tool van onto the ship. With all gear craned aboard and temporarily chained down, work stopped so that the Melville could relocate away from the commercial pier.

Welding started on the morning of May 12th and was completed by the afternoon of May 13th to attach brackets to the steel beams and deck plates so all components could be bolted down in their final operational locations. Once the welding was finished, electrical power was connected to the Hydraulic Power Pack and hydraulic lines were laid to power the winch and LRS.

By the afternoon of May 14th, a complete system test had been run to check the mechanical operations of the LRS as well as running a full deck test of the MR1 tow-fish to verify that the acquisition machines in the main lab could correctly communicate and collect valid data from the MR1 towfish through the tow cable and slip ring. Final system checks were run on the system on the 16th to validate fully all components.

ii. MR1 Surveying

The MR1 sidescan sonar system is an 11/12 kHz near-surface towed sonar system capable of ensonifying large areas of seafloor and collecting co-registered backscatter and phase-bathymetric data (Rongstadt, 1992; Davis et al., 1993). For this survey, because *Melville* is equipped with a Kongsberg EM-122 multibeam sonar, we used only multibeam sonar data to compile the bathymetric maps. Map areas and scales for MR1 backscatter, EM122 acoustic imagery, and EM122 bathymetry are equivalent (Figure 3.b.1). It was only necessary to deploy the MR1 tow-fish one time during the MV1007 leg.

On the morning of May 20th, the MR1 was successfully deployed. Shortly after deployment, a calibration of the tow-fish compass was performed by executing a complete 360° turn at 6° per minute to port followed by a 360° turn, also at 6° degree per minute, to starboard. These turns are used to calibrate the MR1's magnetic compass to the local magnetic field, allowing for a better heading to be determined for each ping. Immediately following the calibration circles, the primary survey began. For a full breakdown of the operations schedule, see Table 3.b.1.

Table 3.b.1. MR1 Survey Timeline

Date (Julian Day) / Time(GMT)	Event
140 / 1300	Begin MR1 Deployment, Tow1
140 / 1343	Begin Compass Calibration
140 / 1410	End Compass Calibration
140 / 1615	Begin Survey
151 / 1400	End Survey
151 / 1400	Begin MR1 Recovery
151 / 1800	End MR1 Recovery

No significant problems occurred during the 264 hours of survey time (a little over 11 days). Over this time period, the MR1 pinged 109,147 times, collecting 15 Gigabytes of raw data. Excluding periods of time when the MR1 system was temporarily halted to check the EM122, the MR1 performed very well. Only 4 time gaps longer than 1 minute occurred (Table 3.b.2). Summing the time of all of these gaps together shows that the MR1 system was only down 0.32% of its operational time (Table Y).

Table 3.b.2. MR1 System Downtime

Start	End	Gap (Minutes)	Reason
2010-05-20 14:09:35	2010-05-20 14:10:44	1.14455	Power Supply Swap
2010-05-25 07:51:12	2010-05-25 08:33:08	41.9287	Full Hard Drive
2010-05-26 14:22:04	2010-05-26 14:28:46	6.69663	Power Switch Accidentally Hit
2010-05-28 15:14:33	2010-05-28 15:15:40	1.11399	Not Logged

Because of the changing modes of the EM122 as it attempted to adjust its swath width and ping rate to account for changes in bottom type and depth, occasionally interference from the EM122 could be seen in the MR1 sidescan data. Attempts to remove the interference by adjusting the delay in pinging the MR1 system or manually adjusting the mode of the EM122 did little to solve this problem. Luckily, this artifact, when present, is easily identifiable in the data and should not cause any confusion in its interpretation.

The MR1 survey was completed on the morning of May 31st and recovery of the system began relatively uneventfully until the depressor weight came into sight. The H-Link, which connects the 1-ton depressor weight to the cable termination, had failed on one of its limbs, directly below a weld. Because of this, the depressor weight was hanging askew and too low to be recovered into its normal channel, on the bed of the LRS. Numerous attempts were made to recover the weight by adjusting the ship speed, changing the LRS bed angle, and tag lining the depressor weight, but nothing was successful. The final attempt brought the depressor in as far as it could onto the guide cone on the LRS, where a lifting strap was put around the weight and the ship's crane was then used to lift the weight onto the bed of the LRS. The MR1 system was then transferred to the LRS' fish winch, allowing the depressor weight to be decoupled from the cables' termination and lifted to the deck with the ship crane. Following this, the actual recovery of the MR1 tow-fish was uneventful. The Melville's res techs and crew were incredibly helpful through this process.

Preparations for demobilization began after the recovery and were completed by June 2nd in order for the HMRG team to disembark in Puerto Ayora, Galapagos.

iii. MR1 System Settings

System settings for MR1 are summarized in Table 3.b.3.

Table 3.b.3. MR1 System Settings

Ping Rate:	MR1 was operated using an external trigger to synchronize the transmit cycle with the *Melville's* EM-122 multibeam sonar. Attempts were made, some with mixed results, to optimize EM-122 cycle to allow greatest possible sidescan return.
Pulse Width:	MR1 pulse width was adjusted based on water depth in order to maintain a full charge on the tow-fish capacitors. The following pulse widths were used based upon the depth mode of the EM-122. 1ms < 1000m 2ms 1000m - 3000m 5ms > 3000m
Power:	Full, for the duration of the survey

iv. MR1 Data Collection

Raw MR1 data were recorded in hour files by the acquisition computer and logged to the acquisition machine's hard drive and then backed up in near real time to the HMRG processing machines. Post-processing of acoustic imagery data was continuous throughout the survey and merged with navigation data collected from shipboard GPS. Bathymetry data collected by MR1 were not used, but were collected. All data (raw and processed) and products (charts, grids, tiff files, etc.) were backed up in near real time to two external USB hard drives and a network storage device, meaning all data and products could be found on any of 4 hard drives at any time.

The HMRG produced final charts of the survey areas at various scales (Figure X, A-D). Maps at each scale include MR1 sidescan data, EM122 acoustic imagery data, and the EM122 bathymetry. Bathymetry data from historic cruises were merged with the MV1007 data for all chart sizes in order to create the most complete bathymetric chart set possible. A summary of charts produced is included below (Tables 3.b.4, 3.b.5).

v. Sonar Data Products Delivered

Final processed data and data products were delivered on a hard drive provided by HMRG and included netCDF Grids, JPEGS, PDFs, and postscript for all chart sizes (1:400K, 1:200K, 1:100K, and 1:50K) and for all systems and data types (MR1 Sidescan, EM122 Bathymetry, and EM122 Imagery). HMRG will load all data and data products on their servers in Hawaii where it can be made available upon request.

Table 3.b.4. Summary of HMRG Charts Produced

MR1 sidescan imagery, EM-122 multibeam bathmetry, and EM-122 acoustic imagery charts produced during MV1007. Bathymetry and imagery from EM-122 were gridded at 50 m, and MR1 data were gridded at a cell size dictated by the scale of the chart.

Scale	Description	Resolution (m)	Number*
1:400,000	Regional MR1 Sidescan	50	1
	Regional EM122 Bathymetry	75	1
	Regional EM122 Imagery	50	1
1:200,000	MR1 Sidescan	25	4
	EM122 Bathymetry	50	5
	EM122 Imagery	50	5
1:100,000	MR1 Sidescan	15	11
	EM122 Bathymetry	50	14
	EM122 Imagery	50	14
1:50,000	MR1 Sidescan	10	40
	EM122 Bathymetry	50	47
	EM122 Imagery	50	47
			Total: 190

*** NOTE:** For each sidescan and imagery chart numbered in the table above, 2 actual charts, page sized and A0 sized, were generated. For each bathymetric chart listed, 4 actual charts were generated, both page sized and A0 sized, as well as one version of each paper size with hill shading and one with no hill shading.

Table 3.b.5. Summary of Size (Gigabytes) of Grids and Charts Generated by HMRG

Product	Size (Gigabytes)
Processed Sidescan Grids & Charts	34
Processed Bathymetry Grids & Charts	9.3
Processed Navigation and Charts	.5

A.

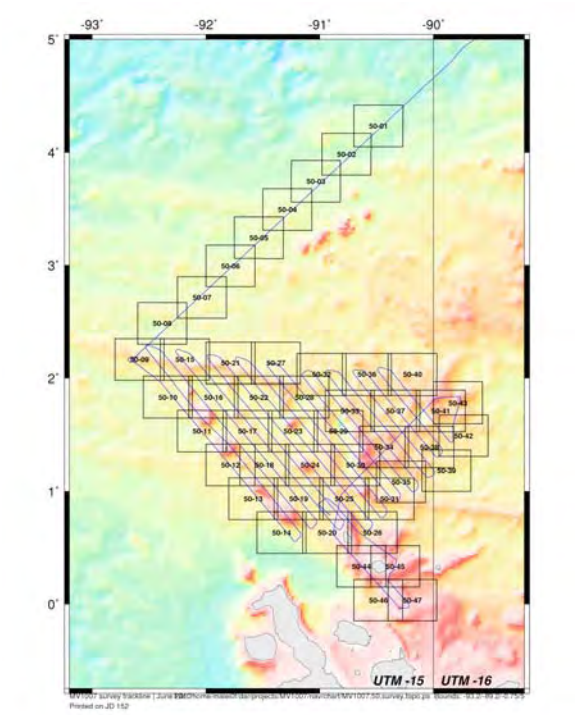

B.

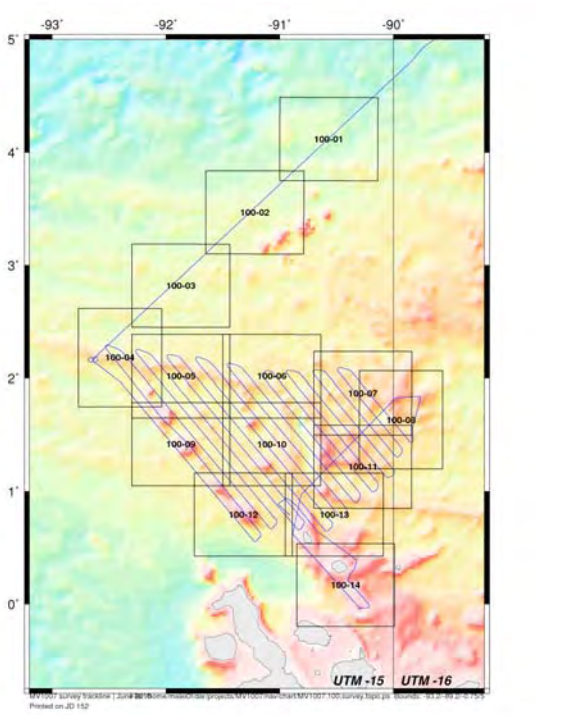

C.

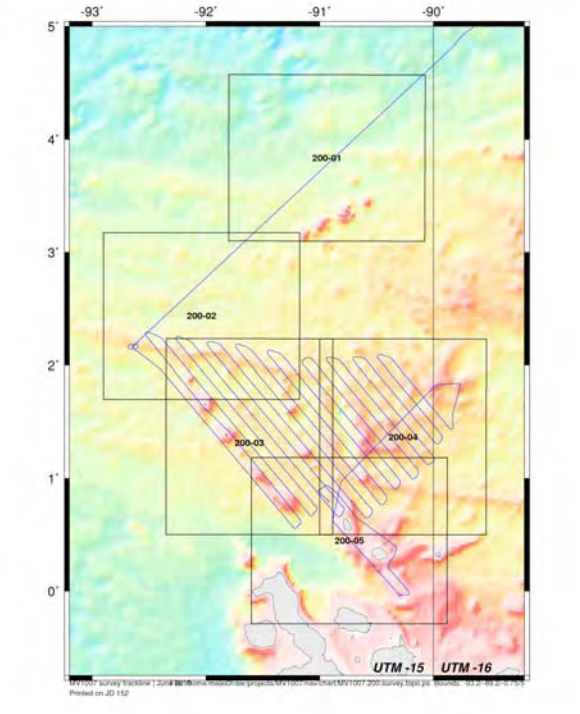

D.

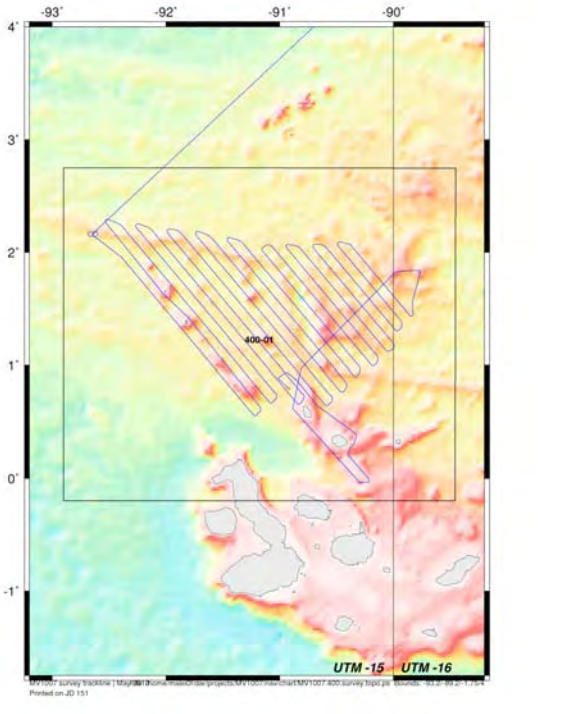

Figure 3.b.1. (A-D) Location maps showing the chart boxes for the scales 1:50K, 1:100K, 1:200K, and 1:400K

c. Dredging Operations

(D. Geist, University of Idaho, D. Fornari and M. Kurz, WHOI, C. Sinton, University of Redlands, A. Koleszar, Oregon State University)

i. Dredging Methodology

Dredging was performed using the 9/16" trawl wire on the Melville and standard SIO dredges with a weak-link system, on the starboard side due to the MR1 installation on the fantail. Protocols were established by SIO Resident Technicians Drew Cole and Brian Rowe in collaboration with Dan Fornari (WHOI). Dredges were lined with tuna netting, which in turn was lined at its base with an inner bag of burlap connected to the netting by tie-wraps to catch glass shards and small samples. The dredge weight was also wrapped in burlap, with all bags being replaced for each new dredge to avoid cross-dredge contamination; in several cases, the burlap provided enough samples for geochemical analysis even when no larger rock samples were collected. A 12 kHz pinger was used for all dredges to determine scope of wire on the bottom; it was placed 300 m above the dredge for all dredging operations. The main weak link was set at 18,000 lbs and side links were set between 5,000 and 7,000 lbs.

Dredge targets were primarily seamounts and fault scarps. Tracks were designed to achieve spatial precision, varying between 200 and 500 m in length and limited to steeply sloping terrain and areas with high reflectivity in the MR1 backscatter data.

All dredges were run at ship's speed over ground of ~0.2 knots using Dynamic Positioning (DP). Approximately 150 m of cable were paid out on bottom behind the ship before it began to move along the dredge track. The pinger depth was typically maintained at ~ 100-150 m during the dredge. The Res. Techs. adjusted wire length during the dredge to maximize effectiveness, resulting in only 2 empty dredges out of 49 total attempts (Appendix II).

Strong currents and at times winds coupled with the use of the starboard overboarding necessitated that most dredge tracks be oriented along a NW to N bearing so as to minimize stress on wire angle and on the dynamic positioning system (particularly the bow thruster, which required repair early in the cruise). The use of the starboard A-frame was required because the MR1 system could only be stored under the aft A-frame, thereby preventing its use for dredging. Some time was lost early in the cruise as the crew had to work out methods to deal with the currents and winds given the sensitivity to problematic wire angles; we were fortunate that the Melville's crew skillfully found a configuration that worked for dredging, that seas were generally calm, and that currents remained consistent during dredging operations. This allowed us to use the same ship orientation and dredge track direction successfully throughout the cruise. We do not recommend this system for intensive dredging use in the future, however, as it is far less flexible for handling variable conditions than an aft dredging configuration, and likely could not have been used if we had encountered rougher seas.

ii. Rock Processing

Samples were primarily retrieved from the seafloor by dredging operations described above. Once on deck, rocks were described and photographed. They were then sub-sampled for thin section production and geochemical analysis. Splits of

glasses (when available) were taken for electron microprobe (major elements; University of Idaho) and inductively coupled plasma-mass spectrometry (ICP-MS; trace elements; Colgate University), as well as radiogenic isotope (WHOI), volatile (Oregon State University), and noble gas analyses (WHOI). Crystalline samples were sub-sampled for Ar-Ar geochronology (University of Redlands/Oregon State University) and X-ray fluorescence (major elements; Colgate University). The detailed rock processing protocol is included as Appendix III; representative images of rock samples are shown in Appendix IV. Additional samples of glass and rock fragments were collected using the wax balls on the Tow Cam.

d. Towed Camera Surveys
(D. Fornari, WHOI)

The WHOI – MISO (Multidisciplinary Instrumentation in Support of Oceanography) Facility TowCam (Fornari, 2003) was used for 5 successful traverses during the MV1007 cruise. The system was configured to collect digital photographs, CTD data, and four wax-ball volcanic glass samples. Camera s/n6004 was used for all lowerings with a delay time of 30-60 minutes and photo interval of 10 seconds. Towing speed was between 0.3-0.4 kt for most lowerings. The two green laser dots, which are visible in each photograph in the middle-right center of the frame, are spaced 15 cm apart.

The TowCam system was used to ground-truth MR1 sonar data over areas with distinct acoustic reflectivity, as well as collect additional samples using the wax-ball glass samplers. Approximately 6000 3.3 megapixel digital color photographs of the seafloor were collected in five camera tows. In addition to the processed, date/time stamped images, files were made of CTD data that include 1 second records of all CTD data and files for each time the camera/strobe were triggered and when each wax ball was deployed.

e. Gravity Survey
(E. Mittelstaedt, CNRS)

i. Pre-cruise Data Verification and Gravimeter Status

In January, 2010, an analysis of sample data from the BGM-3 gravimeter aboard the R/V Melville revealed a standard deviation in the raw gravity counts that ranged between ~300 and 136.2 to 1407.6. When filtered and compared to bathymetry, the data appeared to measure accurately large-scale features, but the high level of noise in the raw signal brought into question the sensitivity of the system to small variations in the gravitational acceleration. The standard deviation of the raw counts from the R/V Melville was comparable to data from the R/V Revelle, but several times larger than data from the R/V Knorr and R/V Atlantis.

NOTE: The majority of the following summary is from Dr. James Kinsey's (WHOI) report on gravity quality status (*Pers. Comm.*, 2010).

Potential causes of noise discussed between January and May, 2010:

1. Platform Shock Mounts: Both the Revelle and the Melville use compact shock mounts (compared to the standard floor mounted shock mounts used on the Knorr, Atlantis, and other ships). Rationale for this cause is that this type of mount is unique to the Melville and Revelle.
2. Degraded Roll Gyro: When the Melville's gravimeter was repaired during the Valparaiso port stop in late February, both during the port stop and sometimes at sea, the roll integrator appears to be biased in one direction. Possible cause for this is a faulty roll gyro. Based on tests onboard the Melville, the roll gyro malfunction value indicates a good gyro and the tilt test was within specifications.
3. Sea State: Data used for comparison were collected during sea states of 1-2. In addition, in-port data also show a larger standard deviation in the raw counts than other vessels (note the Melville was exposed to the swell in Valparaiso).
4. Sensor Signal Conditioner/Clock Board: The signal conditioner board may be causing a problem, but this was considered unlikely as there is an increase in noise level between in-port and at-sea measurements.

Actions taken:

1. The sensor signal conditioner/clock board was replaced.
2. The roll gyro was replaced.
3. Swapped out stabilized platforms. There was a spare platform in the science hold.
4. The shock mounts on the gravimeter stabilization platform were replaced. This did not appear to change the noise level in the data.
5. The control power supply was replaced with a WHOI unit. The unit powered on and stabilized normally.
6. Subsequent attempts to monitor DPM voltages of the unit led to the discovery of a bad 4bit Siliconix analog multiplexer. It appeared that the multiplexer chip was malfunctioning. This did not affect system performance.
7. The pitch gyro was replaced. The system powered up and stabilized normally. After this fix, there was one spare replacement gyro and two useable gyros from the spare gravity platform remaining on board.
8. Because the actions before this did not appear to affect the data quality or noise level, the system is returned to its original configuration (i.e., replaced original signal conditioner clock board, control power supply, and pitch gyro). DPM voltage measurements were then working correctly.
9. A malfunction light indicated that, subsequent to the mount change, the pitch gyro had failed. The control power supply was cycled multiple times to verify that the pitch gyro was really the cause of the problem. After several attempts, the malfunction light did not go off. The pitch gyro was replaced and the system appeared to function normally.

10. The system, which was mounted in a computer rack, was placed on a stock BGM-3 stabilization platform with shock-mounts. The gravimeter mount was affixed to the floor using industrial-strength Velcro.

Result of the actions outlined above: A decrease in the noise level of the data was observed after the mount was replaced. It is difficult to assess whether this is the result of the new mount or other circumstances, but it suggests that the mount is an improvement over the previous situation. No other actions taken above significantly reduced the noise level in the data.

ii. Pre-Cruise Status of Gravimeter and Gravity Ties

The gravimeter appears to be providing accurate data with variable noise levels that are attributed primarily to changes in sea state. Comparison of the underway free-air gravity anomaly to interpolated satellite data shows strong agreement over major seafloor features (Figure 3.e.1). A remaining difficulty is the lack of an established gravity tie record. Few gravity ties were performed since the gravimeter was repaired in March, 2010. To help remedy this situation, a gravity tie was performed just before and just after MV1007 at the head of the Puntarenas pier (Table 3.e.1 and Appendix V).

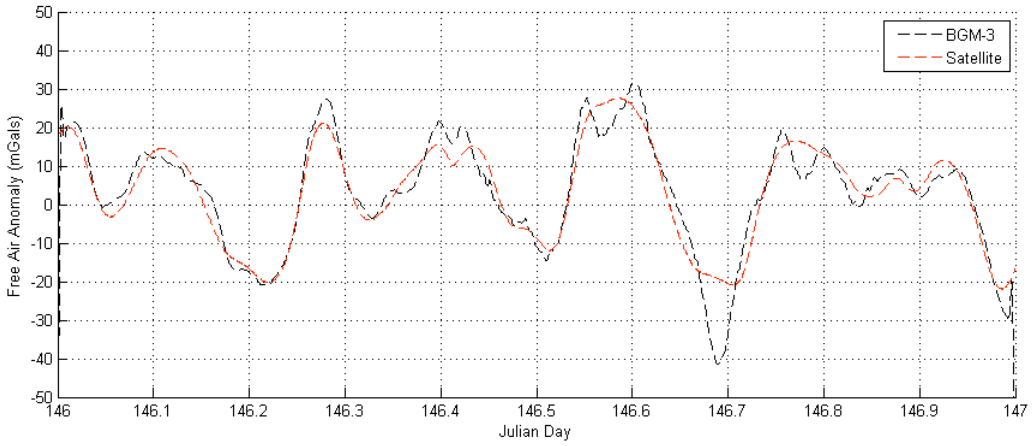

Figure 3.e.1. A comparison between (red) satellite and (black) BGM-3 underway data demonstrate a high correlation suggesting that the BGM-3 is functioning properly.

iii. Underway Gravity Operations

Measurements

Two types of gravity measurements were performed during MV1007: sea-based measurements and land-based measurements. Acquisition of seagoing gravity measurements with the Bell BGM-3 gravimeter began outside of the Costa Rican EEZ on May 20th and continued until the cessation of data collection when the ship re-entered the Costa Rican EEZ on June 16th. The BGM-3 gravimeter experienced no mechanical or software related issues for the duration of the cruise. In addition to the gravity ties at Puntarenas pre- and post-cruise, two land-based gravity measurements

were performed on Wolf Island with the WHOI LaCoste and Romberg land gravimeter (Table 3.e.1).

Table 3.e.1

Gravity Tie Location	Published Gravity Standard	Date	Time (GMT)	Gravimeter Offset After Tie*
Head of Puntarenas Pier	DOD 4551-1	11, May 2010	20:39	855320.35444
Head of Puntarenas Pier	DOD 4551-1	18, June 2010	17:08	855320.65644
Former airport at Puntarenas	DOD 4551-0	18, June 2010	19:27	N/A

The LaCoste and Romberg gravimeter displayed anomalous behavior during the measurements performed on Wolf Island. The measurement needle could not be moved to the extreme left of the measurement window. Email communication with shore-based parties suggested that this may be due to a mirror misalignment shifting the measurement location. To verify the accuracy of the final gravity tie on June 18th, the measurement location was confirmed upon arrival at Puerto Caldera (Appendix V). A roll test and long-line level test indicated that the gravimeter reading line is unchanged, but that the sensitivity is diminished (one turn of dial changed reading position by 7 instead of the standard 10 reading lines).

Gravity Logging

In addition to the existing logging aboard the R/V Melville, a new gravity logging system created by Dr. James Kinsey of the Woods Hole Oceanographic Institution was implemented on MV1007. The system includes both a hardware and software component. The hardware consists of two identical Linux based laptop computers connected to two serial to USB hubs. The software package creates the RGS (Raw Gravity String) with all navigation, depth, and gravity measurements necessary for post-processing of gravity data.

The RGS is created at the native rate of the gravimeter (for the BGM-3 aboard the R/V Melville, once per second) and uses the most recent navigation and depth data. The gravity logging program does not attempt to resolve the asynchronous data streams. Consequently, the navigation and depth data are older than the gravity measurements. The navigation data uses GPS and is less than one second old. The age of the depth data ranges from ~0 to ~12 seconds depending on the site depth. The timestamps of the navigation and depth data are included in the RGS, enabling resolution of the age of the measurement.

For the navigation, only the best available data are logged in the RGS. On the R/V Melville, two separate GPS units (GP-150, GP-90) obtained navigation data. The gravity logging software decides which sensor to use based on a priority table, the staleness of the measurement, and other metrics. Although it is not uncommon for the source of the navigation data to change during a cruise, that was not the case on MV1007 and only data from the GP-150 were logged in the RGS.

f. Underway Magnetometer Operations
(E. Mittelstaedt, CNRS)

The towed Seaspy magnetometer was deployed approximately 300 m behind the ship on the port side. During the first leg of the cruise (May 17 to June 3, 2010), the magnetometer and the MR1 side-scan sonar system were deployed side-by-side. The majority of the magnetometer data was collected continuously between May 20th and May 30th except for two major interruptions. During the second leg of the cruise, the magnetometer was deployed during longer transits between dredging operations and during one north-south transect east of the 90.5°W transform fault (Table 3.f.1).

Data acquisition was interrupted on two occasions during the first cruise leg. The first occurred between May 23rd at 16:30 GMT and May 25th at 20:39. The interruption was caused by deterioration of the data quality number from 99 to 0, caused by water infiltrating the magnetometer cable termination. The re-termination resulted in an extended data loss of ~48 hours due to the 24-hour curing time for each of two layers of epoxy used to seal the termination. The multibeam technician Brandi Murphy carried out the repair effectively and efficiently.

The second major interruption to magnetometer data acquisition occurred near the end of the first leg of the cruise on May 30th at 23:45 GMT. Strong currents caused the MR1 towfish to drift to port. The proximity of the magnetometer and the MR1 resulted in crossed towing cables with the magnetometer cable resting and abrading on the MR1 steel cable. The magnetometer was immediately pulled in and the ship was turned to untangle the two cables. After this interruption, the decision was made to keep the magnetometer out of the water until after the port stop at Puerto Ayora, Galapagos.

Table 3.f.1. MV1007 Magnetometer Use

Magnetometer Leg	Start Date (GMT)	Start Time (GMT)	End Date (GMT)	End Time (GMT)	Reason for End of Leg
1	20 May 2010	16:30	23 May 2010	14:15	Water in cable termination
2	25 May 2010	20:39	30 May 2010	23:57	MR1 and Magnetometer cables crossed
3	9 June 2010	03:06	9 June 2010	04:00	Arrival at dredge
4	10 June 2010	06:22	10 June 2010	10:45	Arrival at dredge
5	12 June 2010	12:59	12 June 2010	15:15	Arrival at dredge
6	13 June 2010	06:03	13 June 2010	09:44	Arrival at dredge
7	13 June 2010	13:33	13 June 2010	16:54	Arrival at dredge
8	13 June 2010	21:27	14 June 2010	01:28	Arrival at dredge
9	15 June 2010	20:12	16 June 2010	07:48	Arrival in Costa Rican waters

4. Preliminary Description of Field Data

a. Mapping

Data from the EM122 bathymetry and MR1 sidescan survey cover the Northern Galápagos region from the Wolf-Darwin Lineament, across the 90.5°W transform fault, to just east of 90°W longitude (Figure 1.2). Bathymetric data are gridded at 50 m spatial resolution and MR1 sidescan data at 10 m resolution. Personnel from HMRG and SIO worked closely together to produce the processed data in real time for shipboard analysis, which was critical to our ability to select appropriate dredge sites. Below we describe a number of important preliminary observations across the study area, all of which will be topics of ongoing research.

Perhaps the most surprising aspect of the mapping survey is the striking difference between the seafloor structure east and west of the 90.5°W transform fault (Figures 4.a.1 and 4.a.2). The area west of the transform fault is dominated by constructional volcanism, primarily arranged in NW-SE lineaments of major seamounts. In contrast, the region east of the transform is dominated by tectonic structures, revealing a series of bathymetric highs and strongly faulted seafloor textures with only small, randomly located cones and one major seamount in the northeastern-most corner of the survey area.

Figure 4.a.1 (next page). MV1007 Bathymetric Data, 1:400,000 scale. Additional shorter surveys were performed across the study area to fill in data gaps, but those data are not included in the map.

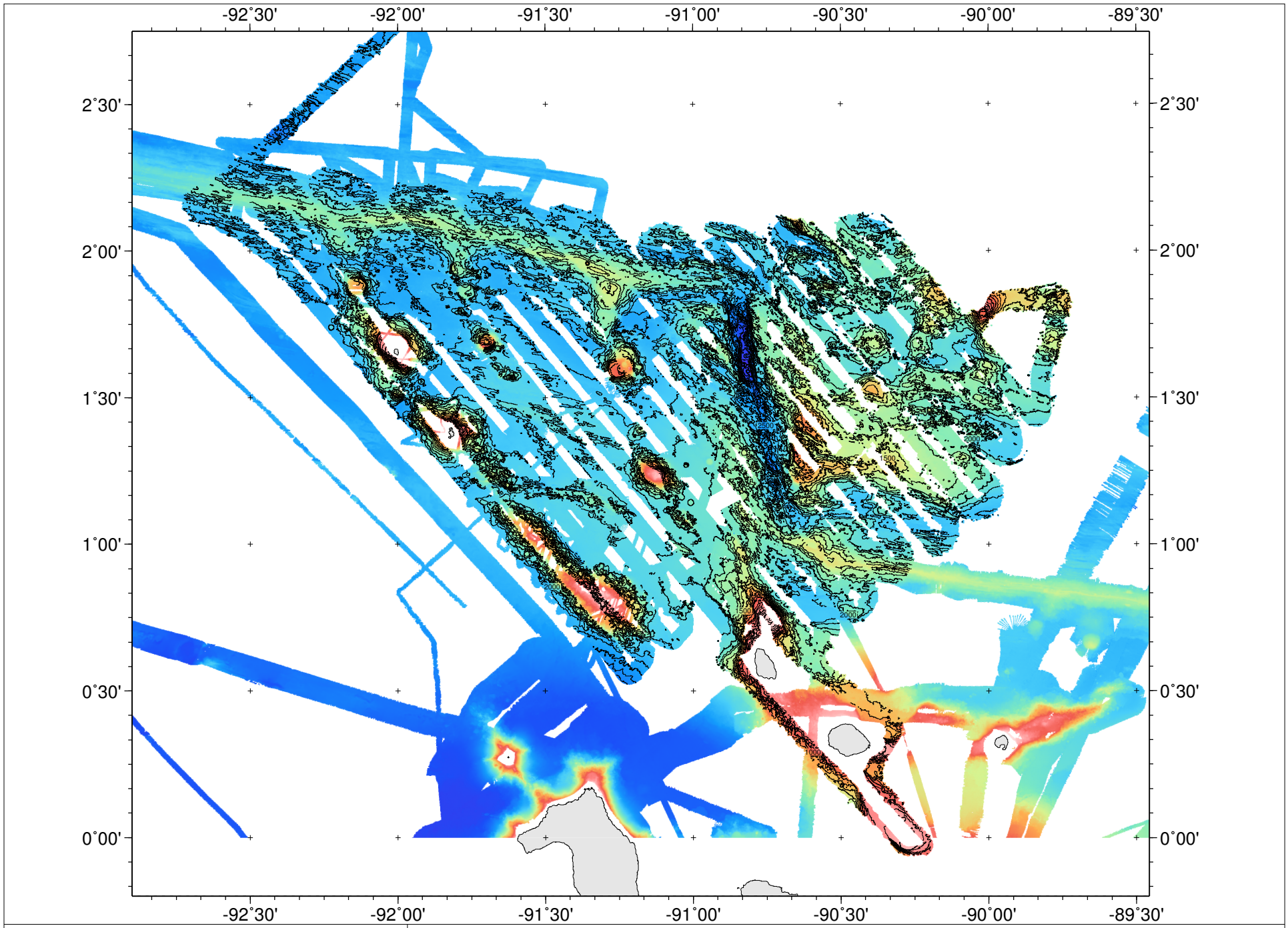

MV1007 : Chart 400-01
North Galapagos Survey

Karen Harpp - Colgate University
R/V *Melville*

EM122 Bathymetry

100 m Contour Interval (500 m Bold)
Grid size: 75 m
Coastline: GMT WVS and WDBII database
NOT FOR NAVIGATION

Universal Transverse Mercator Projection
Scale: 1:1900000 UTM Zone 15 WGS-84

nautical miles
0 40
kilometers
0 40
depth (meters)
-4000 -3000 -2000 -1000 0

8° 4° 0° -4°
-96° -88°

HAWAI`I MAPPING RESEARCH GROUP

Printed:
Tue Jun 1 17:12:31 UTC 2010

- Copyright 2010 - Hawaii Mapping Research Group -

Figure 4.a.2 (next page). MV1007 MR1 Sidescan Sonar Data, 1:400,000 scale.

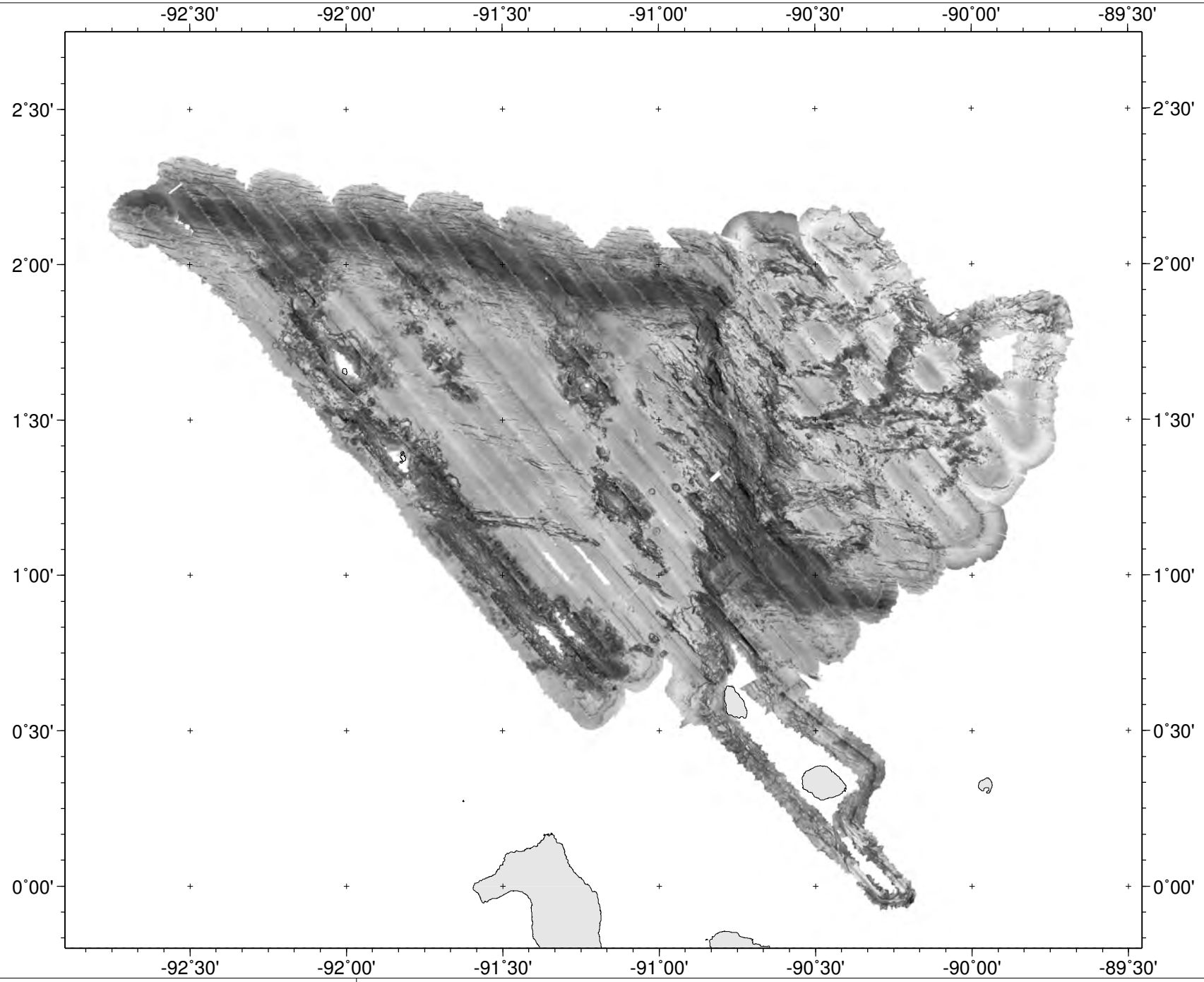

MV1007 : Chart 400-01
North Galapagos Survey

Karen Harpp - Colgate University
R/V *Melville*

MR1 SIDESCAN

High backscatter is black
Grid size: 50 m
Coastline: GMT WVS and WDBII database
NOT FOR NAVIGATION

Universal Transverse Mercator Projection
Scale: 1:1900000 UTM Zone 15 WGS-84

nautical miles
0 40
0 kilometers 40
Backscatter Magnitude
LOW HIGH

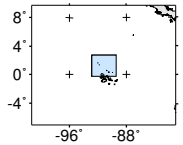

HAWAI`I MAPPING RESEARCH GROUP

Printed:
Tue Jun 1 23:58:46 UTC 2010

- Copyright 2010 - Hawaii Mapping Research Group -

i. West of the 90.5°W Transform Fault

A wide variety of volcanic structures can be observed across the region west of the transform fault. The majority of the constructional activity is concentrated in three major lineaments, the largest and westernmost being the Wolf-Darwin Lineament (Figures 4.a.1 and 4.a.2). The discovery of additional cones outside of these three lineaments, however, indicates that relatively recent volcanism has been widespread throughout the region west of the transform. The geochemistry, petrology, and morphology of these structures coupled with their gravity signals will be critical for testing the plume-ridge interaction models delineated in the original proposal and will be the focus of several of undergraduate projects beginning in late June 2010.

Volcanoes in the western half of the area vary significantly in both volume and morphology. Volumes are broadly bimodal, with small cones 100s of meters in diameter to major polygenetic structures 10s of kilometers in length (Figures 4.a.3, 4.a.4). Many of the smaller, rounder cones have summit craters, whereas some of the larger seamounts have calderas, occasionally with nested structures suggesting complex magmatic histories. The largest volcanoes along the WDL have mesa-like pedestals with prominent sequences of flow fronts that grade upwards into highly reflective terrain and hummocky acoustic textures. This may be a critical observation in terms of understanding the origin of these major volcanic structures. We have a number of hypotheses for the origin of the seamounts, including formation at the GSC, volcanism initiated by regional extensional processes, and activity associated with rift propagation across the ridge-transform intersection. Many of the largest volcanic structures in the western study area, including Wolf and Darwin Islands, have experienced mass wasting of the unbuttressed flanks, resulting in debris flow deposits along their flanks (generally perpendicular to the lineament); similar phenomena are not observed at the small, more conical seamounts in the region. Such observations will help reconstruct the history of these islands and seamounts and their roles in the formation of the volcanic lineaments.

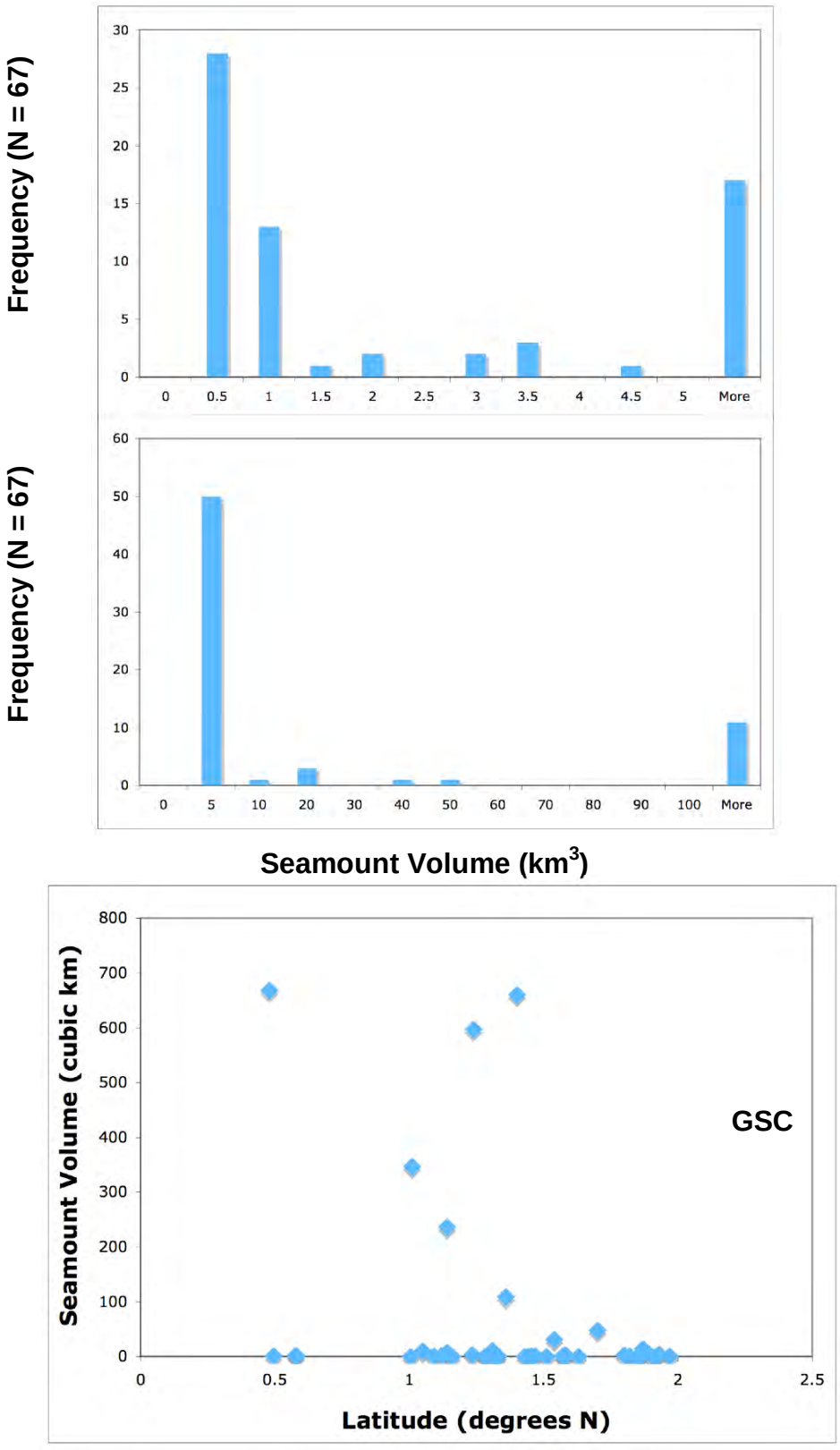

Figure 4.a.3. Preliminary measurements of seamount volumes. Top and middle: distribution of seamount volumes from across the study area; note bimodal distribution of sizes. Bottom: variation in seamount volume with distance from the GSC in the study area west of the transform fault.

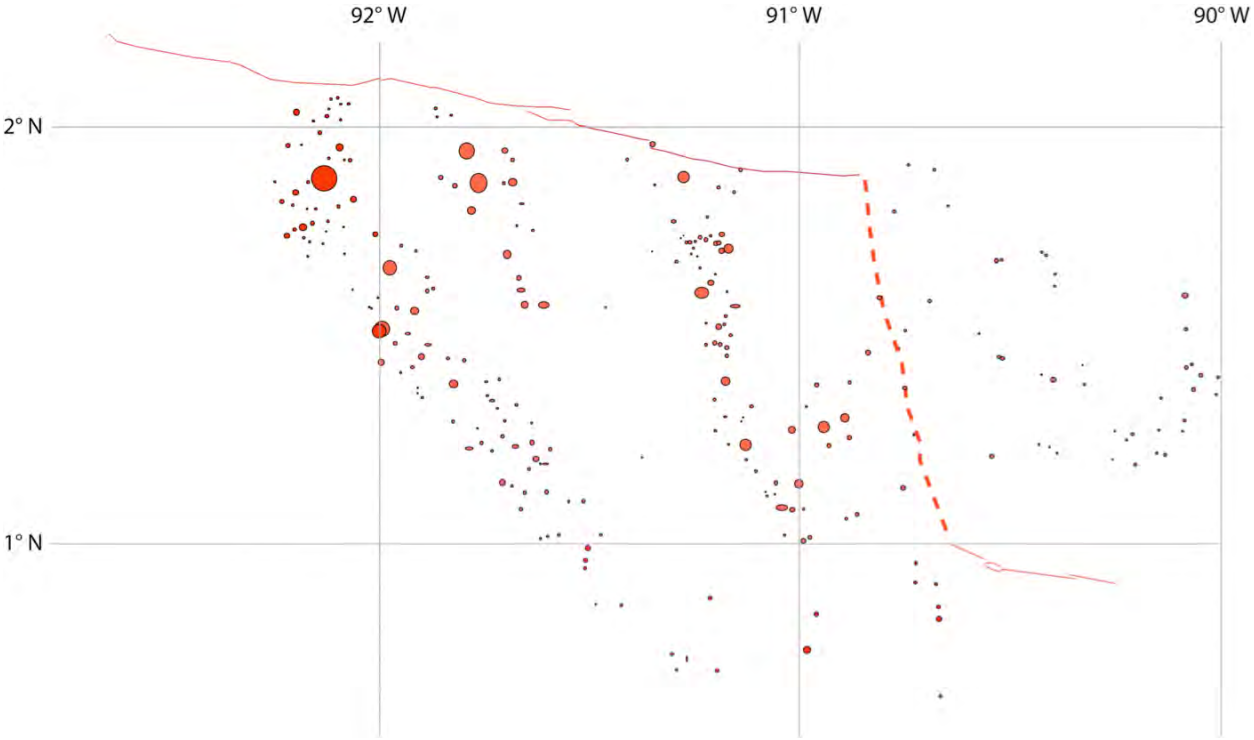

Figure 4.a.4. Map showing preliminary identification of volcanic vents.

There may be a systematic trend in the shapes of major volcanic centers; those close to the GSC have more round, symmetrical structures, whereas those farther from the ridge have increasingly elongate, preferred orientations (Figure 4.a.1). Along the WDL and possibly the smaller lineaments east of the WDL, some of the larger seamounts are arranged in a distinct en echelon pattern, similar to that observed at Genovesa Ridge. Harpp et al. (2003) proposed that this pattern reflects an extensional setting and passive magma upwelling in response to extension. This contrasts with rift zones such as the Puna Ridge, Hawaii, which have linear rift zones believed to be supplied by pressurized volcanic centers (i.e., Kilauea; e.g., Lonsdale, 1989; Clague et al., 1995; Smith et al., 2001). Such observations are particularly relevant for modeling the stress fields across the region, which will be critical for assessing our models for the influence of the transform fault in plume-ridge interaction.

Of particular note in the western study area are two prominent WNW-trending faulted ridges (Figures 4.a.1, 4.a.2). The northernmost ridge extends east from a point between Wolf and Darwin Islands and follows the proposed trace of a pseudofault that originates at the 93^{o}W propagating rift tip on the GSC (Wilson and Hey, 1995; Harpp and White, 2001). The ridges are distinct from numerous, widespread faults across the area west of the transform that are ridge-parallel, north-dipping normal faults. We successfully dredged the southernmost of the faulted ridges, collecting ultramafic rocks (dunites and harzburgites; Appendix III, Dredge 25). We anticipate that petrologic data will reveal more about the nature of these structures and their role in the tectonic evolution of the GSC and its interaction with the Galápagos plume.

ii. Transform Fault Region

The 90.5°W transform fault was thoroughly surveyed, revealing several notable features. The northern part of the transform contains several prominent volcanic cones centrally located in the deepest parts of the trough. As described above, several of these cones were sampled on previous cruises and their chemical data are available in the literature (Christie et al., 2005; Cushman et al., 2004; Detrick et al., 2002; Sinton et al., 2004). The southern half of the transform exhibits a more diffuse shear zone, shallower overall depths, and extensive evidence of volcanism in the form of numerous small cones. The southern transform trough is characterized by numerous volcanic cones that are linked to the bounding walls by narrow, relatively sharp, apparently constructional ridges (Figure 4.a.5). A dredge of a cone and a TowCam survey (TC-04) along one of the connecting ridges revealed that these are relatively young (glassy) unsedimented lavas. These may reflect a transitional setting from primarily strike-slip in the north to partially extensional in the south, with increasing volcanic activity accompanying the transition. This observation would be broadly consistent with the oblique spreading direction of the GSC near the Galápagos plume (e.g., Harpp and Geist, 2002; Taylor et al., 1994).

The entire transform fault is surrounded by a highly tectonized region that extends ~50 km from either side of the fault trough. The area is dominated by NNW-SSE trending faults, some of which (mostly west of the transform) are terminated at their western extents by small volcanic cones. Similarly, in the tectonized zone west of the southern transform fault, many of the linear features curve toward the north approximately 2-10 km beyond the fault trough. Interestingly, the GSC axis to the north and west of the transform ends abruptly at the fault, in contrast to the southern GSC axis, which clearly extends significantly west of the fault trough before trending northward. This fabric may be a reflection of the oblique spreading of the GSC coupled with an enhanced magma supply from the Galápagos plume.

Figure 4.a.5 (next page). Bathymetric map of southern part of 90.5°W transform fault. Note the numerous small cones connected by ridges to the valley walls.

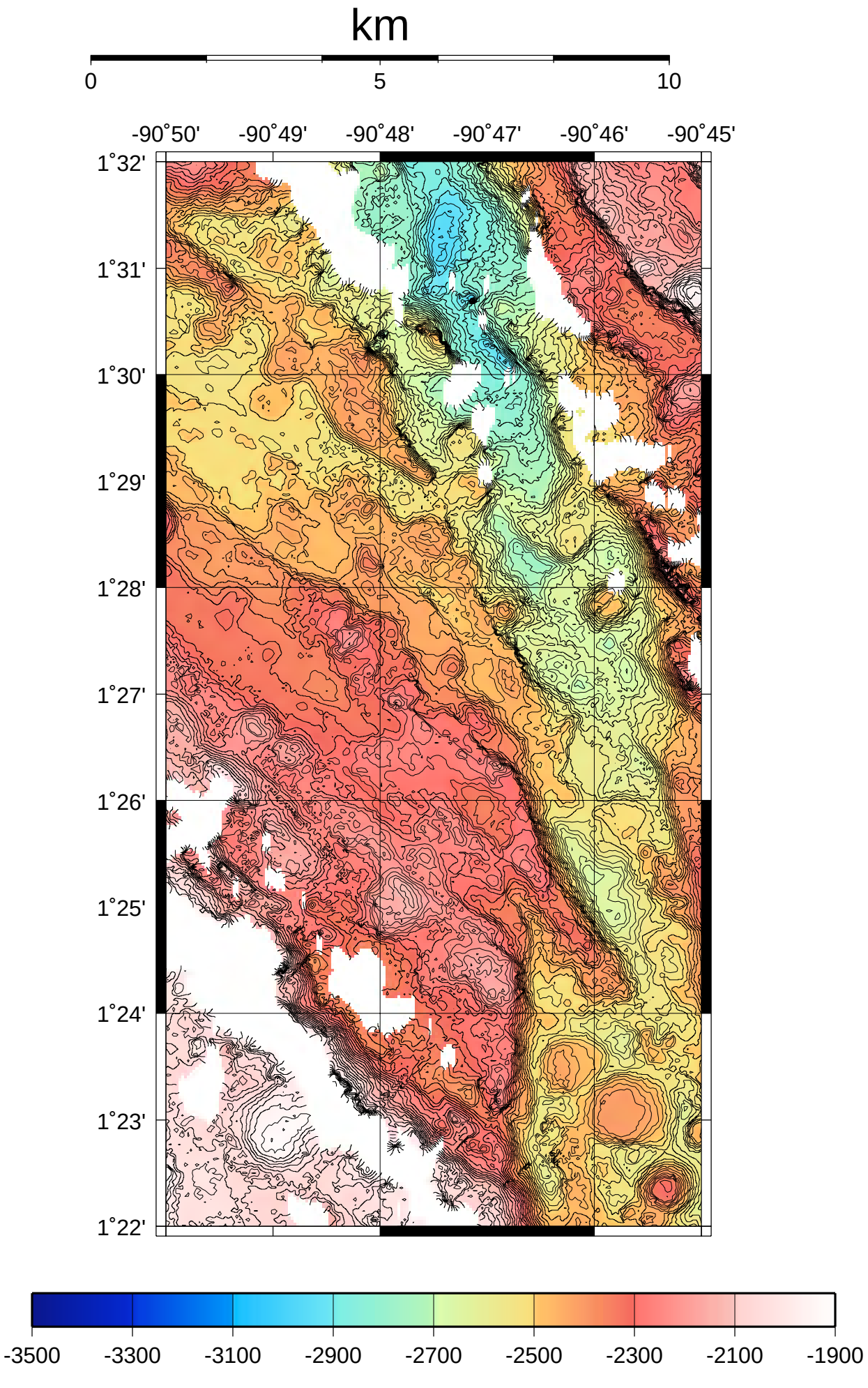
km
0
5
10
-90°50'
-90°49'
-90°48'
-90°47'
-90°46'
-90°45'
1°32'
1°31'
1°30'
1°29'
1°28'
1°27'
1°26'
1°25'
1°24'
1°23'
1°22'
-3500
-3300
-3100
-2900
-2700
-2500
-2300
-2100
-1900

iii. East of the 90.5°W Transform Fault

One of the most striking discoveries of this survey is how strongly the seafloor fabric across the study area east of the transform fault differs from that to the west (Figures 4.a.1, 4.a.2). Instead of volcanic lineaments, this area is characterized by a series of E-W and N-S structures. Five strongly reflective topographic highs are aligned across this region from SW to NE, each at the western end of more linear features that run approximately E-W. Dredging and a TowCam survey (TC-05) revealed pillow fragments and occasional volcanic glass, confirming the constructional origin of some of these structures. Our working hypothesis is that these highs and the ridges that extend from them eastward may be fossil spreading centers that document episodic GSC jumps during the formation of the transform fault ~2-3 Ma (Wilson and Hey, 1995). The areas between the tectonized and constructional seafloor appears to be thickly sedimented. We performed a N-S survey using the 3.5 kHz Knudsen sub-bottom profiler to obtain estimates on sediment cover, as well as a magnetometer survey. We anticipate that the data collected east of the transform may provide critical information toward reconstructing the development of the 90.5°W transform fault and the current configuration of the GSC and the Galápagos plume.

Numerous small, relatively flat cones with summit craters have been observed across the eastern part of the study area as well. The only major seamount in the entire eastern region is located in the NE corner and has a large caldera. Dredges from the upper and lower flanks of this structure yielded Mn-coated pillow basalts but no fresh glass, indicating a lack of recent volcanic activity. Whether this seamount represents a distinct structure from the faulted highs east of the transform remains to be determined.

iv. The Galápagos Platform Extension

Prior to our stop in Puerto Ayora, we were able to perform an EM122 and MR1 survey of the region around Pinta and Marchena Islands, the northern extension of the main Galápagos submarine platform. This area is particularly critical for documenting plume-ridge interaction, owing to the extreme trace element and isotopic compositions observed on the three islands in the area, Pinta, Marchena, and Genovesa. Pinta Island is built of some of the most isotopically enriched lavas of the entire archipelago (lowest $^{143}Nd/^{144}Nd$; Cullen and McBirney, 1987), whereas the most MORB-like, depleted signature is found at Genovesa Island (Harpp et al., 2002; Harpp et al., 2003). Marchena exhibits an intermediate geochemical composition and is located approximately midway between the other two islands (Vicenzi, McBirney et al., 1990.

Our survey revealed that Pinta has a ~30 km long ridge that extends northward from the island. This mirrors the ~50 km long ridge that extends NE from Genovesa Island, first mapped on the DRIFT04 cruise (Harpp et al., 2003). Dredges from Pinta Ridge and from the ridge that connects Genovesa and Marchena Island were glassy and plagioclase-phyric and will provide key information for understanding the distribution of plume material in this critical region.

South of Marchena, we mapped and dredged a feature unique to the northern region and possibly to the entire Galápagos Archipelago. This volcanic structure has a

strikingly flat and shallow surface, with terraced flanks spaced between 10 and 100 m relief. Dredged rocks were sufficiently rounded to suggest possible coastal zone erosion but warrant significant further investigation. Chemical and geochronological analysis will be essential to determine the nature of this structure; if it is a drowned island, it will be the farthest west of any similar structures observed in the Galápagos to date (Christie, Duncan et al., 1992).

b. Dredging

i. Rocks

Altogether, 47 sites were dredged to collect rock samples (Appendix II), and waxed steel weights were dropped at 5 other sites using the TowCam. Lavas were collected at 42 of the dredge sites and coarse-grained ultramafic rocks at one other (D25). At 4 of the dredge sites (D34, D35, D41, D45), only tiny igneous fragments, smaller than 1-2 cm^3, were recovered. At one of the dredge sites (D23), no igneous rocks were recovered. Many of the dredges included foraminifera rich carbonate sediments, which were handled as part of the biology collections.

The vast majority of the collected rocks are basalt (Appendix IV), with plagioclase as the dominant phenocryst phase. Approximately 43% of the basalts are aphyric (defined as having <1% phenocrysts), 39% contain sparse (1 to 5%) plagioclase phenocrysts, and 18% contain abundant, large plagioclase phenocrysts. All lavas are notably poor in mafic phenocrysts; only a few rocks contain phenocrysts of augite, most of which are found as glomerocrysts with plagioclase. Olivine is exceedingly sparse; only a few small grains are observed in the entire cruise suite of basalts, and they are also found as glomerocrysts with plagioclase. The notable exceptions are dredges D25, which recovered mostly ultramafic rocks, and dredge D31, which included one gabbro (D31D), discussed further below.

Several samples were “plagioclase ultraphyric basalts” (D4, D14, D26, D32, D42), which we define as lavas containing >10% plagioclase phenocrysts, some of which have a maximum dimension > 10 mm. Shipboard visual estimation of the mode of plagioclase phenocrysts (Figure 4.b.1) indicates that most of the plagioclase ultraphyric basalts sampled during the MV1007 cruise are located 50 to 80 km from the ridge axis. Interestingly, all five of the islands in the northern Galápagos are also located 50 to 80 km from of the axis of the GSC, and all contain plagioclase ultraphyric basalts.

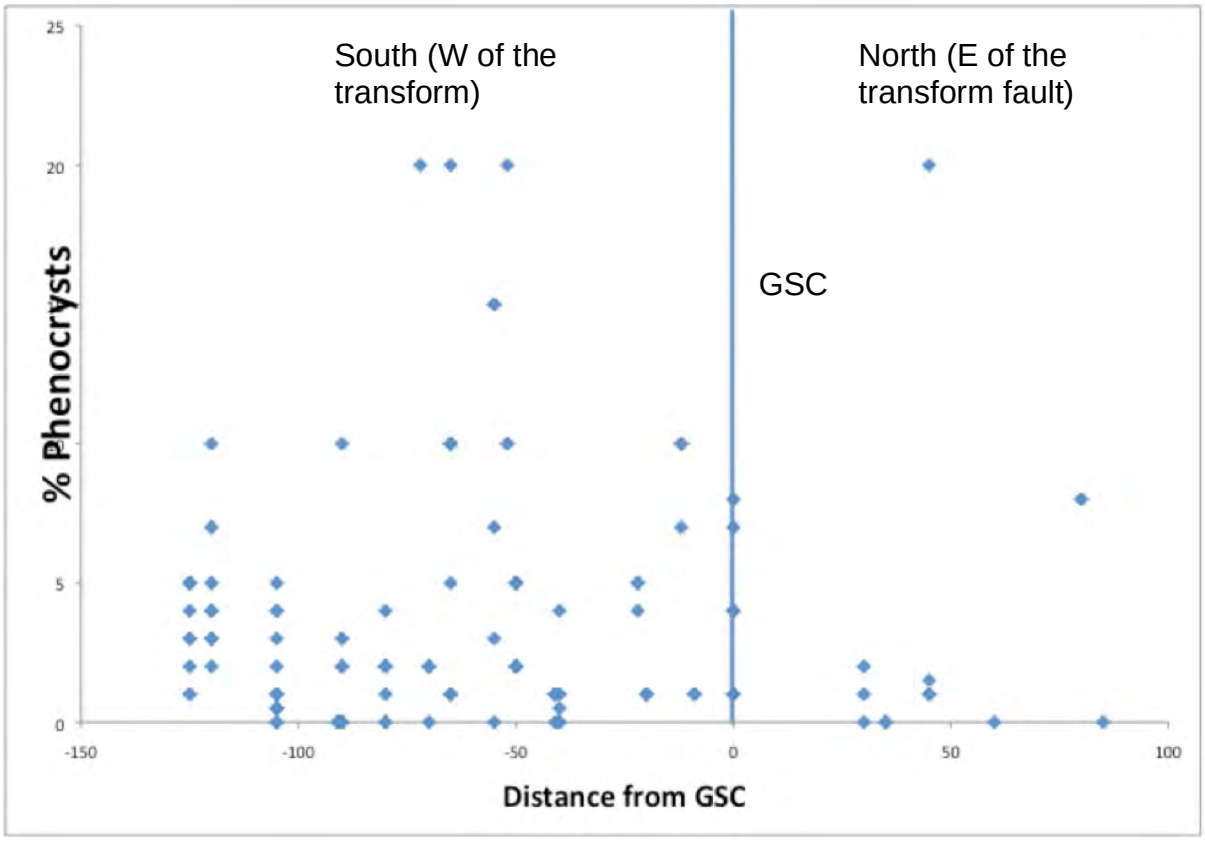

Figure 4.b.1. Mode of plagioclase phenocrysts from dredged rocks on MV1007 compared to the position of the volcano relative to the Galápagos Spreading Center; x-axis is in kilometers.

A suite of ultramafic rocks was collected at dredge site D25, including dunite, harzburgite, and putative wehrlite and pyroxenite. Sample D25B is an ultramafic rock that hosts a thin basalt vein. These are likely samples of the lower oceanic crust and upper mantle, exhumed along an east-west trending fault system (Figure 1.2), and are particularly important samples from the cruise. Sample D31D is a gabbro, in an otherwise basalt-dominated dredge, and is also probably from the oceanic crust. Gabbro was also collected in dredge 47 (samples D47A, D47B, and D47C).

All lava samples contain vesicles. Although vesicle concentration and vesicle sizes range widely throughout the suite, the maximum vesicularity correlates well with the sampling depth (Figure 4.b.2). This crude correlation is expected, as a result of the relationship between confining pressure and volatile saturation, if initial magma volatile contents are approximately similar.

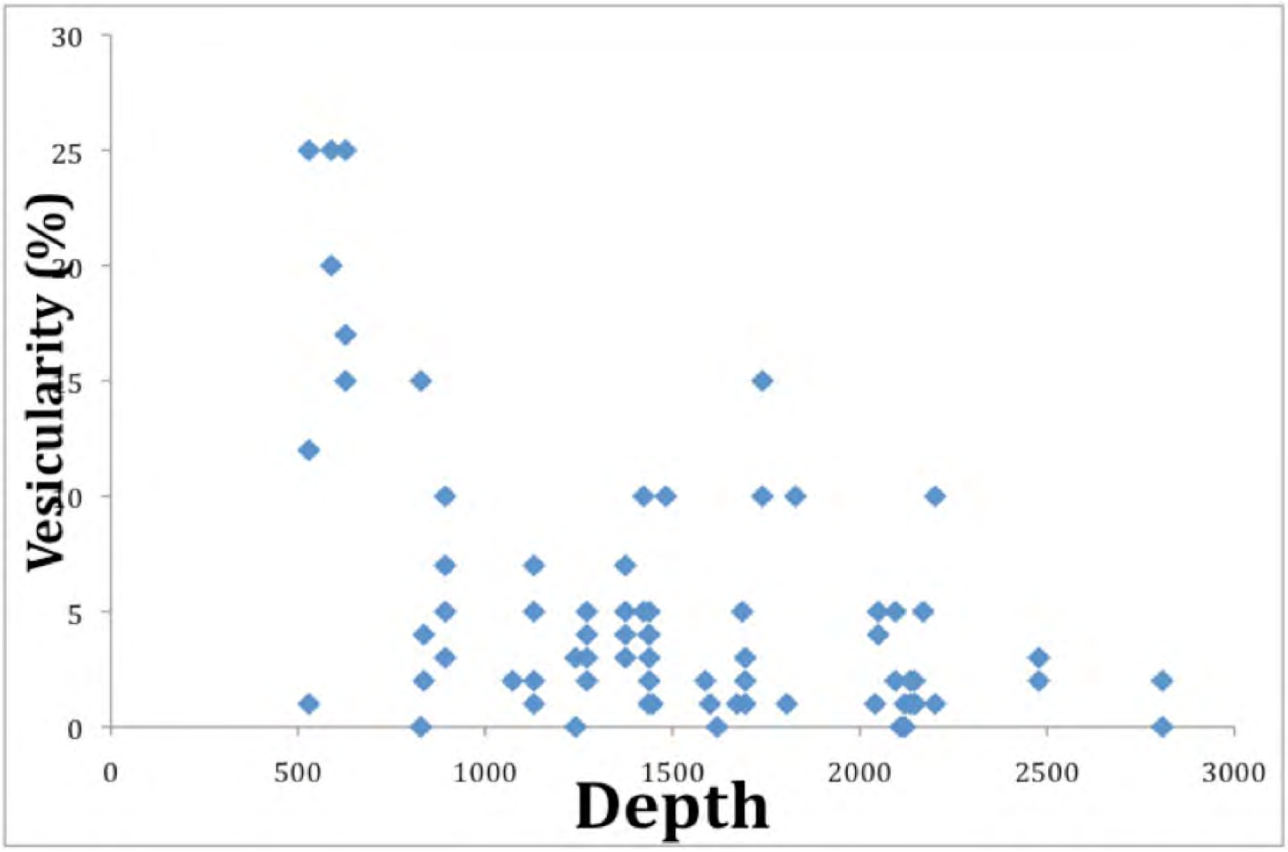

Figure 4.b.2. Maximum vesicularity of lavas sampled on MV1007 correlates negatively with depth (in meters).

Most rocks (both lavas and sediment) are covered with crusts of Mn oxide. The maximum thickness observed is 20 mm (Figure 4.b.3). Although rocks with negligible Mn-oxide crust were sampled throughout the field area, the maximum thickness clearly increases with distance from the GSC. Many of the glasses with Mn-oxide crusts include a layer of orange palagonite between the glass and the crust.

Volcanic breccias and hyaloclastites were collected in several dredges (D19G, D39A,C, D43E, and D47D) and were also heavily coated with Mn oxides. Glassy basaltic clasts were found in most of the hyaloclastites, and are 1-5 cm in size and partially rounded. Manganese oxide-coated carbonate breccia was collected in one dredge (D39D). Glassy rims were observed on a majority of the dredged basalts, but varied significantly with respect to thickness, abundance, and alteration.

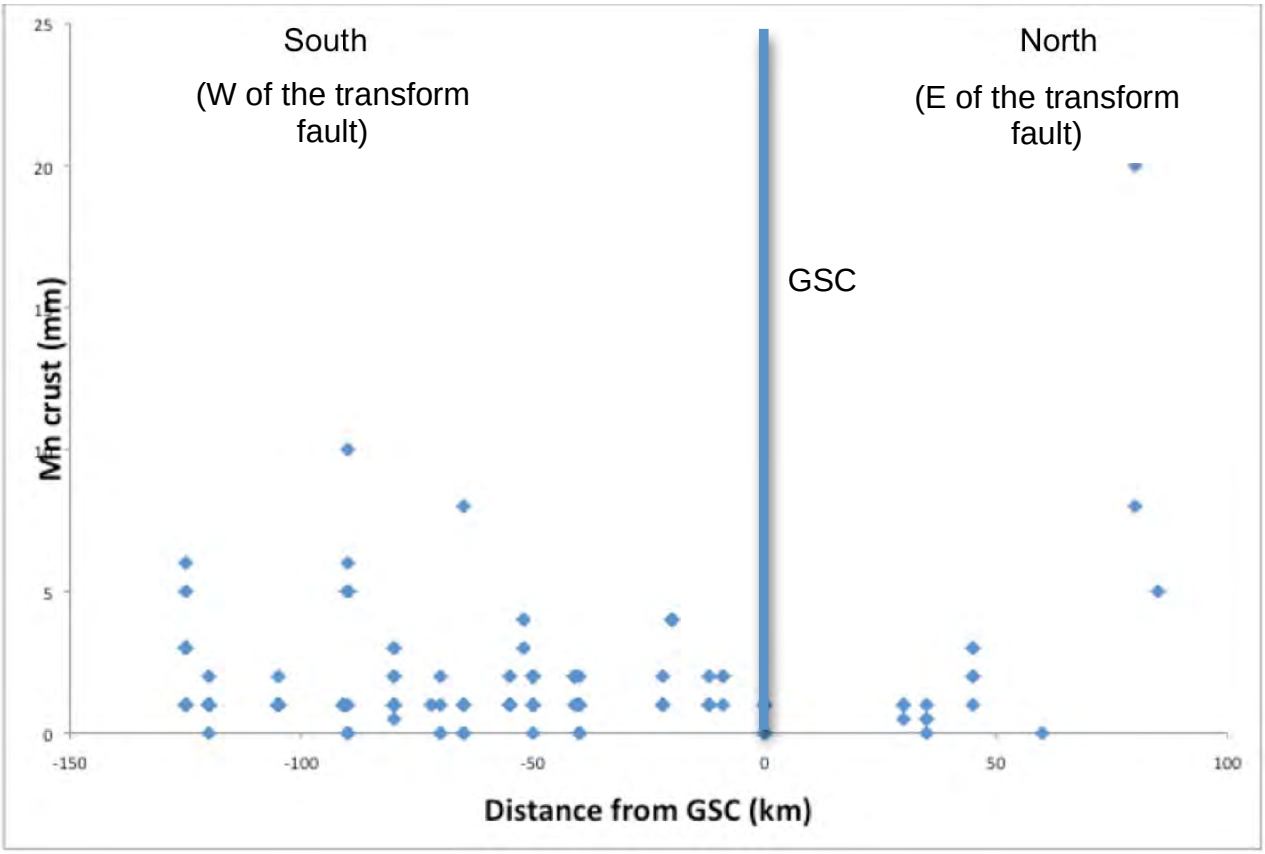

Figure 4.b.3. Thickness of Mn rind versus distance from the GSC.

ii. Biology

The MV1007 expedition has been a successful cruise for biological collections, with a total of 255 specimens recovered. All biological material was placed in chilled seawater (~10°C) immediately after removal from the dredge, and photographed (Appendices VI and VII). Specimens were preserved in either: 1) 4% formaldehyde solution; 2) 95% ethanol; 3) frozen at -85°C; or 4) dried (Appendix VI). Specimens preserved in 4% formaldehyde were transferred to 70% ethanol after 3-5 days.

Cnidarians were the most commonly collected animals on MV1007 (N=74), followed by echinoderms (N=60), arthropods (N=36), annelid worms (N=35), and sponges (N=18) (Figure 4.b.4). Small numbers of fish and salps were also obtained, although at least some of these were likely retrieved from the water column when the dredge was retrieved. The highest abundance and diversity of animals was collected at dredge station D03 (594-627 m; Appendix II) with nine brittle star species, four arthropod species, three scleractinian coral species, three octocoral species, two species of bivalves, one urchin species, and at least one polychaete species. Furthermore, multiple coral fossils and fossilized mollusk shells were collected at this station. The next most diverse dredging stations were D09 (402-589 m) and D26 (923-1073 m).

Most of the biological material collected on MV1007 was obtained through dredges at shallower depths (400-900 m; Figure 4.b.5), and collections at these depths was also most effective when normalizing for sampling effort (Figure 4.b.6).

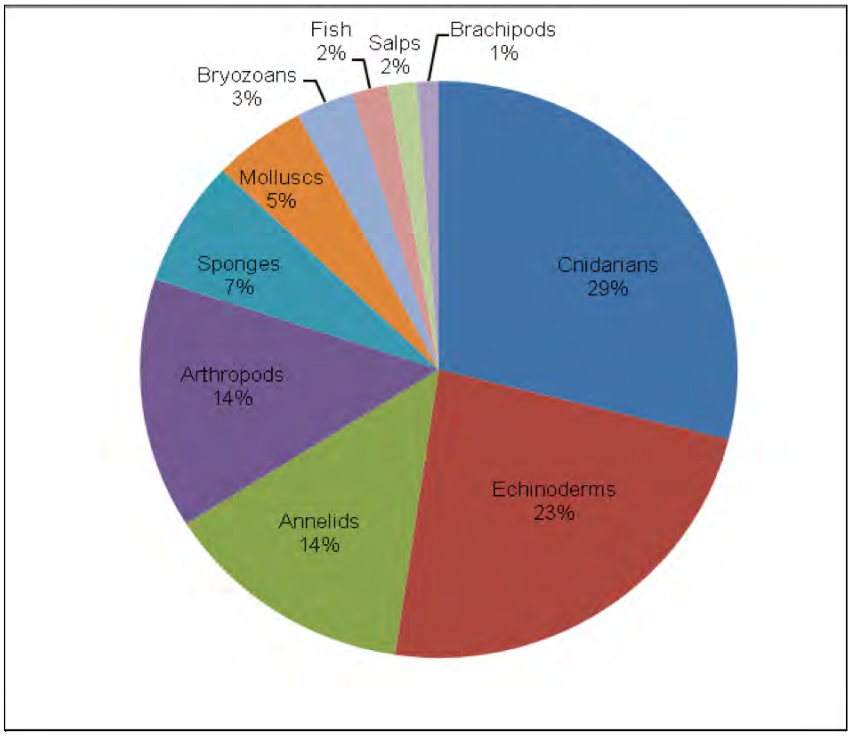

Figure 4.b.4. Number of recovered specimens by taxonomic group.

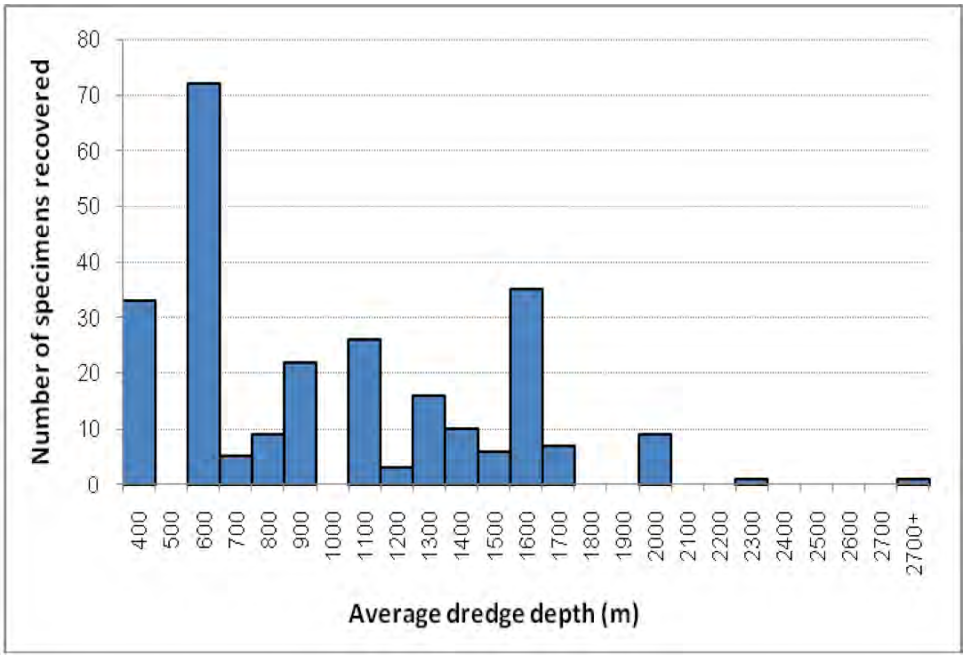

Figure 4.b.5. Number of specimens recovered by depth of dredge.

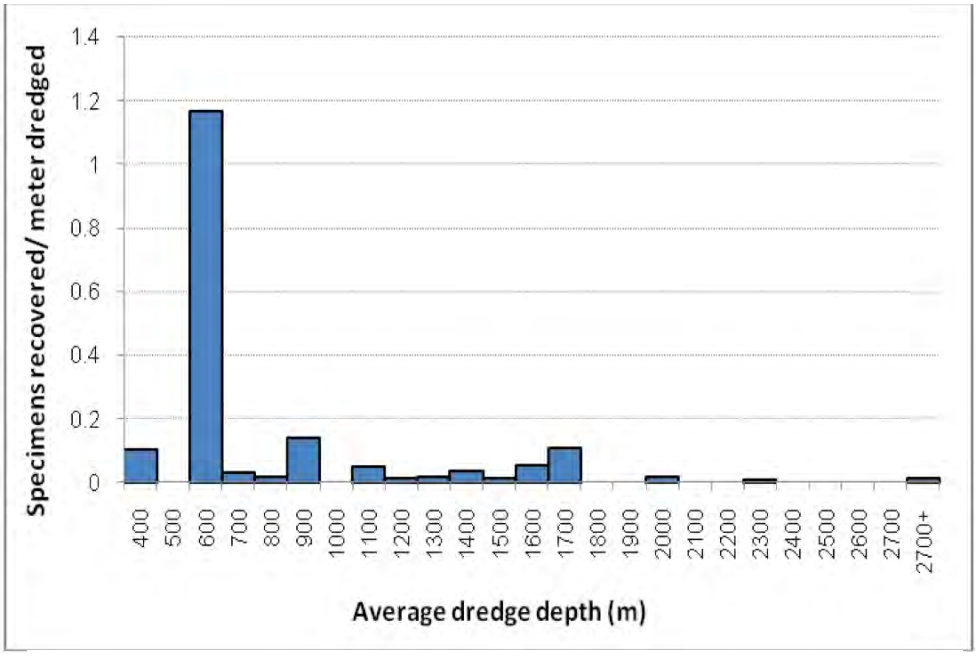

Fig 4.b.6. Number of specimens recovered per meter of seafloor dredged (assuming that all dredged slopes were gradual and continuous).

Biological specimens were collected on 31 of the total 47 dredging stations. Of the dredges where biological material was recovered, 23 were performed within the limits of the Galápagos Marine Reserve. All non-fossil samples collected within the Galápagos Marine Reserve will be returned to the Ecuador National Galápagos Collection housed at the Charles Darwin Research Station in Puerto Ayora, Santa Cruz (Appendix VI for details). The remaining specimens will be taken back to Woods Hole Oceanographic Institution for taxonomic identification and further analyses.

c. Towed Camera Surveys

A total of five TowCam surveys were performed on the cruise. Each survey was designed to address specific questions related to the origins of volcanic structures and for groundtruthing sidescan sonar data.

i. TowCam TC-00

June 2, 2010 (JD153) (10:56Z – 11:44Z)
10 sec rep rate, delay-time 10 minutes DSPL Camera s/n 6004 f-4.2

On this first lowering of the TowCam, the CTD failed at ~125 m depth. Upon recovery it was determined that one of the connectors (J2) on the SBE25 CTD (sn-316) had broken. The CTD was replaced with a spare (sn-370) and prepared for the next lowering. The pressure case battery side did not flood. The electronics side had about a tablespoon of whitish thick fluid, probably seawater mixed with silica gel. The electronics were rinsed with alcohol and dried thoroughly. There were some clearly burned components on one edge of the card stack, and in 3-4 places, the anodizing on the interior of the pressure case was eroded.

ii. TowCam TC-01

June 2-3, 2010 (JD153-154) (21:22Z – 01:55Z)
10 sec rep rate, delay-time 10 minutes DSPL Camera s/n 6004 f-4.2

This tow covered seafloor between ~750 m and 575 m depth over several terraces on the SE margin of a large submarine bank feature SE of Marchena Island. The tow was intended to traverse terrace fronts and intervening benches to determine the nature of the seafloor and distribution of benthic fauna along this slope section (Figure 4.c.1). Start point of tow was at ~0°2.7'S 90°12.4'W and end point was at ~0°1.5'S 90°13.5'W.

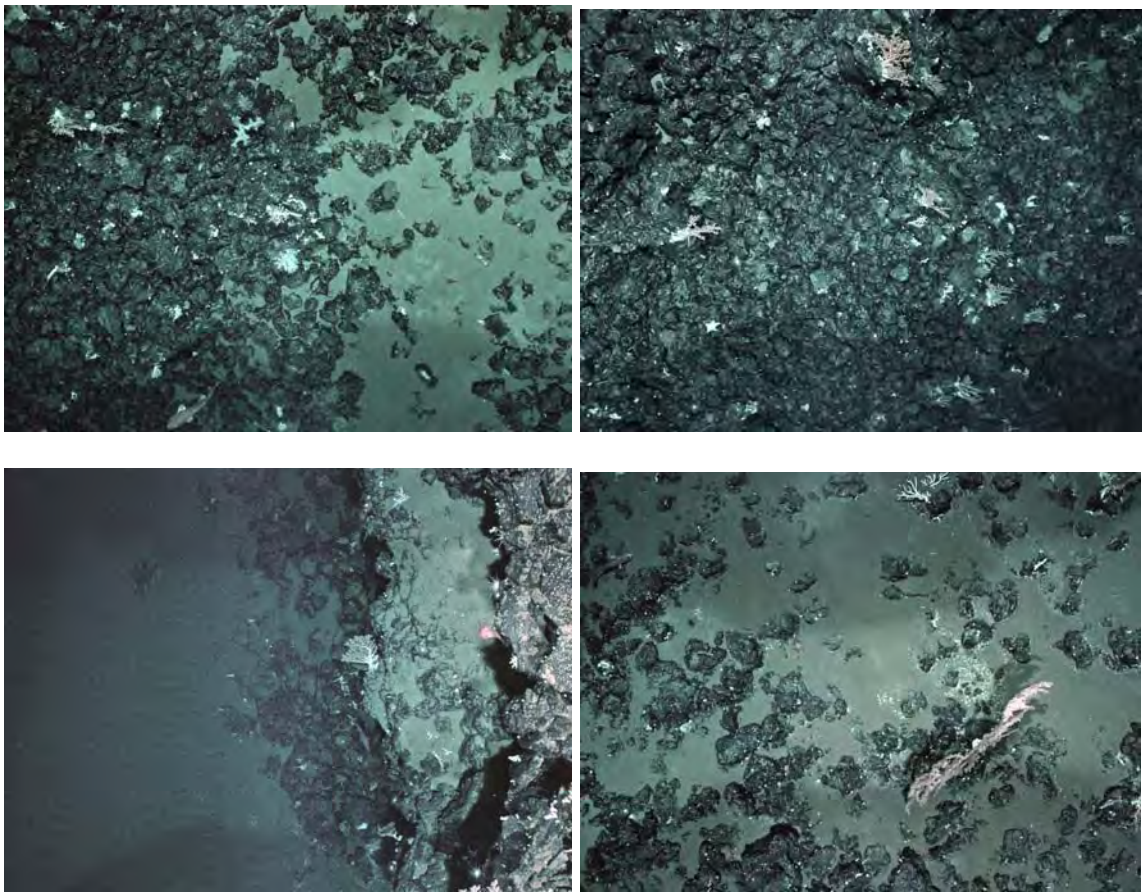

Figure 4.c.1. Selected images from TowCam TC-1 on the SE margin of the large bank south of Marchena Island. Images show variable talus with abundant sessile organisms including gorgonians, stylasteries, anemones, asteroid, fish, sponger, and stony corals. Escarpments are formed by edges of lava flows. Some ripple marks were seen at the base of the escarpments that were traversed, suggesting active current flow.

iii. TowCam TC-02

June 7, 2010 (JD158) (02:17Z – 06:48Z)
10 sec rep rate, delay-time 10 minutes DSPL Camera s/n 6004 f-4.2

This survey was designed to traverse an area at the base of a large flat-topped seamount along the Wolf-Darwin Lineament, south of Darwin Island, that was interpreted to have a lava flow ponded against the SE base of the edifice (Figure 4.c.2). The tow proceeded from SE to NW across two lobes of the flow to ground-truth the sonar interpretation. The imagery confirmed the interpretation, however, it is apparent that the flows are covered by ~0.5 to 1 m of sediment as outcrops of pillows and lobate blisters were only infrequently encountered along the track (Figure 4.c.3).

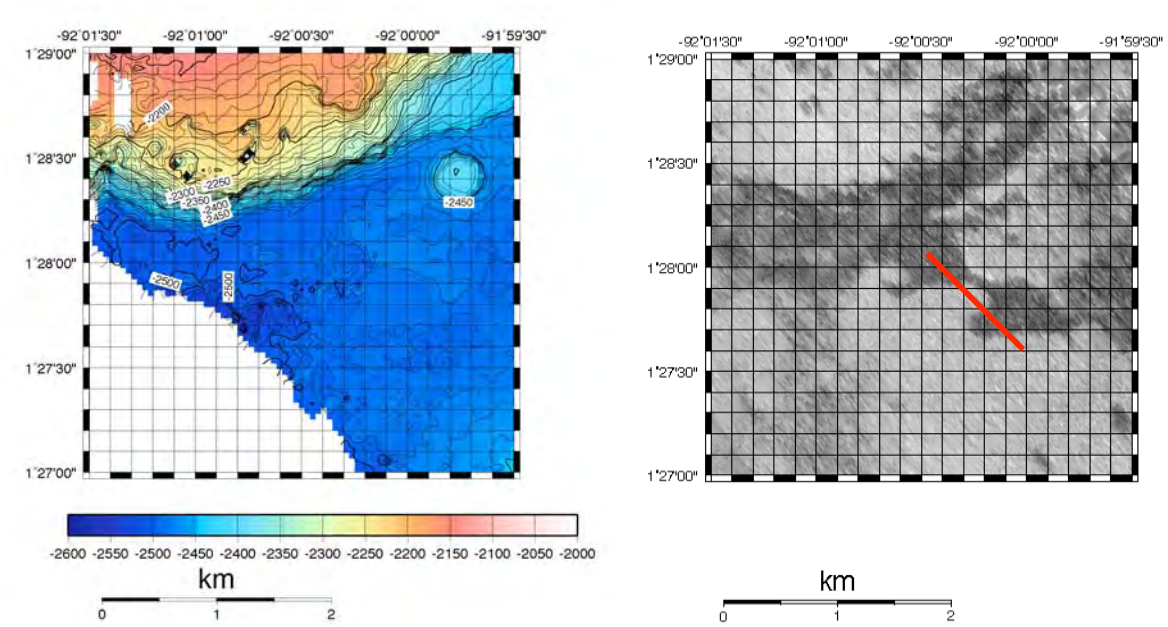

Figure 4.c.2. Multibeam bathymetry (left) and MR1 sidescan (right) maps of the area covered by TowCam TC-02 over several flow lobes identified in the sidescan data.

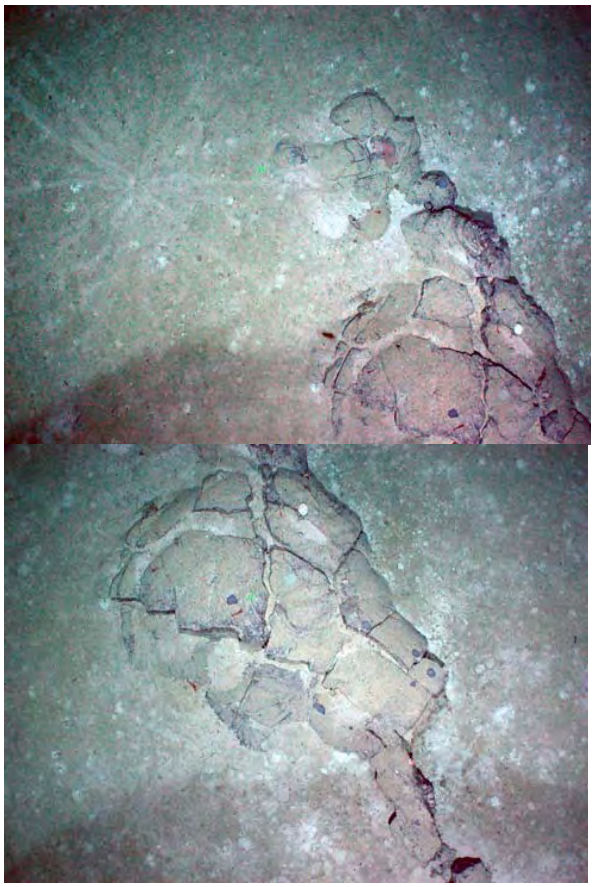

Figure 4.c.3. Examples of outcrops of large bolster-shaped pillows surrounded by variably bioturbated sediment encountered during TowCam TC-02.

iv. TowCam TC-03

June 9, 2010 (JD160) (04:50Z – 10:46Z)

10 sec rep rate, delay-time 10 minutes DSPL Camera s/n 6004 f-4.2

Tow TC-03 was designed to traverse the floor of a nested caldera on a large seamount located near 1°52.5'N and 90°17.5'W (Figure 4.c.4). This seamount is located ~5 km south of the GSC where a known high temperature hydrothermal vent is present at the axis (Haymon et al., in press).

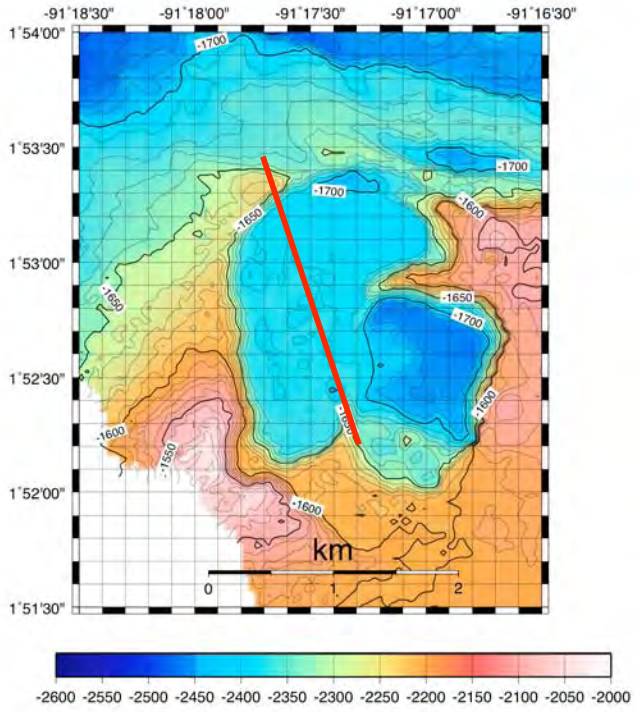

Figure 4.c.4. Multibeam bathymetry of the seamount summit nested caldera traversed during TowCam TC-03; red line shows approximate track.

The TowCam track of TC-03 extended from SE to NW along the caldera floor, encountering variably sedimented pillow terrain with sparse sessile fauna. Along the western margin of the smaller, inner nested crater, we observed apparent low-temperature hydrothermal deposits, orange/yellow in color that in places completely covered the lava terrain. We have preliminarily identified small chimneys, probably tens of centimeters high (Figure 4.c.5).

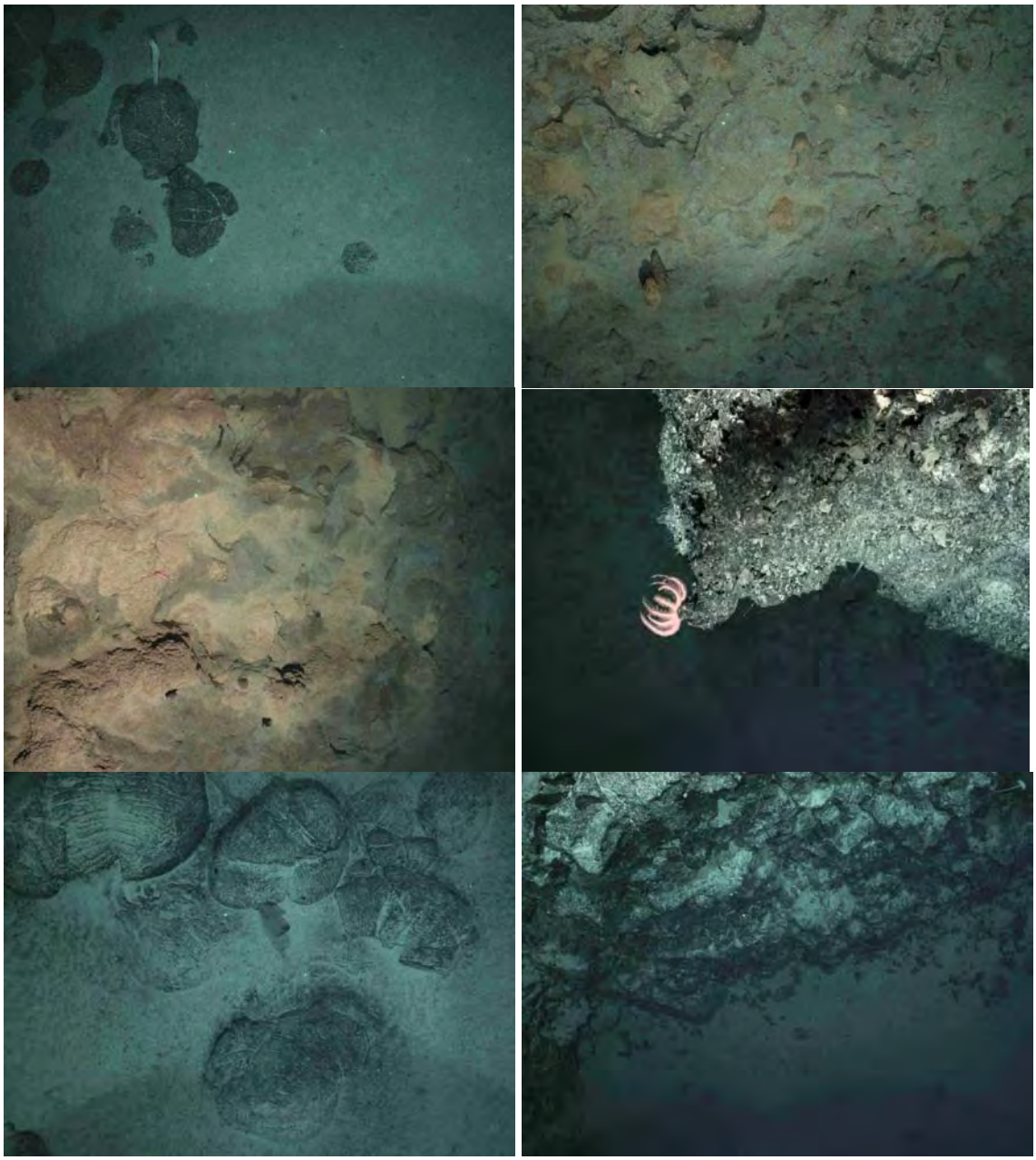

Figure 4.c.5. Photos from TowCam TC-03. Upper left: partially sedimented pillow lava along the southern margin of the inner crater at the beginning of the tow. Upper right: low-temperature hydrothermal sediment and deposits, including what appear to be small chimneys 10s of cm high in left central part of image. Center left: hydrothermal sediment completely covering lava terrain. Center right: flow front along ridge that separates the inner crater from the outer caldera floor. Lower left: sedimented pillows approaching the NW rim of the caldera. Lower right: scarp that forms the NW rim of the seamount caldera.

v. TowCam TC-04

June 11, 2010 (JD162) (17:26Z – 23:07Z)
10 sec rep rate, delay-time 10 minutes DSPLCamera s/n 6004 f-4.2

TowCam TC-04 traversed a presumed volcanic ridge along the western margin of the central 91°W transform fault (Figure 4.c.6). The ridge links the transform bounding wall on the east to a small cone, an apparently characteristic morphological element to the central and southern portion of this transform that may reflect extension within the transform domain.

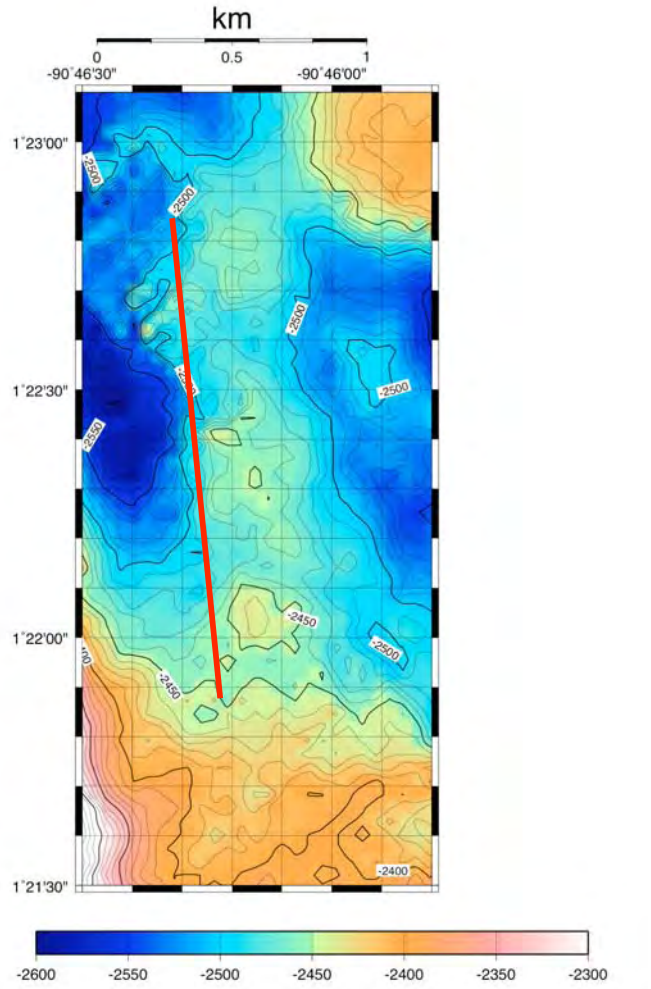

Figure 4.c.6. Track of TowCam TC-04 (red line) along a volcanic ridge that extends northward from the west margin of the 91°W transform domain.

The terrain encountered during TC-04 included extensive areas of well-formed pillow and lobate lavas as well as escarpments with broad talus slopes. One interesting feature is a series of linear structures filled with pillows that may be sites of primary eruptive fissures. The features are flanked by more heavily sedimented terrain (Figure 4.c.7). No obviously faulted terrain was encountered along the traverse, suggesting that the ridge is, indeed, constructional in origin and that these features are an important component of the transform terrain over at least half of its ~80 km length.

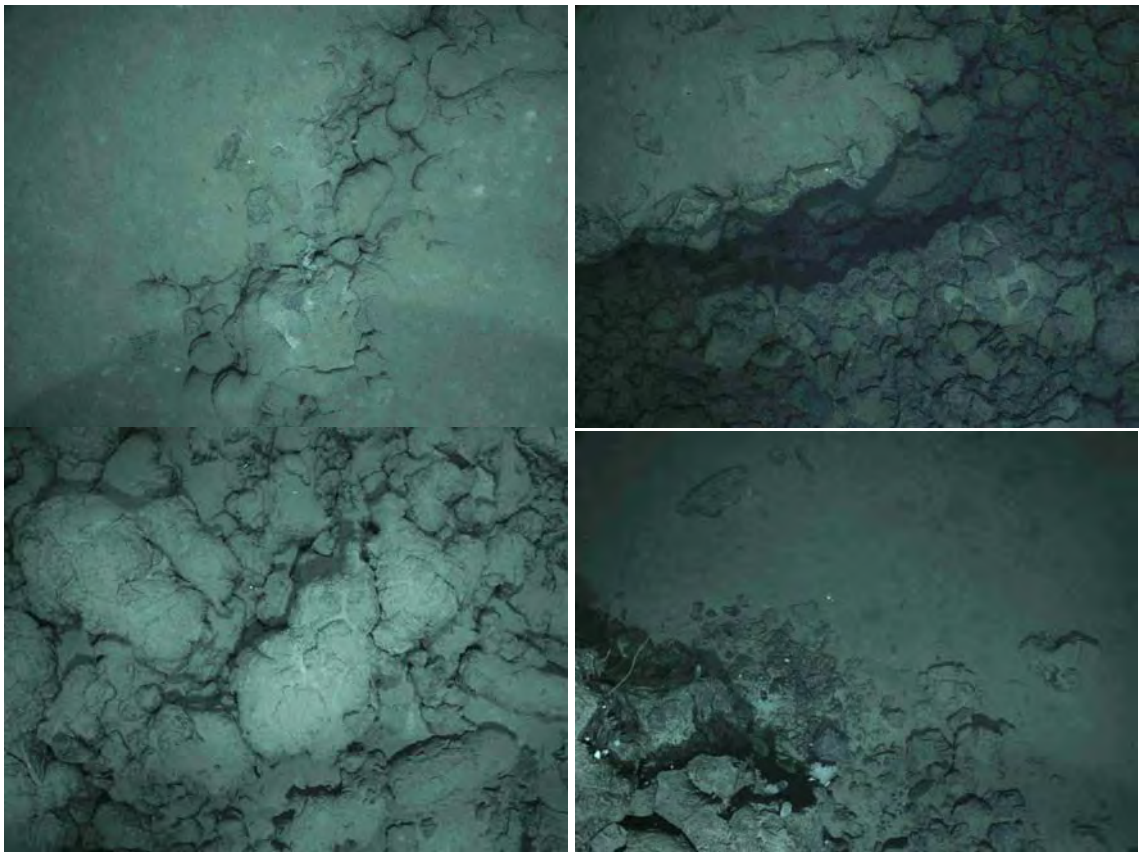

Figure 4.c.7. Photographs from TowCam TC-04. Upper left: linear fissure-like feature exposing pillows, which may be an eruptive fissure. Upper right: lobate flow and collapse margin. Lower left: well formed pillow lavas on a flow front escarpment. Lower right: flow front escarpment with numerous sessile organisms (crinoids and sponges) and talus at the base.

vi. TowCam TC-05

June 15, 2010 (JD166) (02:54Z – 04:415Z)

10 sec rep rate, delay-time 10 minutes DSPLCamera s/n 6004 f-4.2

This survey was designed to traverse a small area of the summit of Pyramid Seamount at 1°38'N and 90°15.2'W that had been sampled on Dredge D44. The total on-bottom coverage amounted to ~140 m along a heading due north, starting from the above position (Figure 4.c.8). The primary objective of the camera survey was to determine whether the highly reflective areas that characterize the ridge-like 'patterned terrain' east of the 90.5°W transform are well formed pillows or simply bare rock terrain that is more tectonic in nature. The imagery confirms that the seafloor is characterized by intact, large diameter (0.5-2 m) pillows (Figure 4.c.9) and elongate pillows with only moderate interstitial sediment between the lava forms. In a few images, faint traces of ripple marks are observed suggesting variable current activity sweeping the seamount summit.

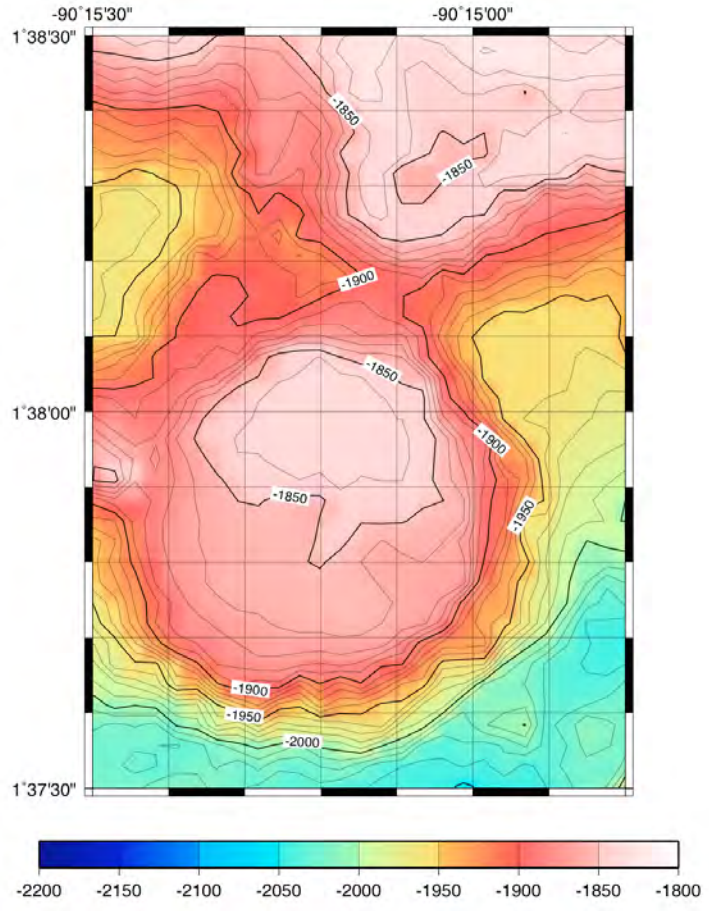

Figure 4.c.8. Map showing location of TowCam TC-05 survey on the summit of Pyramid seamount.

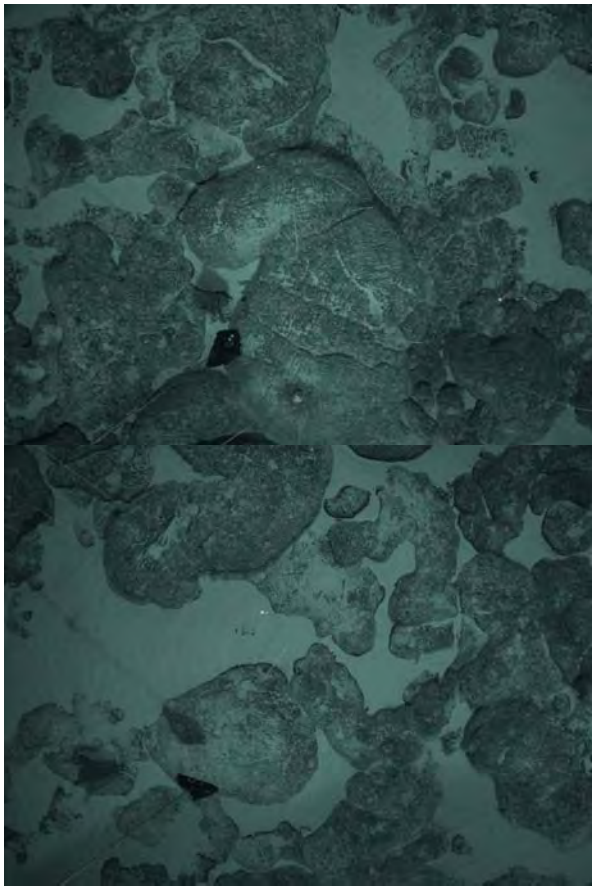

Figure 4.c.9. Images from TowCam TC-05 survey showing well formed, large pillows with sediment pockets in between the lava forms. Left image (center bottom) shows one of the wax ball rock corers that landed on the pillow surface.

d. Gravity Survey

In general, the free-air gravity anomaly data are consistent with satellite-derived gravity, but there are several significant differences. For example, two linear, northwest trending features at approximately 91.4°W, 1.2°N and 91.4°W, 1.45°N display sharper, larger signals in the BGM-3 data set than that detected in the satellite data (Figure 4.d.1). A similar difference is observed over all of the large seamounts in the study area. The MV1007 data set is considerably more precise and has greater resolution than the satellite gravity data. This precision is essential to our analysis and modeling plans that will examine the crustal thickness beneath the volcanic lineaments, the thermal structure and crustal thickness beneath the proposed fossil spreading centers east of the transform, and the variations in mantle temperature associated with plume spreading. Incorporation of gravimeter data from the PLUME02 and DRIFT4 cruises, as well as post-processing by cross-over analysis and drift removal will further enhance this preliminary data set.

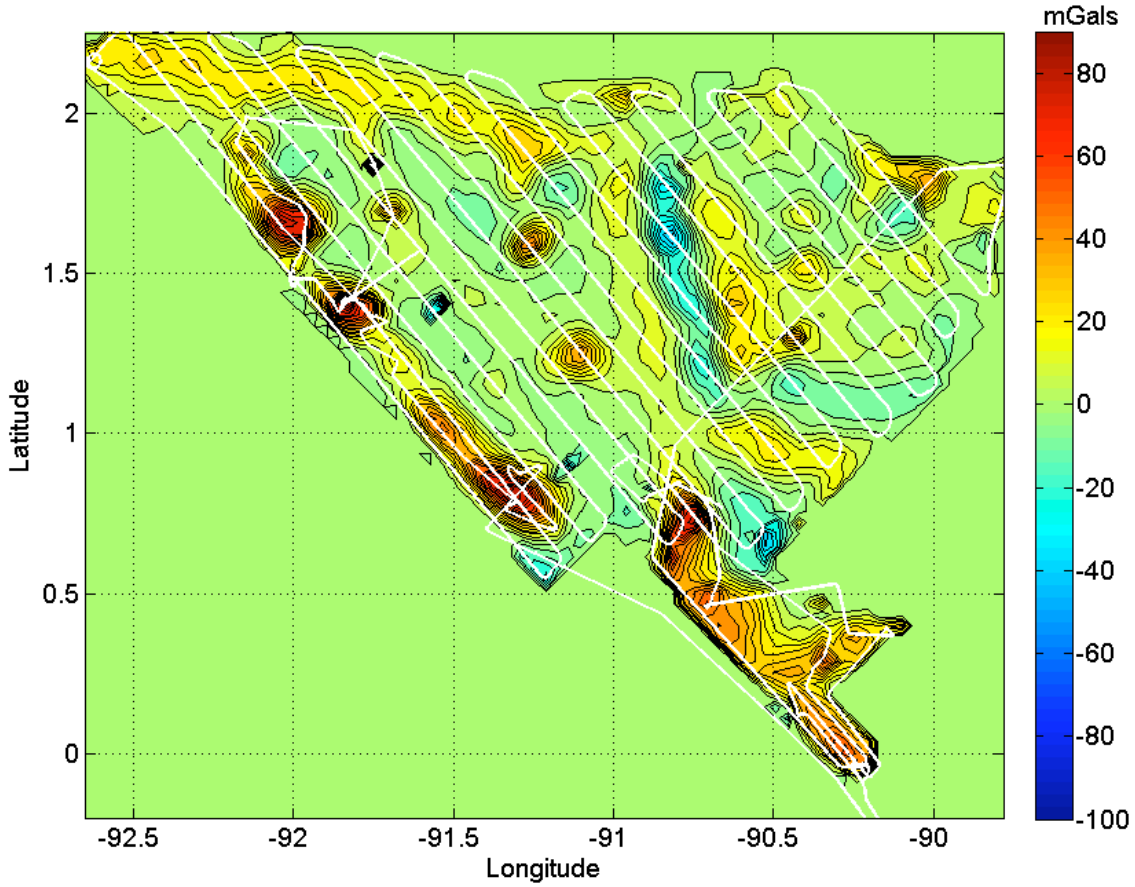

Figure 4.d.1. The free-air gravity anomaly map gridded at 5 km and track lines (white lines) of the survey through the 6th of June, 2010.

e. Magnetics Survey

Preliminary examination of the magnetometer data reveal that magnetic anomalies along the GSC axis are clearly visible to the east and west of the transform fault at 90.5°W. Off-axis anomalies are also detectable, with well-defined positive and negative polarities. The anomalies are traceable parallel to the ridge axis and should prove useful in reconstructing of ridge evolution.

To the east of the transform fault, over what may be several fossil spreading centers, the magnetic anomalies do not appear to agree with the magnetic polarity time scale expected for normal oceanic spreading. This provides support for the hypothesis that the anomalous linear features observed east of the transform are either fossil ridges or sites of anomalous, off-axis volcanism and faulting (Figure 4.e.1).

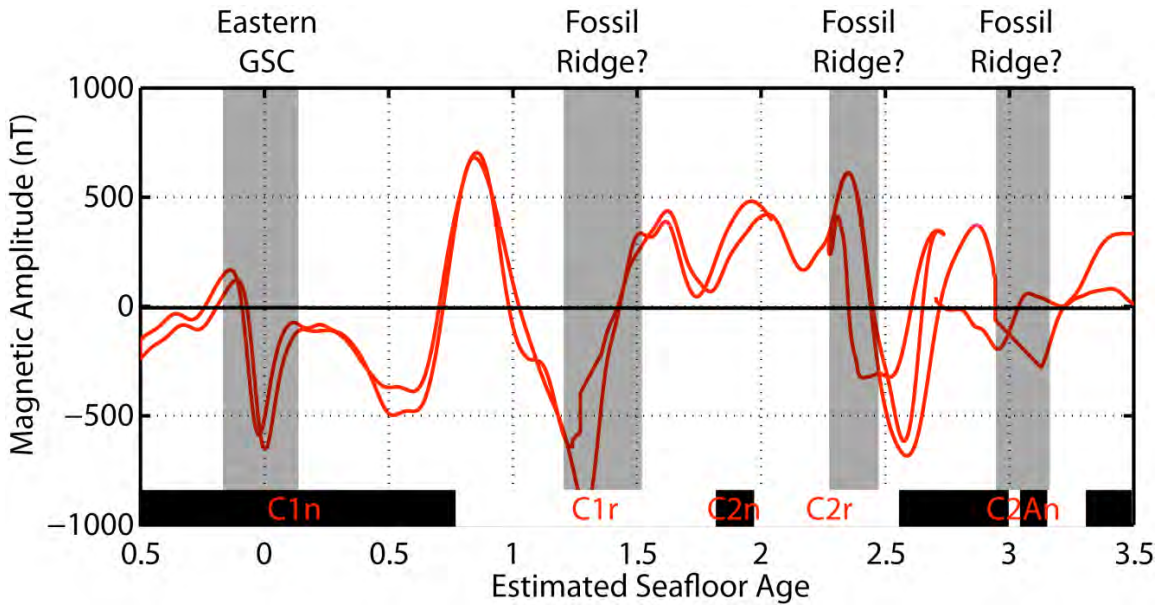

Figure 4.e.1. Changes in polarity of the observed magnetic anomalies (red lines) along a north-south transect of the proposed fossil ridge do not appear to agree with the standard magnetic polarity time scale (black and white boxes, red lettering).

f. Knudsen 3.5 kHz Sub-Bottom Profiler Survey

A north-to-south survey just east of the 90.5°W transform fault using the Knudsen 3.5 kHz sub-bottom profiler reveals a series of sedimentary basins separating each of the proposed fossil ridge axes. Several 10s of meters of sediment lie within each of the basins (Figure 4.f.1). Some of the underlying basement has an undulating pattern that may, after further analysis, be indicative of inward dipping normal faults associated with former ridge axes.

A second, short 3.5 kHz survey performed over a seamount east of the transform fault (Dredge 41, Appendix II) revealed hard returns indicating little to no sediment. This is surprising because the distance of the seamount from the ridge axis would initially indicate that it is a few million years old; with its gentle slope, there should be significant sediment accumulation on the structure. One hypothesis is that the surface of this seamount is covered in manganese-encrusted sediment, similar to some of the material dredged from this seamount.

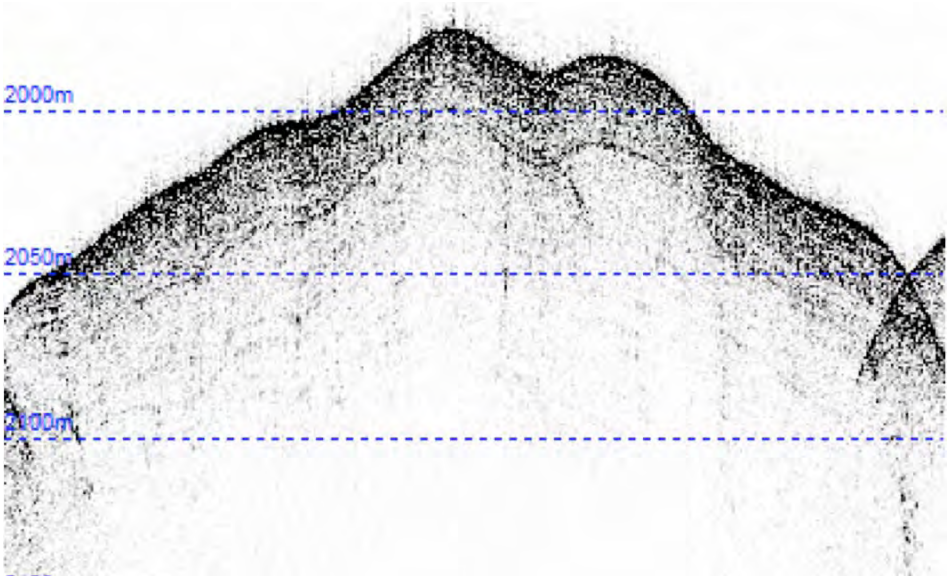

Figure 4.f.1. The sub-bottom profile near a proposed fossil ridge axis shows undulating terrain and several 10s of meters of sediments.

5. Preliminary Research Plan and Timeline

The goal of this project is to carry out an integrated geophysical and geochemical study of the Northern Galápagos Province to address two fundamental questions about plume-ridge interaction: 1) how does mantle flow occur between the hotspot and the ridge axis; and 2) what is the response of the lithosphere to plume-ridge interaction? We are taking an interdisciplinary approach by integrating bathymetric, geochemical, geochronological, and geophysical methods to investigate these questions.

1) EM122 and MR1 Data: Bathymetric and sidescan data will be used to produce a geologic map of the study area that will complement the geochemical, geophysical, and geochronological data as it is collected. A major goal will be to establish the relative timing of volcanic activity along the lineaments, at isolated seamounts, and eruptive fissures. Adam Soule and Dan Fornari (WHOI) will be the leaders of this effort, in collaboration with the participating undergraduate students (see Section 6), as well as Harpp, Geist, and Mittelstaedt. Efforts will include detailed fault mapping, volcanic cone identification, analysis of proximity of volcanoes to the GSC, hotspot, and transform, and lava flow type identification.

2) Major and Trace Element Analysis: Geochemical analysis will be accomplished using a team approach in which the undergraduates play essential roles. All representative lithologies from each dredge will be characterized for major and trace elements. Major element analysis of glasses will be carried out by electron microprobe by Dennis Geist (University of Idaho) and Marques Miller (University of Idaho student). Samples without glass will be processed by x-ray fluorescence (XRF) at Colgate University as a component of several undergraduate projects, which will include sample preparation and use of the XRF by the students. All samples will also be analyzed for trace element content

by inductively coupled plasma-mass spectrometry (ICP-MS) at Colgate by the Colgate and University of Idaho student team. Whole rock and glass samples will be dissolved using a mixture of hydrofluoric and nitric acid, then analyzed by ICP-MS using matrix-matched external standards (e.g., Harpp et al., 2003). Students will all learn to operate the ICP-MS and XRF independently. Petrographic analysis will be carried out using thin sections from representative lithologies, which we will also produce at Colgate. Our optimistic but feasible goal is to complete analyses of representative samples from all lithologic units from the cruise by the end of the fall in time for the AGU meeting in December, 2010. Geochemical data are essential to addressing the majority of the objectives of this proposal, including melt generation conditions, differentiation processes, mineral composition variations, eruptive processes, and magma source identification.

3) Isotopic Analysis: Radiogenic isotopes (Sr, Nd, and Pb) will be measured in selected samples from each dredge, in order to characterize their source characteristics (i.e., plume vs. ridge sources). This work will require acid leaching, dissolution, and ion exchange chemistry on glasses and rock chips, to separate the elements of interest. The leaching, dissolutions, and ion exchange chemistry will be carried out collaboratively at WHOI and Colgate, and the isotopic measurements will be performed by ICP-MS at WHOI with students participating under the supervision of Mark Kurz and WHOI technicians. Our objective is to have samples from the range of compositions from each dredge analyzed for radiogenic isotopes by the end of summer, 2011.

The first priority for noble gas measurements will be a survey of the dredges for helium concentrations and isotopic concentrations. We envision dividing the samples into three regional groups for the purposes of undergraduate projects: Pinta-Marchena-Genovesa area, the WDL and 2 other lineaments west of the transform fault, and the region east of the transform fault. The first step will be obtaining measurements from clean (hand picked) glasses by crushing in vacuum to extract magmatic helium. A subset of the samples may then be further analyzed by melting in vacuum to determine the abundance of the radiogenic helium for geochronology (and also to evaluate the robustness of the magmatic measurements). It may be possible to date the samples using Th-U-He, a possibility that has never been properly explored or exploited. Samples with high helium contents may be further analyzed for magmatic neon and argon, to compare their rare gas compositions to samples from the Galápagos Islands (e.g., Kurz et al., 2009).

4) Volatile Contents: Volatiles (H_2O, CO_2, S, Cl, and F) will be measured in submarine glasses from seamounts in the northern Galápagos Archipelago to constrain the mantle source, initial volatile load, and degassing history of the magmas. These components will be measured by electron microprobe and FTIR spectroscopy. These analyses will likely begin in late 2011 and constitute the post-doctoral project of Alison Koleszar, currently a graduate student at OSU.

5) Ar-Ar Age Determinations: Chris Sinton (University of Redlands) will perform the geochronological analysis at Oregon State University. Sinton was

responsible for age dating the PLUME02 samples, and thus has experience working with rocks similar to those collected during MV1007 (Sinton, Christie et al., 1996).

Careful sample selection and preparation is critical to obtain a meaningful crystallization age for submarine basalts. There are several ways that basalt can be prepared for analysis, in increasing order of complexity: mini-cores, crushed rock, or mineral separates. Mini-cores are obtained by using a 5 mm diamond coring bit in a drill press. This method works well for fresh, massive rock. Crushed rock is used for vesicular basalt that cannot be drilled or for altered basalt that will require leaching to remove secondary minerals such as clays, calcite, and zeolites. In the Northern Galápagos region, plagioclase ultraphyric rocks are common and many of the recovered basalts are of this type. These are particularly challenging because the plagioclase is typically anorthitic (and therefore has essentially no potassium) and most host melt inclusions that may contain magmatic ^{40}Ar. As a result, the plagioclase ultraphyric basalts are best prepared by crushing the whole rock and separating the groundmass for analysis. Radiometric dating will be conducted at the ^{40}Ar-^{39}Ar lab at Oregon State University (OSU).

Sample preparation will be based on information from the thin sections, which will reveal texture and degree of alteration, as well as major element geochemistry, which will indicate the amount of K_2O. Therefore, most of the radiometric dating will be conducted after initial geochemical analyses and petrographic analysis has been completed.

The timing of radiometric analysis depends on several factors and must take into account the three to four months required for sample irradiation and the subsequent “cooling” period to reduce radioactivity. Mass spectroscopic analysis requires approximately one day per sample. On the basis of these assumptions, a general timeline for acquisition of geochronology data is as follows:

July 2010: Initial five to six samples will be sent to OSU for irradiation
October 2010: Initial samples will be analyzed
Fall-Winter 2010: Remaining samples will be prepared
May-August 2011: Completion of analyses and data reduction

All sample preparation will be done by Chris Sinton. Mass spectroscopy will be performed in part by Sinton and also by the lab technician.

6) Gravity and Magnetics: Processing, analysis, and modeling of gravity and magnetic data will be the focus of the post-doctoral position of Eric Mittelstaedt at WHOI. This position is scheduled to begin in February, 2011, when work on this aspect of the project will begin in earnest. Prior to that time, Mittelstaedt will consult on geophysical and structural issues with the students working on projects during the 2010-2011 summer and academic year; he will advise students directly working during the summer of 2011 on more geophysically focused projects.

6. Undergraduate Participation and Broader Impacts

a. Undergraduate Research Program

One of the primary aspects of this project is the wholesale involvement of undergraduates in all aspects of the research and data acquisition. In addition to the collaboration between WHOI, Colgate, and the University of Idaho, we have expanded our program to include the University of Redlands, another predominantly undergraduate institution. In total, 9 undergraduates participated in the cruise (from CU: Michael Carbone, Krista Moser, Nicholas Pollock, William Cushman, Caitlin Mello, Cameron McKee, and William Schlitzer; from UI: Marques Miller; from UR: Allison Tinnin). One graduate student from Oregon State University (Alison Koleszar; see Section 5, volatiles) and a recent Colgate graduate (Gretchen Swarr) also participated. Swarr will be overseeing the analytical efforts of the undergraduates at Colgate, in her final months as a technician in training.

In the semester preceding the cruise, all students participated in a seminar on ocean island geology, led by the senior scientists on the project (Harpp, Geist, Mittelstaedt, Fornari, Kurz, Sinton, Soule, and Koleszar). We focused on previous research in the Galápagos, emphasizing the petrologic, geochemical, and geophysical methods used on the cruise, culminating in the design of individual research projects. The seminar emphasized a cooperative approach in which everyone contributed to cruise preparation, paralleling the type of scientific collaboration required for most marine geological and geophysical field efforts. Each of the senior scientists contributed to the seminar through either campus visits or videoconferences, and the group visited WHOI to help with cruise preparation and to visit the institution. Consequently, students joined the cruise equipped with an intellectual investment in the project and established collaborations with the scientists.

Over the course of the cruise, students have been involved in most aspects of the planning and execution of our objectives. Each individual designed and supervised dredges, learned how to describe and process rocks, used GMT to produce bathymetric and sidescan maps, interpreted bathymetry and sidescan data to produce geologic maps that they presented to the science party in daily meetings, participated in science planning meetings, learned some aspects of the biological sampling, and been members of watch teams while mapping. They also all crossed the equator.

During the course of the cruise, we developed the research projects for the students to pursue this summer and for the upcoming academic year as thesis projects. Students will investigate research questions substantive enough for presentation at AGU this fall (2010) yet sufficiently broad to contribute significantly to our overall research goals. Research projects will focus on interpretation of bathymetric, sidescan, and geochemical data, including:

1) Investigation of the 90.5^{o}W transform fault: This project will focus on integrating bathymetric and sidescan data analysis in the form of geologic

mapping (with an emphasis on fault identification and measurement) with geochemical data from samples dredged from inside the transform and images from a TowCam survey in the southern part of the trough (TC-04). Student researcher: Michael Carbone.

2) Analysis of tectonized fabric east of the transform: Our working hypothesis for the sequence of nearly E-W trending, highly faulted and reflective ridges that extend across the eastern study area is that they may represent fossil ridges from the formation of the transform between 2-3 Ma (Wilson and Hey, 1995) and the present. This project will focus on the integration of a detailed geologic map of these features with geochemical analysis of dredges that targeted the major bathymetric highs across the area. Student researcher: Caitlin Mello.

3) Seamount morphology: The wide range in seamount morphologies across the study area raises important questions about their origins, which will be the focus of a project that integrates analysis of seamount dimensions, development of models for their growth, and their petrologic and geochemical evolution. Student researcher: Cameron McKee.

4) Volcanic lineaments in the western study area: The origin of the WDL and the two other major lineaments west of the transform fault is a critical question in our research program. This project will consist of geochemical analysis of all dredge samples from the lineaments, which were major dredge targets on the cruise. The goal will be to interpret chemical variations in the context of spatial data, including preferred orientation of elongate seamounts and seamount volume, to develop a model for lineament formation. Helium isotopic and possibly preliminary geochronology data will be components of this work as well. Student researcher: William Cushman.

5) Investigation of the Northern Galápagos platform extension: An interdisciplinary approach will be taken to investigate the region that connects the main Galápagos Archipelago with the Northern Galapagos. This area, which is centered on Pinta and Marchena Islands, was investigated in detail on this cruise and likely plays an important role in understanding plume interaction with the GSC; trace element and isotopic data (including helium) will be essential in this investigation, in addition to spatial analysis of ridge orientations. Student researcher: William Schlitzer.

6) Melt generation and magma differentiation in the Northern Galapagos: In an attempt to constrain melt generation parameters across the region, this project will use microprobe data on glasses collected during the cruise to model depths of melt generation and crystallization. These data will inform our understanding of the origins of the major volcanic centers as well as explore the role of the lithosphere in melt generation. Student researcher: Marques Miller.

7) Exploration of a possible drowned island: The large, flat-topped, shallow seamount that is located south of Marchena has several characteristics that indicate it may have been subaerial at one time. This project will focus on integrating bathymetric and sidescan data with geochemical results from several dredges on the shoal as well as a TowCam

survey (TC-01) to determine the origin and history of this structure. Additional work will include collaboration with biologists and oceanographers at the Charles Darwin Research Station to assess the influence of the shoal on fisheries and biological communities. Preliminary Ar-Ar data will also be generated for this project in the first round of analyses. Student researcher: Allison Tinnin.

All students working this summer (those listed above) will present their work at AGU in December, 2010. Several of the students will continue their work in the summer of 2011 and into the following academic year; depending on our progress, additional undergraduates are likely to be recruited to contribute to research efforts. Projects in year 2 will incorporate geophysical data into their interpretations, with the help of Eric Mittelstaedt who will be a post-doctoral fellow at WHOI as of February, 2011.

b. Outreach

During the cruise, the undergraduate students were responsible for constructing a blog, available at http://galapagos-expedition.blogspot.com. The students shared responsibilities for the daily reports, which included explanations of their activities and duties on board, interviews with the crew, and explanations of the oceanographic technology used on the cruise. The goal of the blog, as designed ahead of the cruise during the seminar, was to develop an outreach venue appropriate for all levels of science background, with particular emphasis on younger audiences. We know from advance planning and from contact since that time that many people followed the blog on a daily basis, including several elementary school classes around the country.

One of the participating students, Krista Moser, is pursuing her teaching certification; she was the main coordinator for the blog and will be using it as a starting point for her senior project. She and an oceanographer from the Charles Darwin Research Station who participated on the cruise (Stuart Banks) will be collaborating over the next year to design a series of outreach activities for Galápagos teachers and classes. Current efforts from the CDRS are focused on the biological aspects of the Galápagos Archipelago, and one of the newest programs brings information about sharks and their migratory habits in the Northern Galápagos to the Ecuadorian schools. Krista will work with Stuart and several Ecuadorian teachers to design materials to add a geological perspective to the educational efforts of the CDRS, focusing on the role of the seamounts and flanks of the islands we have mapped during this project in the behavior of the sharks throughout the region. Krista will be emphasizing materials that can be conveyed to teachers and used in classrooms via the web, to maximize their transportability and ease of use. She will also present her work at AGU this year (2010). Should this pilot project be successful and the materials be used effectively in the Galápagos schools, we will be discussing a more long term collaboration between US teachers in training and the research station in the Galapagos, in which we will help develop educational materials to integrate geological concepts into the CDRS' ongoing outreach efforts.

c. International Collaboration

This project has resulted in two new and promising international collaborations with Ecuadorian scientific organizations. Two representatives from the oceanographic institute of the Ecuadorian Navy, INOCAR, participated in the cruise (Carlos Martillo Bustamante and Miguel Calderon Torres). Both are geologists with expertise in GIS and mapping technology and will be using data collected during the cruise for projects related to defining Ecuador's exclusive economic zone. Furthermore, through the work of Dan Fornari (WHOI) and Giorgio de la Torre (Teniente de Navío, INOCAR) over the last few months, WHOI and INOCAR have forged an agreement to collaborate on future oceanographic projects, in an effort to capitalize on complementary resources and interests.

Two oceanographers form the Charles Darwin Research Station (CDRS) in Galápagos also joined us for the cruise, Stuart Banks and Angela Kuhn. Both contributed to analysis of biological samples and assisted in other cruise efforts. All of the bathymetric and sidescan data, as well as ADCP and meteorological records from the cruise will be used by the CDRS in ongoing studies of the Galapagos Marine Reserve, a critical region in terms of biological resources. Data from the TowCam surveys will also be analyzed in detail by the station scientists, providing an unprecedented perspective on the ocean floor in this region. The bathymetric data from the WDL and the other large seamounts in the study area will contribute to ongoing studies of shark migratory behavior in the Northern Galapagos, a major focus of research by the CDRS (Cesar Penaherrera; A. Hearn, http://www.Galápagos.org/2008/index.php?id=149). Penaherrera and Harpp have collaborated for over a year on questions related to Wolf and Darwin Islands. The CDRS's recent coastline mapping data will be incorporated into the EM122 grids we are producing. This will produce maps of unprecedented precision and detail for these two islands, where only a few years ago the islands were not even properly located on navigation charts. We anticipate continuing to collaborate with the CDRS, as several of us have for decades, on projects related to this cruise and other ongoing projects.

As described above, with the involvement of a Colgate teacher in training (K. Moser), we are also embarking on a pilot project to develop educational materials to complement their ongoing program. With CDRS, we will develop materials that explain the geological aspects of the region, including the origin and evolution of the seamounts, their three-dimensional morphology, and how these relate to the unique marine ecosystem.

7. Final Word

Thanks to the impressive efforts of the R/V Melville crew, SIO personnel, HMRG personnel, the senior scientists, visiting scientists, and undergraduates, we successfully achieved all of the objectives of the MV1007 cruise, including a complete sidescan survey of the Northern Galápagos, a detailed EM122

bathymetric survey of the same area, TowCam studies of selected targets, dredge sample collection from all of the major seamounts, and gravity and magnetic data acquisition. Together, this dataset represents an unprecedented study of a potentially critical region for understanding both plume-ridge interaction and biological phenomena related to the Galápagos Islands. We anticipate an exciting few years ahead of us as we delve into the project in greater depth.

We would like to express our profound thanks to Captain Murray Stein, the R/V Melville crew, and SIO personnel on shore who have been exemplary in their effective, efficient, tireless, and enthusiastic support of our operations. We are grateful for their ongoing efforts and wish them the best in future endeavors.

8. References

Barr, J. A., K. S. Harpp, et al. (2004). "Plagioclase-Ultraphyric Basalts of the Northern Galapagos and Plume-Ridge Interaction." Eos Trans. **Jt. Assem. Suppl.**(Abstract V43C-05).

Blair, S. W., L. A. Reed, et al. (2002). "The Role of Plume-Ridge Interaction in Magma Genesis II: Wolf Island, Galápagos." Eos Trans. **AGU**(Fall Meet. Suppl., San Francisco, CA).

Christie, D. M., R. A. Duncan, et al. (1992). "Drowned islands downstream from the Galapagos hotspot imply extended speciation times." Nature **355**(6357): 246-248.

Christie, D. M., R. Werner, et al. (2005). "Morphological and geochemical variations along the eastern Galapagos Spreading Center." Geochemistry, Geophysics, Geosystems **6**(1): doi:10.1029/2004GC000714.

Clague, D. A., J. G. Moore, et al. (1995). "Petrology of submarine lavas from Kilauea's Puna Ridge." J. Petrol. **36**: 299-349.

Cullen, A. and A. R. McBirney (1987). "The volcanic geology and petrology of Isla Pinta, Galapagos Archipelago (Pacific)." Geol. Soc. Am. Bull. **98**(3): 294-301.

Cushman, B., J. Sinton, et al. (2004). "Glass compositions, plume-ridge interaction, and hydrous melting along the Galápagos Spreading Center, 90.5°W to 98°W." Geochemistry, Geophysics, Geosystems **5**(doi:10.1029/2004GC000709).

Davis, R., S. Zisk, et al. (1993). "Davis, R., S. Zisk, M. Simpson, M. Edwards, A. Shor, E. Halter, Hawaii Mapping Research

Group Bathymetric and Sidescan Data Processing, Oceans '93 Proceedings, IEEE, p. II-

449 to II-453, 1993." Oceans '93 Proceedings, IEEE: II-449 to II-453.

Detrick, R. S., J. M. Sinton, et al. (2002). "Correlated geophysical, geochemical, and volcanological manifestations of plume-ridge interaction along the Galapagos Spreading Center." Geochemistry, Geophysics, Geosystems **3**(10): 8501, doi:10.1029/2002GC000350.

Fornari, D. J. (2003). "A New Deep-sea Towed Digital Camera and Multi-rock Coring System." Eos Trans. **84**: 69, 73.

Geist, D. J., T. R. Naumann, et al. (2005). "Wolf Volcano, Galapagos Archipelago: Melting and magmatic evolution at the margins of a mantle plume." J. Petrol. **46**: 2197-2224.

Geldmacher, J., B. B. Hanan, et al. (2003). "Interaction in the Northern Galápagos Islands: Hafnium isotopic variations in volcanic rocks from the Caribbean Large Igneous Province and Galápagos hotspot tracks." Geochemistry, Geophysics, Geosystems **4**(1062): doi:10.1029/2002GC00477.

Graham, D. W., D. M. Christie, et al. (1993). "Mantle plume helium in submarine basalts from the Galapagos Platform." Science **262**(5142): 2023-2026.

Harpp, K. S., D. J. Fornari, et al. (2003). "Genovesa Submarine Ridge: A Manifestation of Plume-Ridge Interaction in the Northern Galápagos

Islands." Geochemistry, Geophysics, Geosystems **4**: doi:10.1029/2003GC000531.
Harpp, K. S. and D. J. Geist (2002). "The Wolf-Darwin Lineament and plume-ridge interaction in the Northern Galapagos." Geochemistry, Geophysics, Geosystems **3**: doi:10.1029/2002GC000370.
Harpp, K. S., V. D. Wanless, et al. (2004). "The Cocos and Carnegie Aseismic Ridges: A trace element record of long-term plume-spreading center interaction." J. Petrol. **46**(1): 109-133.
Harpp, K. S. and W. M. White (2001). "Tracing a mantle plume: Isotopic and trace element variations of Galapagos seamounts." Geochemistry, Geophysics, Geosystems **2**: 200GC00137.
Harpp, K. S., K. R. Wirth, et al. (2002). "Northern Galapagos Province: Hotspot-induced, near-ridge volcanism at Genovesa Island." Geology **30**: 399-402.
Haymon, R. M., E. T. Baker, et al. (in press). "Hunting for hydrothermal vents along the Galapagos Spreading Center." Oceanography **20**(4).
Kokfelt, T. F., C. Lundstrom, et al. (2005). "Plume-ridge interaction studied at the Galapagos Spreading Center: Evidence from 226Ra-230Th-238U and 231Pa-235U isotopic disequilibria." Earth Planet. Sci. Lett. **234**: 165-187.
Kurz, M. D., J. Curtice, et al. (2009). "Primitive neon from the center of the Galapagos hotspot." Earth Planet. Sci. Lett. **286**(1-2): 23-34.
Lonsdale, P. (1989). "A geomorphological reconnaissance of the submarine part of the East Rift Zone of Kilauea Volcano, Hawaii." Bull. Volc. **51**: 123-144.
Pistiner, J. S., K. S. Harpp, et al. (2000). "Petrographic insight into plume-ridge interactions: Genovesa's fascinating phenocrysts (Galapagos Islands)." GSA Ann. Mtg., Reno, NV: abstract 50192.
Reed, L. A., S. W. Blair, et al. (2002). "The Role of Plume-Ridge Interaction in Magma Genesis III: Darwin Island, Galápagos." Eos Trans. **Fall Meet. Suppl., San Francisco, CA**.
Rongstad, M. (1992). HAWAII MR-1: A new underwater mapping tool. *International Conference on Signal Processing and Technology, Institute of Electrical and Electronic Engineers*. San Diego, CA.
Schilling, J.-G., D. Fontignie, et al. (2003). "Pb-Hf-Nd-Sr isotope variations along the Galapagos Spreading Center (101°-83°W): Constraints on the dispersal of the Galapagos mantle plume." Geochemistry, Geophysics, Geosystems **4**(10): 8512, doi:10.1029/2002GC000495.
Schilling, J.-G., R. H. Kingsley, et al. (1982). "Galapagos hotspot-spreading center system 1: Spatial, petrological, and geochemical variations (83°W-101°W)." J. Geophys. Res. **87**: 5593-5610.
Sinton, C. W., D. M. Christie, et al. (1996). "Geochronology of Galapagos seamounts." J. Geophys. Res. **101**: 13,689-13,700.
Sinton, J., R. S. Detrick, et al. (2003). "Morphology and segmentation of the western Galapagos Spreading Center, 90.5°-98°W: Plume-ridge interaction at an intermediate spreading ridge." Geochemistry, Geophysics, Geosystems **4**(12): 8515, doi:10.1029/2003GC000609.

Smith, D. K., M. A. Tivey, et al. (2001). "Magnetic anomalies at the Puna Ridge, a submarine extension of Kilauea Volcano: Implications for lava deposition." J. Geophys. Res. **106**: 16,047-10,060.

Taylor, B., K. A. W. Crook, et al. (1994). "Extensional transform zones and oblique spreading centers." J. Geophys. Res. **99**(1707-1719).

Vicenzi, E. P., A. R. McBirney, et al. (1990). "The geology and geochemistry of Isla Marchena, Galapagos Archipelago: An ocean island adjacent to a mid-ocean ridge." J. Volcanology and Geothermal Research **40**(4): 291-315.

White, W. M., A. R. McBirney, et al. (1993). "Petrology and geochemistry of the Galapagos Islands: Potrait of a pathological mantle plume." J. Geophys. Res. **98**: 19,533-19,564.

Wilson, D. S. and R. N. Hey (1995). "History of rift propagation and magnetization intensity for the Cocos-Nazca spreading center." J. Geophys. Res. **100**: 10,041-10,056.

Appendix I: MV1007 Personnel List

Scientific Personnel

Chief Scientist: Karen Harpp
Co-Chief Scientists: Eric Mittelstaedt, Dan Fornari, Dennis Geist

Last Name	First Name	Affiliation
Calderon	Miguel	INOCAR (Leg 1)
Carbone	Michael	Colgate University undergraduate
Cushman	William	Colgate University undergraduate
Fornari	Daniel	WHOI
Geist	Dennis	University of Idaho
Harpp	Karen	Colgate University
Koleszar	Alison	Oregon State University graduate student
Kurz	Mark	WHOI (Leg 2)
Martillo	Carlos	INOCAR (Leg 2)
McKee	Cameron	Colgate University undergraduate
Mello	Caitlin	Colgate University undergraduate
Miller	Marques	University of Idaho undergraduate
Mittelstaedt	Eric	Universite de Paris Sud
Moser	Krista	Colgate University undergraduate
Pollock	Nicholas	Colgate University undergraduate
Schlitzer	William	Colgate University undergraduate
Sinton	Christopher	Redlands University (Leg 2)
Swarr	Gretchen	Colgate University undergraduate
Tinnin	Allison	Redlands University undergraduate
Wagner	Daniel	University of Hawaii graduate student
Davis	Roger	Hawaii Mapping Research Group (Leg 1)
Johnson	Paul	Hawaii Mapping Research Group (Leg 1)
Tottori	Steven	Hawaii Mapping Research Group (Leg 1)
Wanless	Dorsey	Hawaii Mapping Research Group (Leg 1)
Banks	Stuart	Charles Darwin Research Station (Leg 2)
Kuhn Cordova	Angela	Charles Darwin Research Station student (Leg 1)

R/V Melville Crew List

Last Name	First Name	Rank
Stein	Murray	Master
Hammond	Christopher	1st Officer
Turner	Melissa Ann	2nd Officer
Kirby	Jeffrey Calab	3rd Officer
Keenan	Edward	Boatswain
Sergio	Matthew	Able Seaman
Gilmartin	David	Able Seaman
Ingalls	Kent	Able Seaman
Gerhardt	Robert	OS
Buck	Richard	Sr. Cook
Martires	Leoncio	Cook
Bueren	Paul	Chief Engineer
Fitzgerald	Patrick D.	1st Assistant Engineer
Mack	Elizabeth	2nd Assistant Engineer
Navarrete	Luis Enrique	3rd Assistant Engineer
Boing	John	Electrician
Sill	Joseph Eugene	Oiler
Juhasz	Robert	Oiler
Brown	Wiliam	Oiler
Slater	Matthew	Oiler
Bouvier	William	Wiper
Kerlee	Drew	Cadet

Appendix II

MV1007 Rock Sample Collection List

	General Information:	
Dredge Number	**General location**	**Approximate Dredge Recovery**
D01	Flow boundary W of Pinta	<1/4 bag, giant pillow wrapped on cable
D02	Pinta Ridge	<1/4 bag
D03	Fractures at Pinta and Marchena	1/3 bag
D04	Seamount between Genovesa and Marchena	2/3 bag
D05	small flat cone near the SE corner of shoal S of Marchena	>2/3 bag
D06	SE corner of shoal S of Marchena	2/3 bag
D07	Upper flanks of shoal S of Marchena	>2/3 bag
D08	Southern WDL seamount base	1/4 bag
D09	Southern WDL seamount summit	2/3 bag
D10	WDL lava field S of Wolf	1/4 bag
D11	Base of Wolf	1/3 bag
D12	Mid-slope of Wolf	<1/4 bag
D13	Base of seamount on WDL near Pseudofault	1/3 bag
D14	Top of seamount near Pseudofault on WDL	1/4 bag
D15	Base of Darwin	1/3 bag
D16	Western-most drip on the GSC	1/2 bag
D17	Northern-most seamount on lineament 1	1/3 bag
D18	Second most northern seamount on lineament 1	<1/4 bag
D19	Cheerio seamount: third seamount from North on lineament 1	>2/3 bag
D20	Nubbin: fourth seamount from north on lineament 1	2 kg
D21	Tea Cup Dredge: first seamount on lineament 2, drip on GSC	1/2 bag
D22	Big Round Seamount, second seamount from north on Lineament 2	150 kg
D23	Small seamount, third from north on lineament 2	sediment only
D24	Pseudofault north, between lineament 1 and 2	handful
D25	Pseudofault south, between lineament 1 and 2	10 kg
D26	The BFS: large seamount on lineament 2, fourth from north	single rock, glass from burlap
D27	Lava field south of BFS	2 kg
D28	Wiener Seamount: small seamount east of BFS	1/4 bag
D29	Cone at ridge tip, same latitude as BFS, between BFS and transform	1 large rock (50 cm diameter)
D30	Southern of two cones dredged within the transform valley	burlap only
D31	Bbray Dos: southern inside corner high, east of transform	5 kg
D32	EPIC dredge: inside corner high, north of Bbray Dos, east of transform	<1/4 bag
D33	Northern of two cones dredged within the transform valley	three rocks, max 17 cm diameter
D34	north fossil ridge, east of transform	burlap only
D35	Lone Survivor seamount, between D34 and D36	two rocks, max 5 cm diameter

	General Information:	
Dredge Number	**General location**	**Approximate Dredge Recovery**
D36	second-nothern-most fossil ridge	25 kg
D37	southern-most fossil ridge, east of transform	5 kg
D38	east GSC drip, south of GSC	15 kg
D39	fossil ridge #3, between south fossil ridge and second from north fossil ridge	15 kg
D40	Lil Noname: seamount southwest of Noname Seamount and west of third-from-north fossil ridge	1 rock (14 cm diameter)
D41	Noname Seamount: large seamount on fossil ridge #3	burlap only
D42	Skull Mountain, seamount north of Noname Seamount	1/5 bag
D43	Redredge of Noname Seamount	70 kg
D44	Pyramid: small cone on broad high east of Noname	15 kg
D45	Tortuga: potential extension of a fossil ridge	burlap only
D46	Mount Schlitzky (summit crater), east of north fossil ridge, largest seamount in area	20 kg
D47	Base of Mount Schlitzky	handful

Dredge Number	General Description	Samples
D01	pillow and pillow fragments	A-F
D02	pillow blocks and rind	A-F, extras
D03	prismatic blocks and flow chunks	A-F, extras
D04	pillows and prismatic blocks	A-F
D05	old altered pillows	A-D, extras
D06	old altered pillows	A-D, extras
D07	old altered flow/pillow pieces, some potetially subaerial rounded cobbles	A-H, extras
D08	pillow and flow fragments	A-G, extras
D09	pillows and pillow fragments	A-E, extras
D10	pillow fragments	A-E, extras
D11	pillows and pillow fragments	A-E
D12	pillow fragment and glassy rinds	A-C, extras
D13	basalt clasts, glass, abundant sediment	A-H, extras
D14	altered basalt fragments	A-D
D15	pillow fragments	A-E, burlap
D16	pillows and pillow fragments	A-D
D17	pillow fragments	A-E
D18	basalt and glass fragments	A-D
D19	pillow and pillow fragments	A-G, extras
D20	pillow fragments	A-E
D21	basalt and Mn nodules	A-E
D22	pillow and flow fragments with green/blue alteration	A-H
D23	no rock recovery	n/a
D24	small basalt and Mn pieces, sediment	A-C, burlap
D25	breccia and ultramafic nodules, some debate on mineral IDs	A-H, extras
D26	plag ultraphyric basalt, glass	A-B
D27	basalt fragments with glass	A-D, extras
D28	ol-bearing pillow and pillow fragments	A-D, extras
D29	weathered pillow fragment	A, burlap
D30	pillow fragments and glass	A-C
D31	pillow and flow fragments, gabbroic rock	A-D, extras
D32	pillow and flow fragments, one plag-phyric fragment	A-E, extras
D33	pillow margin and rind	A-C
D34	no rock recovery	burlap
D35	Mn crusts, rock fragment	A-B

Dredge Number	General Description	Samples
D36	pillow fragments	A-B, extras
D37	aphyric fragments and glassy fragments	A-D, extras
D38	pillow fragments	A-F, extras
D39	breccia, basalt, hyaloclastite	A-E, extras
D40	flow top, weathered glass	A, burlap
D41	altered diabase	A
D42	large log-shaped prismatic fragment	A, extras
D43	prismatic pillow fragments	A-H
D44	pillow fragment	A
D45	no igneous material	n/a
D46	fine to medium grained basalt	A-E, extras
D47	gabbro and breccia fragments	A-D, extras

	On bottom:								
Dredge Number	Date (GMT)	GMT	Depth (m)	Latitude (deg)	Latitude (min)	N/S	Longitude (deg)	Longitude (min)	W/E
D01	5/31/10	20:21	2095	0	47.294	N	90	54.716	W
D02	6/1/10	4:39	1438	0	50.549	N	90	47.624	W
D03	6/1/10	17:01	627	0	27.593	N	90	42.563	W
D04	6/2/10	1:00	893	0	23.582	N	90	7.223	W
D05	6/2/10	15:57	836	0	2.719	S	90	12.111	W
D06	6/2/10	18:55	828	0	2.392	S	90	12.3	W
D07	6/3/10	3:13	529	0	2.125	S	90	14.984	W
D08	6/5/10	13:41	1600	0	52.633	N	91	17.665	W
D09	6/5/10	21:03	589	0	47.3	N	91	18.129	W
D10	6/6/10	2:58	1619	1	13.57	N	91	40.457	W
D11	6/6/10	8:31	2093	1	20.895	N	91	42.579	W
D12	6/6/10	12:06	1241	1	22.29	N	91	45.69	W
D13	6/6/10	22:50	2201	1	29.166	N	91	59.869	W
D14	6/7/10	8:34	1423	1	30.294	N	91	59.989	W
D15	6/7/10	12:33	1447	1	35.582	N	91	57.948	W
D16	6/7/10	19:29	2135	1	59.098	N	92	8.76	W
D17	6/8/10	1:30	1805	1	56.765	N	91	48.367	W
D18	6/8/10	6:14	2120	1	50.263	N	91	44.764	W
D19	6/8/10	11:21	1271	1	40.346	N	91	41.122	W
D20	6/8/10	23:02	1587	1	34.045	N	91	36.693	W
D21	6/9/10	12:19	1694	1	52.789	N	91	16.932	W
D22	6/9/10	17:14	1130	1	36.21	N	91	15.207	W
D23	6/9/10	22:14	1946	1	22.63	N	91	10.54	W
D24	6/10/10	3:14	2169	1	21.166	N	91	23.933	W
D25	6/10/10	12:31	2109	1	9.655	N	91	27.518	W
D26	6/10/10	19:16	1073	1	13.037	N	91	6.034	W
D27	6/11/10	0:57	1740	1	4.252	N	91	1.5	W
D28	6/11/10	5:45	2041	1	15.779	N	91	1.106	W
D29	6/11/10	10:08	1828	1	14.896	N	90	52.74	W
D30	6/11/10	14:42	2478	1	22.181	N	90	45.179	W
D31	6/12/10	2:11	1436	1	16.463	N	90	38.996	W
D32	6/12/10	5:36	1374	1	23.2	N	90	37.9	W
D33	6/12/10	10:16	2808	1	32.605	N	90	48.106	W
D34	6/12/10	16:53	1724	1	52.264	N	90	31.801	W
D35	6/12/10	21:49	2100	1	40.364	N	90	31.91	W

	On bottom:								
Dredge Number	Date (GMT)	GMT	Depth (m)	Latitude (deg)	Latitude (min)	N/S	Longitude (deg)	Longitude (min)	W/E
D36	6/13/10	1:55	2049	1	39.901	N	90	29.15	W
D37	6/13/10	11:24	1482	1	15.215	N	90	32	W
D38	6/13/10	18:37	2090	0	44.819	N	90	28.853	W
D39	6/14/10	2:25	1638	1	28.555	N	90	29.484	W
D40	6/14/10	5:53	1686	1	28.359	N	90	27.623	W
D41	6/14/10	10:57	1579	1	30.062	N	90	22.728	W
D42	6/14/10	15:09	1672	1	41.368	N	90	24.811	W
D43	6/14/10	19:50	1442	1	30.763	N	90	23.496	W
D44	6/15/10	0:58	1975	1	37.601	N	90	15.047	W
D45	6/15/10	7:44	1710	1	34.413	N	90	5.9786	W
D46	6/15/10	14:51	894	1	47.868	N	90	1.412	W
D47	6/15/10	17:50	1358	1	45.466	N	90	0.612	W

	Off bottom								
Dredge Number	Date (GMT)	GMT	Depth (m)	Latitude (deg)	Latitude (min)	N/S	Longitude (deg)	Longitude (min)	W/E
D01	5/31/10	22:53	1942	0	47.211	N	90	54.093	W
D02	6/1/10	6:24	1268	0	50.6	N	90	48.149	W
D03	6/1/10	17:42	594	0	27.735	N	90	42.823	W
D04	6/2/10	3:03	719	0	23.745	N	90	8.783	W
D05	6/2/10	17:38	834	0	2.423	S	90	12.288	W
D06	6/2/10	20:27	682	0	1.912	S	90	12.515	W
D07	6/3/10	5:15	430	0	1.7465	S	90	15.219	W
D08	6/5/10	15:43	1456	0	52.925	N	91	17.917	W
D09	6/5/10	22:09	402	0	47.377	N	91	18.255	W
D10	6/6/10	4:13	1428	1	13.686	N	91	40.581	W
D11	6/6/10	9:16	1987	1	20.996	N	91	42.686	W
D12	6/6/10	13:04	1072	1	22.376	N	91	45.775	W
D13	6/7/10	0:40	2013	1	29.372	N	92	0.073	W
D14	6/7/10	9:49	1349	1	30.463	N	91	0.157	W
D15	6/7/10	14:23	1261	1	35.697	N	91	58.059	W
D16	6/7/10	20:50	1891	1	59.297	N	92	8.995	W
D17	6/8/10	3:00	1670	1	56.935	N	91	48.539	W
D18	6/8/10	7:47	2120	1	50.488	N	91	44.99	W
D19	6/8/10	12:36	1003	1	40.501	N	91	41.274	W
D20	6/9/10	0:22	1464	1	34.22	N	91	36.857	W
D21	6/9/10	13:39	1600	1	52.958	N	91	16.956	W
D22	6/9/10	18:28	1070	1	36.378	N	91	15.375	W
D23	6/9/10	23:34	1835	1	22.63	N	91	10.54	W
D24	6/10/10	4:55	2002	1	21.465	N	91	24.013	W
D25	6/10/10	14:34	1900	1	9.897	N	91	27.771	W
D26	6/10/10	20:35	923	1	13.227	N	91	6.218	W
D27	6/11/10	2:37	1555	1	4.501	N	91	1.621	W
D28	6/11/10	7:00	1905	1	15.877	N	91	1.182	W
D29	6/11/10	11:04	1769	1	14.96	N	90	52.883	W
D30	6/11/10	15:57	2318	1	22.3	N	90	45.298	W
D31	6/12/10	3:16	1160	1	16.62	N	90	38.996	W
D32	6/12/10	6:50	1171	1	23.4	N	90	37.8	W
D33	6/12/10	11:27	2752	1	32.791	N	90	48.235	W
D34	6/12/10	17:53	1508	1	52.421	N	90	31.834	W
D35	6/12/10	23:18	1858	1	40.492	N	90	32	W

	Off bottom								
Dredge Number	Date (GMT)	GMT	Depth (m)	Latitude (deg)	Latitude (min)	N/S	Longitude (deg)	Longitude (min)	W/E
D36	6/13/10	3:27	1888	1	40.053	N	90	29.257	W
D37	6/13/10	12:27	1388	1	15.34	N	90	32	W
D38	6/13/10	20:23	1957	0	45.06	N	90	26.893	W
D39	6/14/10	3:26	1555	1	28.703	N	90	29.555	W
D40	6/14/10	7:16	1542	1	28.61	N	90	27.714	W
D41	6/14/10	12:04	1391	1	30.223	N	90	22.766	W
D42	6/14/10	16:49	1566	1	41.471	N	90	24.868	W
D43	6/14/10	21:31	1290	1	30.935	N	90	25.448	W
D44	6/15/10	1:43	1856	1	37.752	N	90	15.154	W
D45	6/15/10	9:20	1542	1	34.578	N	90	6.022	W
D46	6/15/10	15:55	760	1	47.994	N	90	1.486	W
D47	6/15/10	19:01	1249	1	45.634	N	90	0.673	W

Appendix III: Rock Processing Protocol

A. Fifteen minutes before dredge comes up, alert biologist for sampling.
B. When the dredge lands on deck, biologist samples any organisms, then we clean off any sediment using hose out on deck. *Never use sinks to clean the rocks.*
C. Take the rocks into lab. Never put rocks from more than one dredge on a table. If we are behind and all of the inside tables are full, keep the rocks outside on a tarp with a sheet of paper labeled with the dredge number, or buckets with a sheet of paper indicating dredge number in each bucket. Make sure that the inside table has a sheet indicating dredge number.
D. Clean the deck with the saltwater hose and brooms.
E. Sort the individual rocks by size and petrographic/lithologic type. Biggest one is called A, smallest H. If there are ~8 or more rocks and not a great deal of diversity, the extra samples will go straight into a bucket labeled “Dredge X: Extra Rock”
F. Label bags (cloth sample bags).
G. Photograph each labeled sample with a written label (the labeled sample bag can be used or a white board) indicating the sample number using the digital camera in lab. Rename the photo file by sample number (e.g., D24A.jpg)
H. Most rocks should be sawn, to render visible the crystals and their texture. A thin section billet of each lithological type should also be cut.
I. For each sample:
    i. Chip ~10 g of clean glass (preferably on the high side, for isotopes and ICP-MS).
    ii. Put most of the sample in a plastic envelope and label with sample name.
    iii. Put a few grains of glass in a labeled gel cap for volatile sample analysis, then the cap in another envelope and label with sample name.
    iv. Make a microprobe probe mount with 5-10 glass fragments, following separate directions. Take a photo of probe mount with label and re-title the file name.
J. If an important rock has no glass, chip fresh pieces (no weathered crust) about 1 cm in diameter; total volume should be the equivalent of a tennis ball. Put this in a labeled bag, adding “XRF” to the name.
K. Put additional unlettered samples in bucket labeled with dredge name.
L. Put lettered cloth bag samples in buckets, or their own bucket if too big.
M. All buckets need to be labeled on their lid and twice on the sides, once on tape with the dredge and sample numbers.

Appendix IV: MV1007 Representative Rock Types

D01A: Giant pillow basalt.

D03D: Pillow rind.

D04A: Pillow basalt toe lobe. Glassy and plagioclase-rich.

D04E: Altered pillow basalt.

D05C: Altered pillow toe lobe.

D07A: Altered vesicular pillow fragment.

D07D: Altered dense pillow fragment.

D07E: Inclusion of vesicular pillow fragment within a dense pillow fragment

D07H: Plagioclase phyric acicular lava.

D08A: Glassy radial pillow fragment.

D08E: Intricate folded flow fragment.

D08G: Flat tabular flow fragment with glass on both sides.

D10A: Prismatic pillow fragment.

D16C: Glassy pillow fragment with more plagioclase in the outer 1 cm near the rim than in the interior.

D13H: Unconsolidated sediment with Mn crust.

D19G: Hyaloclastite (photomicrograph)

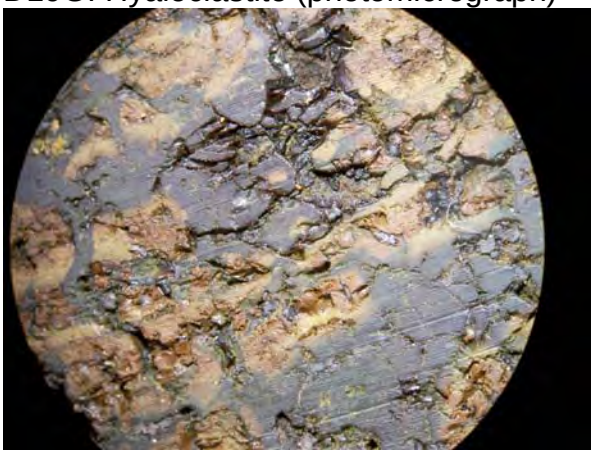

D15A: Dense pillow fragment with no glass.

D21A: Massive unfractures basalt piece with a 1 cm weathering rind.

D21D: Mn crust with red mud (likely evidence of a low temperature hydrothermal system).

D31D: Gabbroic, magnetic rock (photomicrograph)

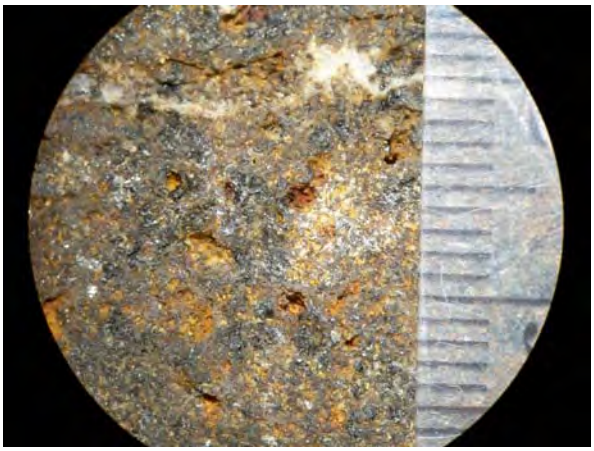

D25A: Dunite of grayish olivine with trace chromite and a thick Mn crust.

D37C: Obsidian: like glassy fragments with 10% vesicles.

D25B: Breccia with clasts of basalt.

LAND GRAVITY ABSTRACT

PORT / CITY PT CALDERA METER NO. G70 OBSERVER ERIC MITTELSTAEDT FIELD CHECKER

COUNTRY COSTA RICA FIELD BK. NO. RECORDER BUD HALE OFFICE CHKR.

VESSEL RV MELVILLE DATE 18 JUNE 2010 ABSTRACTER PAGE OF

STATION: NAME AND/OR NUMBER	LOCAL DATE	LOCAL TIME	ZULU J. DAY	ZULU TIME	Δ TIME	ELAPSED TIME	D D READING	MGAL READING	DRIFT RATE	DRIFT CORR'N	DRIFT CORR'D READING	Δ g
SHIP SIDE	6/18/10	~~13:27~~	169	~~19:27~~			1807.93	1870.18	0.0042105 MGALS/MIN	—	—	
DOD 4551-0	6/18/10	14:00	169	20:00:00	33 MIN	33 MIN	1787.24	1848.28		0.13895	1848.641	21.54
SHIP SIDE	6/18/10	14:43	169	20:43	43 MIN	76 MIN	1807.90	1870.50		0.32	1870.18	-21.54

DATE: DAY-MONTH
Δ TIME (MINS.): A→B, B→C, C→D
ELAPSE TIME (MINS.): A→B, A→C, A→D,...
D D READINGS: TO HUNDREDTHS
MGAL READINGS: TO HUNDREDTHS
DRIFT RATE: TO 6 PLACES
DRIFT CORR'N: TO HUNDREDTHS
Δ g: TO HUNDREDTHS: A→B, B→C, C→D

This Δg not used to calculate changes in the BGM-3 bias.
We used the gravity tie from DOD 4551-1 on June 18th 2010

STATION: NAME AND/OR NUMBER	N φ S	E λ W	ELEV. (meters)	g	REMARKS:
DOD 4551-0	9° 58.881	84° 46.541	11.8	978 201.52	
Ship side	9° 54.763'N	84° 43.111'W		978 223.06	(Δg added to DOD 4551-0)
BGM-3 uncorrected	9° 54.763'N	84° 43.111'W	4.3m	978223.51	(at BGM-3 height of 0.6 m above water line)
BGM-3 corrected to pier	—	—	—	978222.37	Δg = 0.69452 mGals

correction to pier = 1.14182

↑ ship side − BGM3-corrected

LAND GRAVITY ABSTRACT

PORT / CITY Port Caldera METER NO. G-70 OBSERVER Eric Miltelstaedt FIELD CHECKER

COUNTRY Costa Rica FIELD BK. NO. RECORDER Bud Hale OFFICE CHKR.

VESSEL R/V Melville DATE 18 JUNE 2010 ABSTRACTER PAGE OF

STATION: NAME AND/OR NUMBER	LOCAL DATE	LOCAL TIME	ZULU J. DAY	ZULU TIME	Δ TIME	ELAPSED TIME	D D READING	MGAL READING	DRIFT RATE	DRIFT CORR'N	DRIFT CORR'D READING	Δ g
		11:08										
Ship side	6/18/10	[illegible]	169	17:08			1808.07	1870.33	-0.001587 MGALS/MIN	-		
DOD 4551-1 Portarenas Head of pier	6/18/10	11:57	169	17:57	49 min	49 min	1802.076	1864.13		0.0777	1864.208	6.122
Ship side	6/18/10	12:40	169	18:40	43 min	92 min	1807.93	1870.184		0.1460	1870.3300	-6.122

DATE: DAY-MONTH
Δ TIME (MINS.): A→B, B→C, C→D
ELAPSE TIME (MINS.): A→B, A→C, A→D,...
D D READINGS: TO HUNDREDTHS
MGAL READINGS: TO HUNDREDTHS
DRIFT RATE: TO 6 PLACES
DRIFT CORR'N: TO HUNDREDTHS
Δ g: TO HUNDREDTHS: A→B, B→C, C→D

Current BGM-3 bias = 855320.35444
correction = + 0.302
new BGM-3 bias = 855320.65644

STATION: NAME AND/OR NUMBER	N φ S	E λ W	ELEV. (meters)	g	REMARKS:
DOD 4551-1	9° 58.4'N	84° 49.9'W	3.81	978217.22	
Ship side	9° 54.763'N	84° 43.111'W	[illegible] (4.5m)	978223.342	(Δg added to DOD 4551-1 value above)
BGM-3 observed	9° 54.763'N	84° 43.111'W		978224.77	(at BGM-3 height of 0.6m above waterline)
BGM-3 corrected to pier	—	—	—	978223.04	Δg = -0.302 mGals

correction = 1.20354 mGals

Ship side - BGM 3 corrected

```
# t1, t2, t3 are UTC times of: first pier measurement, base station measurement
# and second pier measurement (seconds since 1/1/1970 00:00:00)
t1=1273588560
1273588560
t2=1273605900
1273605900
t3=1273610340
1273610340
# p1, p2, p3 are the L&R portable gravity meter #70 measurements converted
# to mgals at first pier, base station, second pier.
p1=1861.98+7.65*1.03460
1869.89469
p2=1861.98+1.80*1.03460
1863.84228
p3=1861.98+7.84*1.03460
1870.091264
# dPg is the L&R drift correction (mgals/sec)
dPg=(p3-p1)/(t3-t1)
0.00000982543618
# dp1p2 is the difference between portable gravity meter measurements
# at t1 and t2, corrected for drift.
dp1p2=p2-dPg*(t2-t1)-p1
-6.208911863361
# h1 & h3 are the pier height (m) above sea level at t1 and t3.
h1=3.35
3.35
h3=2.43
2.43
# h2 is the pier height interpolated at t2.
h2=h1+(h3-h1)*(t2-t1)/(t3-t1)
2.6175482093664
# bh1 & bh3 are the bgm-3 height above sea level at t1 and t3.
bh1=3.04-2.44
0.6
bh3=3.96-2.44
1.52
# bh2 is the bgm-3 height interpolated at t2.
bh2=bh1+(bh3-bh1)*(t2-t1)/(t3-t1)
1.3324517906336
# gpub is the published gravity value for the tie location (DOD 4551-1).
gpub=978217.22
978217.22
# gpier is calculated gravity at the pier at t2.
gpier=gpub-dp1p2+h2*0.3
978224.2141755
# gbgm3obs is the observed smoothed bgm-3 gravity at t2.
gbgm3obs=978214.86
978214.86
# gbgm3 is the bgm-3 gravity at t2 corrected to sea level.
gbgm3=gbgm3obs+bh2*0.3
978215.2597355
# oldbgm3offset is the old offset value (11/2003) used to calculate
# gbgm3obs.
oldbgm3offset=855311.4
855311.4
# bgm3offset is the correction to apply to the old offset to match pier gravity.
bgm3offset=gpier-gbgm3
8.954448826195
# newbg3offset is the new offset value for bgm-3 #224.
newbg3offset=oldbgm3offset+bgm3offset
855320.35444
```

Gravity Tie

at Head of Pier in Puntarenas, Costa Rica

4.9826266

11 May 2010

Appendix VI: MV1007 Table of Collected Biological Specimens

Station	Phylum	Species ID on ship	Frozen	EtOH	Formalin	Dry	Fate
MV1007-D01	Porifera	Tube sponge			2		CDF
MV1007-D01	Annelida	Polychaete			1		CDF
MV1007-D01	Cnidaria	Small anemone			1		CDF
MV1007-D01	Cnidaria	Fossil Scleractinians				2	CDF
MV1007-D02	Cnidaria	Fan-shaped scleractinian			1		CDF
MV1007-D02	Cnidaria	Gorgonian fragments			4		CDF
MV1007-D02	Porifera	Assorted sponges (3 different)			3		CDF
MV1007-D03	Cnidaria	Flabellum sp.	28 (1 bag)				CDF
MV1007-D03	Cnidaria	Madrepora oculata	2 bags				CDF
MV1007-D03	Cnidaria	Green Primnoid octocoral			1		CDF
MV1007-D03	Cnidaria	Gorgonian			1		CDF
MV1007-D03	Arthropoda	Crustacean#1		2			CDF
MV1007-D03	Arthropoda	Crustacean#2		4			CDF
MV1007-D03	Arthropoda	Crustacean#3		5			CDF
MV1007-D03	Arthropoda	Crustacean#4		1			CDF
MV1007-D03	Echinodermata	Urchin (2 large and 1 small)	3				CDF
MV1007-D03	Mollusca	Bivalve#1	5				CDF
MV1007-D03	Mollusca	Bivalve#2	5				CDF
MV1007-D03	Cnidaria	Golden axis gorgonian fragments	1 bag				CDF
MV1007-D03	Annelida	Assorted polychaetes			6		CDF
MV1007-D03	Echinodermata	Assorted ophioroids			9		CDF
MV1007-D03	Cnidaria	Colonial scleractinian fossils				5 bags	LFR
MV1007-D03	Cnidaria	Solitary scleractinian fossils				1 bag	LFR
MV1007-D03	Mollusca	Mollusk fossils				1 bag	LFR
MV1007-D04	Annelida	Assorted polychaetes			2		CDF
MV1007-D04	Porifera	Yellow sponge	1 bag				CDF
MV1007-D04	Porifera	White sponge	1 bag				CDF
MV1007-D05	Cnidaria	Golden axis gorgonian (2 fragments)	1 bag				CDF
MV1007-D05	Chordata	Assorted sea squirts			3		CDF
MV1007-D06	Cnidaria	Tanacetipathes sp. w/galatheid crab		1	1		CDF
MV1007-D06	Annelida	Polychaete			1		CDF
MV1007-D06	Porifera	Glass sponge	1 bag				CDF
MV1007-D06	Cnidaria	Coral fragment	1 bag				CDF
MV1007-D07	Cnidaria	Solitary scleractinian			1		CDF
MV1007-D07	Vertebrata	Fish	1				CDF
MV1007-D07	Arthropoda	Shrimp	1				CDF
MV1007-D07	Porifera	Sponge #1	1 bag				CDF
MV1007-D07	Porifera	Sponge #2	1 bag				CDF
MV1007-D09	Porifera	Barrel sponge			1 vial		CDF
MV1007-D09	Porifera	White sponge			1 vial		CDF
MV1007-D09	Echinodermata	Holothurian		3			CDF
MV1007-D09	Echinodermata	Asteroid	1 → Formalin				CDF
MV1007-D09	Vertebrata	Fish			1		CDF
MV1007-D09	Annelida	Assorted polychaetes			12		CDF
MV1007-D09	Echinodermata	Urchin (no spines left)			1		CDF
MV1007-D09	Arthropoda	Crustacean	1 → ETOH				CDF
MV1007-D09	Mollusca	Brachiopod			1		CDF
MV1007-D09	Cnidaria	Primnoids			2		CDF
MV1007-D09	Cnidaria	Colonial scleractinian	1 → Formalin				CDF
MV1007-D09	Cnidaria	Hydroids			1		CDF
MV1007-D09	Cnidaria	Stylasterids	1 → ETOH				CDF
MV1007-D09	Cnidaria	Colonial scleractinian fossils				1 bag	LFR

Station	Phylum	Species ID on ship	Frozen	EtOH	Formalin	Dry	Fate
MV1007-D10	Cnidaria	Pink octocoral (Corallium?)	1 → ETOH				CDF
MV1007-D10	Echinodermata	Ophioroid			1		CDF
MV1007-D12	Bryozoa	Bryozoan				1 bag	CDF
MV1007-D12	Echinodermata	Assorted ophioroids			2		CDF
MV1007-D12	Porifera	Assorted sponge fossils				1 bag	LFR
MV1007-D12	Cnidaria	Fan-shaped stylasterid	1 → ETOH				CDF
MV1007-D15	Cnidaria	Anthozoan fossils				1 bag	LFR
MV1007-D15	Porifera	Sponge			1 bag	1	CDF
MV1007-D15	Echinodermata	Ophioroid			1		CDF
MV1007-D15	Cnidaria	Assorted stylasterids	1 → ETOH				CDF
MV1007-D18	Echinodermata	Ophioroid			1		CDF
MV1007-D19	Cnidaria	Anemone?			1		CDF
MV1007-D19	Porifera	Assorted sponges			1		CDF
MV1007-D19	Bryozoa	Bryozoan fossils				1 bag	LFR
MV1007-D19	Brachipoda	Brachiopod			1		CDF
MV1007-D19	Arthropoda	Assorted crustaceans (3 different)			3		CDF
MV1007-D19	Cnidaria	Stylasterid			1		CDF
MV1007-D20	Echinodermata	Ophioroid			1		CDF
MV1007-D20	Echinodermata	Urchin			1		CDF
MV1007-D21	Cnidaria	Golden axis gorgonian				fragment	CDF
MV1007-D21	Echinodermata	Ophioroid			3		CDF
MV1007-D21	Arthropoda	Galatheid crab		1			CDF
MV1007-D21	Annelida	Tubeworm? (tube only)			1		CDF
MV1007-D22	Porifera	Sponge				1 fragment	CDF
MV1007-D22	Porifera	Assorted sponges			1		CDF
MV1007-D22	Echinodermata	Assorted ophioroids			6		CDF
MV1007-D22	Bryozoa	Bryozoans (large)				1	CDF
MV1007-D22	Arthropoda	Isopod		1			CDF
MV1007-D22	Chordata	Salp			1		CDF
MV1007-D22	Cnidaria	Assorted stylasterids		1 vial			CDF
MV1007-D22	Bryozoa	Bryozoan (long)			1		CDF
MV1007-D22	Brachipoda	Brachiopod			1		CDF
MV1007-D25	Arthropoda	Shrimp			1		CDF
MV1007-D25	Cnidaria	Fossil coral				1 bag	LFR
MV1007-D26	Cnidaria	Alcyonacean			1		CDF
MV1007-D26	Cnidaria	Primnoid			1		CDF
MV1007-D26	Bryozoa	Large white bryozoan				1 bag	CDF
MV1007-D26	Annelida	Polychaete			2		CDF
MV1007-D26	Cnidaria	Stylasterid				1	CDF
MV1007-D26	Bryozoa	Bryozoan				1 bag	CDF
MV1007-D26	Porifera	Sponge			1		CDF
MV1007-D26	Annelida	Nermetean worm			6		CDF
MV1007-D26	Echinodermata	Assorted ophioroids			4		CDF
MV1007-D26	Cnidaria	Flabellum sp.? (fragments)			1 bag		CDF
MV1007-D26	Arthropoda	Assorted crustaceans (3 different)		3			CDF
MV1007-D26	Arthropoda	Snail			1		CDF
MV1007-D27	Echinodermata	Urchins			5		CDF
MV1007-D27	Echinodermata	Assorted ophioroids		4			CDF
MV1007-D27	Annelida	Nermetean worm			1		CDF
MV1007-D27	Brachipoda	Brachiopod		1			CDF
MV1007-D27	Mollusca	Chiton		2			CDF
MV1007-D29	Cnidaria	Small solitary scleractinian		1			CDF
MV1007-D29	Porifera	Assorted sponges			1 vial		CDF

Station	Phylum	Species ID on ship	Frozen	EtOH	Formalin	Dry	Fate
MV1007-D29	Echinodermata	Assorted ophioroids (2 different)			2		CDF
MV1007-D29	Cnidaria	Assorted sylasterids		1 vial			CDF
MV1007-D29	Annelida	Nermetean worm			1		CDF
MV1007-D29	Echinodermata	Holothurian			1		CDF
MV1007-D30	Annelida	Polychaete			1		CDF
MV1007-D31	Bryozoa	Bryozoan				1	CDF
MV1007-D31	Echinodermata	Assorted ophioroids (2 different)			2		CDF
MV1007-D33	Vertebrata	Eugraulid sp. (Anchovy)		1			TMS
MV1007-D34	Echinodermata	Ophioroid			1		TMS
MV1007-D34	Echinodermata	Urchin			1		TMS
MV1007-D37	Echinodermata	Seastar		1			CDF
MV1007-D37	Annelida	Tubeworm			1		CDF
MV1007-D37	Echinodermata	Ophioroid			1		CDF
MV1007-D39	Echinodermata	Yellow crinoid			1		TMS
MV1007-D39	Cnidaria	Golden axis gorgonian			1		RGW
MV1007-D41	Vertebrata	Fish (clupeid?)		1			TMS
MV1007-D41	Echinodermata	Ophioroid			1		TMS
MV1007-D41	Cnidaria	Hydromedusae			1		TMS
MV1007-D41	Arthropoda	Assorted shrimps (3 different)			3		TMS
MV1007-D41	Echinodermata	Urchin fragments		1 vial			TMS
MV1007-D43	Echinodermata	Urchin			1		TMS
MV1007-D43	Cnidaria	Hydroid			1		RGW
MV1007-D43	Cnidaria	Octocoral			1		RGW
MV1007-D45	Cnidaria	Bamboo coral				Fragments	RGW
MV1007-D45	Arthropoda	Assorted shrimps (3 different)			3		TMS
MV1007-D45	Echinodermata	Ophioroid fragments			1 vial		TMS
MV1007-D45	Arthropoda	Assorted isopods (2 different)		2			TMS
MV1007-D46	Vertebrata	Fish (eel-like)			1		TMS
MV1007-D46	Bryozoa	Bryozoan fragments				1	TMS
MV1007-D46	Arthropoda	Red small shrimps (N=2)			2		TMS
MV1007-D46	Arthropoda	Large clawed crustacean		1			TMS
MV1007-D47	Cnidaria	Fossil Coral				1 fragment	LFR
MV1007-D47	Arthropoda	White crab		1			TMS

APPENDIX VII: MV1007 Selected Biological Specimen Photographs

1. Cnidarians

1.1. Octocorals

Gr Green Primnoid (D03)

Gorgonian (D03)

Bamboo coral (D45)

Golden axis gorgonian (D39)

Primnoid (D09)

Pink octocoral (D10)

Alcyonacean (D26)

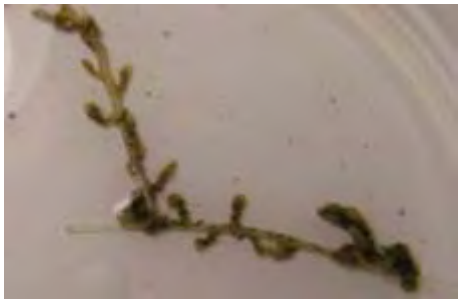

Octocoral (D43)

Gorgonian (D02)

1.2. Scleractinians (Stony corals)

Cladopsammia sp. (D07)

Javania? sp. (D03)

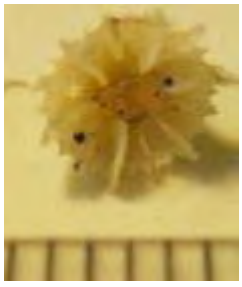

Solitary scleractinian (D29)

Madrapora occulata & *Lophelia pertusa*? (D03)

1.3 Other corals

Stylopathes sp. (black coral) with symbiotic galatheid crab (D06)

Pink stylasterid (D09)

Crypthelia sp. (Stylasterid, D02)

2) Echinoderms

2.1 Ophioroids (brittle stars)

Ophioroid (D10)

Assorted ophioroids (D03)

Ophioroid (D12)

Ophioroid (D18)

2.2 Asteroids (sea stars)

Asteroid (D09)

Asteroid (D37)

2.3 Urchins

Urchins (D03)

Urchin (D09)

Urchins (D20)

Urchin fragments (D41)

2.4 Other echinoderms

Holothurian (D09)

Holothurian (D29)

Yellow crinoid (D39)

3) Annelida (worms)

Polychaetes (D04)

Polychaetes (D09)

Nermetean worms (D26)

3) Arthropods (shrimps and crabs)

Shrimp (D07)

Crab (D03)

White crab (D09)

4) Sponges

Yellow sponge (D04)

White sponge (D04)

Sponge (D09)

Appendix VIII: Dredging Primer by Dan Fornari

Originally prepared for the seminar for students participating on the cruise, spring, 2010.

Seafloor Rock Dredging – A Primer

Dan Fornari
Geology & Geophysics Dept.
Woods Hole Oceanographic Institution
Woods Hole, MA 02543

April 6, 2010

1. Introduction

Imagine you are in a helicopter about 1.5 miles (2800 meters) above a slope by your home that has rock outcrops and you want to collect some representative samples exposed on that slope. You have a winch in the helicopter that lets you lower a line and a basket to scoop up the rocks and sediment. However, clouds block your view, so you have to do this without being able to see where the basket is or where the objects are. You have a general map of what's down there perhaps to 50-100 m pixel resolution, but you cannot see anything! All you know is the position of the helicopter, your height above the ground, and how much of the line you have let out to drag the basket over the ground.

What I have just described is a realistic equivalent to what is done to dredge rocks from the seafloor! This technique has been employed for over 100 years to characterize rocks exposed on the seafloor throughout the world's ocean basins since the Challenger Expedition in the late 1800s.

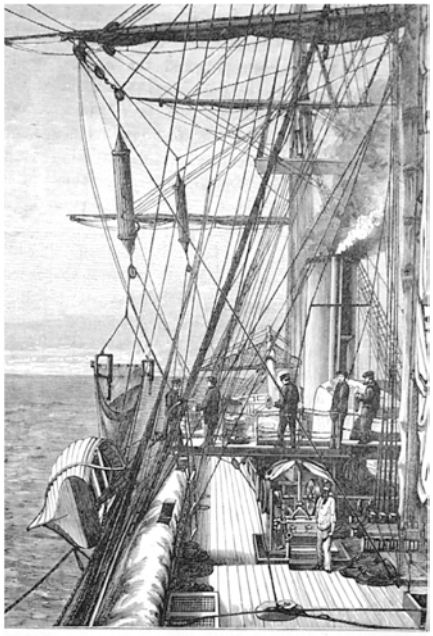

Fig. 12.—Dredging and Sounding arrangements on board the Challenger.

Line drawing from the HMS Challenger volumes showing the port side dredging and trawling winch.

2. What you need to dredge rocks from the ocean floor

Seafloor rock dredging involves several important components involving both equipment and scientific approach:

- A ship with GPS positioning so you know where you are on the globe
- The ship has to have a 'trawl' winch with a very strong steel rope – usually 1/2" or 9/16" diameter that can be controlled from a lab on the ship.
- An A-frame and sheave system or other suitable and mechanically strong mechanism to get the steel rope from the winch over the side of the ship.
- A deep-sea dredge, including a chain bail system that allows for the dredge to be dragged along the bottom and scoop up rocks, and also for it to 'release' in specific ways if it gets snagged on an outcrop, so that you don't lose the dredge, the wire, or the samples. The weak-link system is part of the chain bail and either relies on the shear-strength of standard bolts (SIO system) or shear pins of different strength materials (WHOI system).
- A 12 kHz pinger that is attached to the steel rope about 150 m above the dredge so you can acoustically determine whether the dredge is on the seafloor and how much of the steel rope is laying on the bottom (this is called the 'scope' of wire on the bottom – at least 50-70 m of scope is needed to be sure that the dredge mouth digs into the bottom as it moves along the seafloor).
- A scientific hypothesis and justification for delineating the sampling site and choosing a dredging strategy.
- Onboard expertise in describing, cataloging and processing the rocks in preparation for shore-based geochemical analytical studies.

Once you have made a detailed, multibeam bathymetric map of the area to be sampled and analyzed available side-scan sonar data so you have a good working hypothesis regarding the tectonic and volcanic context of the various seafloor features and their relationships, you can begin to identify dredging targets where you want to collect rocks so that you can analyze them and better understand their magmatic origin.

3. What is a rock dredge, and how do you put together a dredge system

A basic configuration for a seafloor rock dredge is show in the following figure. You have the steel wire rope that is lowered and recovered using a traction winch, the rock dredge that is made of heavy galvanized steel, a chain basket under the dredge that is where the rocks are captured (often this is lined with a heavy fishing net so that small chunks of rock are retained and not washed out), a bridle made of heavy chain so that the dredge can bump along the seafloor and be relatively flexible as it responds to the irregular seabed it is dragged across, and a swivel and system of weak-links on the chain bridle to provide calibrated breaking points at strategic locations above the dredge in case it gets 'hung-up' on a rock outcrop - effectively anchoring the ship to the seafloor.

Getting hung-up is one of the most dangerous aspects of dredging and is why constant surveillance is required by the technical and science operators in the lab, and the ship's bridge watch – all of whom are involved each dredging operation.

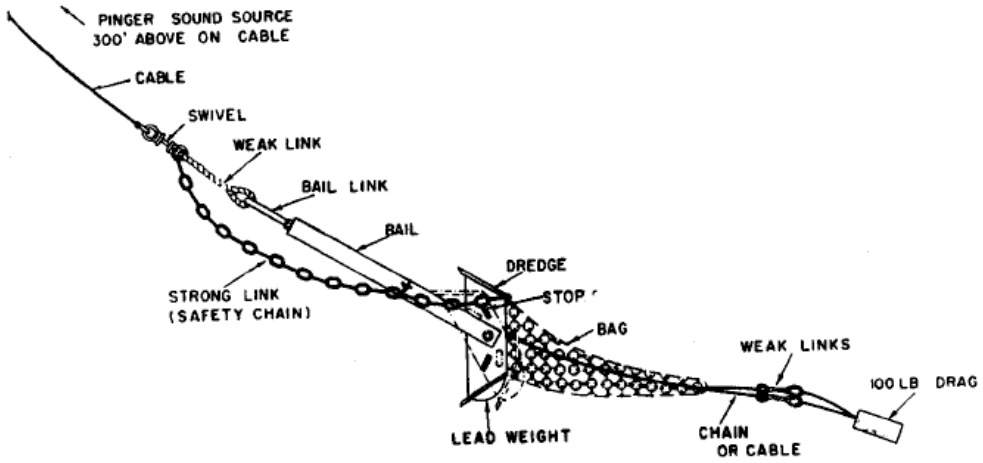

Fig. 1. Diagrammatic sketch of the dredge.

Diagrammatic sketch of a seafloor rock dredge from Nawalk et al., (1962).

Dr. Maurice "Doc" Ewing, dredging on the Lamont vessel Vema in the early 1960's. What safety problems can you identify in this photograph?

Dredging is part science, part safe shipboard practices, and part 'occult' art. There are a number of standard techniques but the key objective is to recover representative samples from a restricted portion of seafloor or a specific feature, over a specified depth range, and not lose the equipment and not hurt anyone. The dredge itself weighs many hundreds of pounds, the tension on the 9/16" steel wire rope is usually thousands of pounds, the sheaves, or wheels, that the wire runs over, which fairleads the wire from the winch to the A-frame and over the side are all dangerous places where fingers can get chopped off in a split second; and if the steel rope breaks unexpectedly, it can cut a person in half – safety on deck during dredging is paramount. In

addition, because there are many places where you can hurt your feet – good safety shoes with steel toes or heavy hiking shoes are important when working on the ship's deck during dredging operations. No sandals or open toed shoes are permitted.

Photos of a Scripps dredge. Left photo shows Ron Comer an expert SIO ResTech who has done thousands of successful dredges throughout the worlds' oceans. Right photo shows the author during deployment of a dredge on the R/V Melville in 2001. The chain bail and weak links are noted. The two lines on the deck are 'tag' lines used to steady the dredge as it is deployed and recovered. They are slipped off once the dredge is in the water.

As shown in the photos above, the dredge is a heavy walled galvanized box, sometimes with small snub teeth, that has a chain bag and a liner made from strong fish netting attached below the opening. The dredge bag is weighted down with a pig weight to keep the netting or the chain from flipping inside out as the dredge is lowered to the bottom. The pig weight is placed inside a burlap sack twisted shut and flipped upside down. Four long pieces of twine are then tied onto the top edge of the bag to tie the bag and weight into the bottom of the dredge bag just before deploying. The weight is put in the burlap sack to collect any fine silt, sand, or glass.

4. The Weak Link System

Weak links are used in rock dredging to ensure safe and efficient operations and help prevent loss of expensive equipment. **The principle is based on NEVER exceeding the elastic limit of the steel rope.** The plot below shows the method used by SIO to calculate the shear pin values for both the main weak link and the 2 side links.

SIO DREDGING INFORMATION SHEET

DATA

1. Wire weighs 1.4042 lbs/meter in water
2. Elastic limit of wire is 24,375lbs.
3. Yield strength is 28,600 lbs.
4. Breaking load is 32,500 lbs.

INSTRUCTIONS

1. Determine maximum amount of wire to be put out.
2. Enter graph at that point on vertical axis.
3. Follow Horizontally to diagonal line intersect.
4. Follow Vertical line to Horizontal axis and read Main shear Pin value to be used
5. Never use this value, I.e. Use this value or a lower value shear pin.

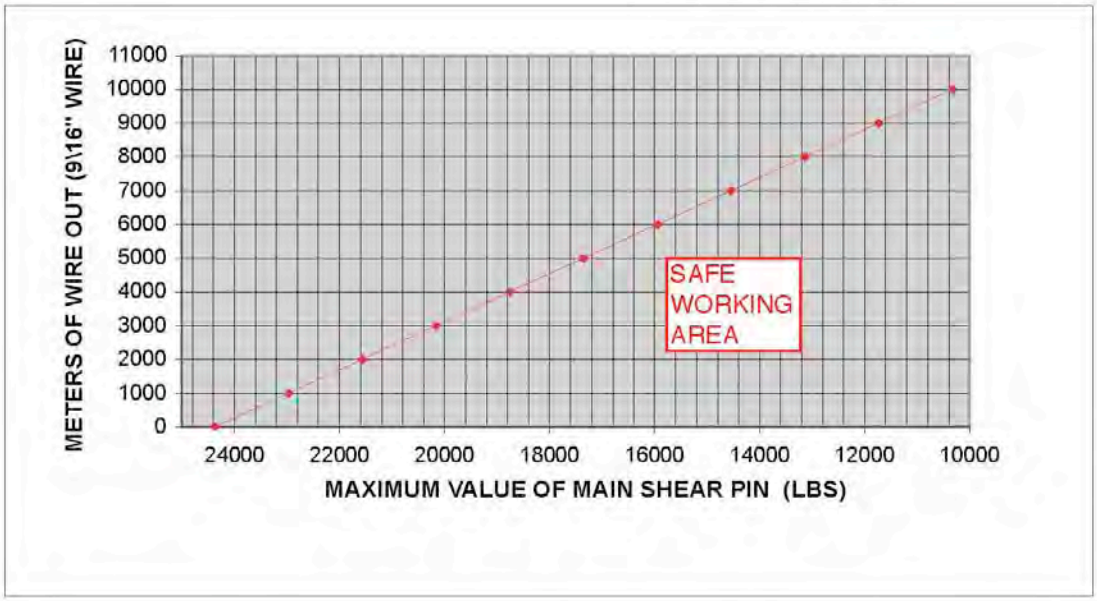

Tables by Ron Comer and John Boaz. May 1985

Rev. G.P. and T.E. 13 April 2001

There are 3 weak links on a SIO type dredge. One weak link is inserted between the bridle of the dredge and the end of the steel rope- that is the 'main' weak link. Two (2) side links are installed on opposite corners of two of the chains that extend from each of the 4 corners of the dredge box. These chains allow for the first release of the dredge should it get hung up. Releasing one of the side weak links should allow the dredge to swing free of the outcrop and release the tension. If the main weak link releases, then the dredge should be recovered by the single chain that is attached ABOVE the weak link and runs to the bottom of the dredge bag.

THE MOST IMPORTANT RULE IS NEVER EXCEED THE ELASTIC LIMIT OF THE STEEL ROPE. FOR UNOLS 9/16" TRAWL WIRE THAT VALUE IS 24,375 LBS.

The key pieces of information required to properly 'rig' the weak link system on a rock dredge are as follows:

• Determine your maximum wire out for the dredge you will be doing by seeing what the deepest depth is where you will land the dredge. Let's say that is 3000 m. Add 20% to that value as a safety margin, so add 600 m. The total length of wire expected to be deployed during the dredge is then equal to 3600 m.

• Calculate the weight of the wire. As shown in the information on the graph above, the steel rope weighs 1.4042 lbs per meter in seawater. Hence the total weight of wire for the dredge will be 3600 x 1.4042 = 5,055 lbs.

• Subtract 5,055 from 24,375 (the elastic limit of the wire rope) = 19,320. THIS NUMBER IS VERY IMPORTANT TO REMEMBER FOR EACH DREDGE AS IT GIVES YOU THE MAXIMUM PULL OR TENSION. **NEVER EXCEED THIS VALUE**, IN FACT IT IS BETTER IF YOU TRY TO SET YOUR MAX PULL TO 500-1000 LBS LESS THAN THIS VALUE. THE ONLY REASON FOR EXCEEDING THIS VALUE IS IF YOU ARE HUNG UP AND YOU DETERMINE YOU MUST TRY TO BREAK ONE OF THE SIDE OR MAIN LINKS TO FREE THE DREDGE. THAT EFFORT IS DONE UNDER VERY CONTROLLED CIRCUMSTANCES, WITH THE SHIP STOPPED AND THE BRIDGE, CHIEF ENGINEER AND CHIEF SCIENTIST ALL AGREEING ON A PLAN FOR FREEING THE DREDGE.

• To get the value of the main shear pin, using the graph above, you see that plotting 3600 m of wire on the Y axis, and following that value to the right to the red line, leads you down from the line to a maximum value for the shear pin of ~19,000 lbs – matching what was calculated above by subtracting the weight of the wire from the yield strength of the wire. ALWAYS SELECT A MAIN SHEAR BOLT WITH A VALUE OF ~500-1000 LBS **LESS THAN** THE CALCULATED VALUE OF YIELD STRENGH MINUS WEIGHT OF WIRE.

• From the above calculations, you determined that the correct main shear bolt should be ~18,500 lbs.

• The side weak links bolt shear values are determined by taking the main weak link bolt and dividing it by 4 since they are part of a 4 part bridle. This means that the load on the wire is theoretically evenly distributed among the 4 chains attached to the 4 corners of the dredge bucket. For our example, each of the 2 side weak links should be fitted with a bolt that has a shear strength of 4,625 lbs

• The shear strengths of various types of 5/16" bolts used in the SIO weak link system has been calculated by repeated testing to destruction of many different types of bolts (i.e., brass, plain steel, stainless steel, galvanized, etc.). Normally a box of 100 bolts of a certain type are given to a machine shop or testing lab and they will 'break' 10 of the bolts to determine the shear strength of that box of bolts. These are then labeled and placed into service in the SIO ResTech dredge supplies.

5. The Pinger

Pingers are a 12 kHz sound source with a self-contained battery supply in an 11,000 m rated stainless steel housing that emits a 1 Hz (1 per second) ping. This ping is used to determine the distance between a pinger that is mounted on the dredge wire using special clamps and the seafloor. Here is how this method works. The figure below outlines in general the geometry between the pinger, the dredge and the seafloor, and the ship's bathymetry system transducer that is mounted on the hull.

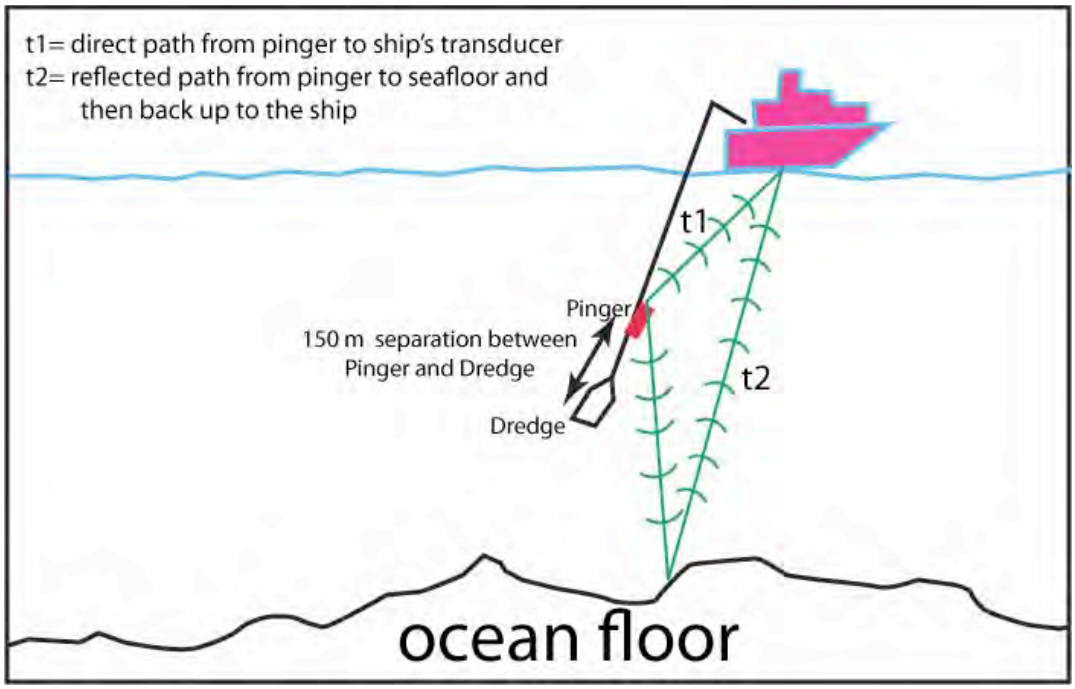

The pinger is mounted on the dredge wire a fixed distance above the dredge – usually 150 m. **Remember that number**, it will be critical for properly interpreting the acoustic returns displayed on the PDR – Precision Depth Recorder, which is where the pinger trace will be displayed in the ship's lab. The figure below shows a good example of a pinger trace. They key to understanding these acoustic recordings is to realize that you are seeing two (2) returns from the pinger – one is a direct path from the pinger to the ship, and the other is a reflected return from the bottom. The difference between these two travel-times represents the height - or altitude above the bottom of the pinger. As the dredge wire is lowered, or paid-out, the pinger gets closer to the seafloor so the time difference between the direct return and the reflected return gets smaller. In our case, with the pinger mounted 150 m above the dredge – **once the separation between the t1-direct return, and t2-reflected return equals ~150 m, that means that the dredge is about to land on the seafloor.**

In order to convert from time (which is what is displayed on the PDR record) to distance, you need to assume the sound speed of 1500 m/sec in seawater (that is 2-way time, so 750 m = approximately 1 second of travel time on the PDR record). Usually a PDR record is divided into 10 equally spaced vertical gridlines so the approximate distance between each gridline is 75 m. We use the pinger trace to lay out wire on the seafloor – about 50-75 m of 'scope' so that as the ship pulls the wire and dredge the dredge mouth digs into the seafloor as it moves and collects rocks. If the pinger trace and the bottom trace meet and there is no separation – then the pinger is ON THE BOTTOM – too much wire has been let out and you need to slowly recover it so that the pinger is not bashed against the rocks. Never use the pinger as a dredge!

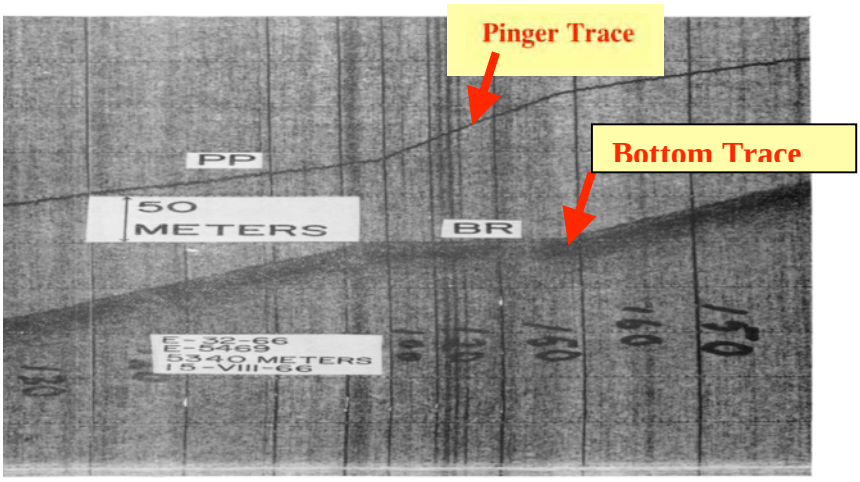

(left) Gene Pillard, a SIO ResTech mounting a pinger on the dredge wire. Right hand figure shows a PDR (Precision Depth Recorder) record with a pinger trace (fine black line) and the bottom trace (fuzzier return below it). The distance between the two lines varies as the wire is hauled in – note that the distance separating the two traces increase on the right side of the record – because the wire was hauled in, thereby increasing the distance between the pinger and the bottom.

5. Dredging – Active & Passive Methods, and ALWAYS watching/recording the tensiometer and the ship's position, wire out and water depth and noting these data in a logbook keyed to GMT time

From experience and the bathymetric maps that you make prior to dredging and in planning the sampling strategy for your experiment, you know what the seafloor slope is, what general kinds of volcanic and structural features are on the ocean floor, and what is the best direction to drag the dredge (usually up the steepest slope). In advance of planning a final dredge track, you have to consult with the ship's Bridge and Mates, and determine what the optimal dredging direction will be. Keep in mind that if the ship has Dynamic Positioning, the ship can actually be heading (meaning the direction that the bow of the ship is pointing) in a different direction to best accommodate the seas and wind, while traversing over the seafloor in another direction. Speed during dredging is usually kept low - between ¼ to ½ knot, and again depends on wind, weather, and general towing conditions. It is also important to know if the over-boarding point of the steel dredge wire is over the stern or over an A-frame on the side of the ship. Where the wire is overboarded may limit your ability to turn in certain directions, although in general it is important to keep your dredge tracks short and straight so you can best determine where your samples are from. It is very important to maintain good contact with the bridge at all times during dredging and especially if there are problems, like getting the dredge hung-up.

As one pulls in and lets out the wire to keep the dredge moving across the seafloor, you can "feel" the bites that the dredge makes by looking at the tensiometer display. Bites are what all dredgers like to see -- an increase in the tension on the wire followed by the sudden release of tension when the rocks break free. Hopefully, those rocks end up in the dredge bag!

There are two basic types of dredging technique, and their use is mostly dependent on the weather (sea state and wind direction) and the direction you need to move the ship during dredging in order to go up slope (dredging down slope is a BAD idea). **There is 'active' dredging and 'passive' dredging.** The main difference is whether you are moving the ship slowly as you 'play' the wire by hauling in and paying out slowly – this is 'active' dredging, or whether you lay out wire on the seafloor slowly by moving the ship up slope and then stop the ship and use the winch to drag the dredge across the seafloor as you haul in wire – this is 'passive' dredging.

Here is the 'occult' art-part of dredging - when I dredge, I imagine myself on the seafloor, at the mouth of the dredge, with the detailed bathymetric map in my subconscious and my brain synched to the wire tension, meters of wire out and the pinger trace. My motto is: **"See the dredge, be the dredge!"**

The author with his 'dredge hat' on, at the winch controls during dredging operations on the Atlantis II during dredging operations in the Siqueiros Transform in the mid 1980s – concentrating on having the rocks jump into the dredge.

6. Procedures to follow if the dredge gets hung up
Stop the Ship – Notify the Bridge – Pay out wire to keep the tension down until the ship stops

There should always be several watch standers monitoring the ship's track along the dredge path, the wire tension, and one person 'flying' the dredge – i.e., at the controls of the winch to haul the wire in and out. That person should be focused on the tensiometer and watching that the tension never exceeds the maximum value determined for each dredge (remember that if you are dredging at shallower depths or deeper depths, that maximum tension value will change depending on the maximum amount of wire out and its weight in water, subtracted from the elastic limit of the wire).

If the dredge is hung up you will see that the wire tension will not go up and down with the ocean swells in rhythmic fasion, but will constantly increase monotonically. That is when you have to either slow the ship or slow your rate of hauling in the wire so you control the tension increase and DO EVERYTHING SLOWLY. If it appears that the tension is only increasing and

you are approaching ~75% of your maximum allowed tension for that dredge, stop the ship immediately, notify the Bridge that you may be hung up and pay out wire slowly to keep the tension from increasing.

There are various methods to get Un-stuck from the seafloor. Again, stop the ship and keep tension under control and below your max limit. Remember that one of the best ways to get un-stuck is to move in a slightly different direction with respect to the topography – i.e., try to move the ship and dredge across the slope or down slope. This involves changing the direction of ship's travel. Communication with the Mate on watch is essential so they can best determine what the safest direction to move the ship is, depending on weather and the over-boarding point is. Slowly paying the wire in/out as the ship moves in a different direction usually works to get the dredge un-stuck. In extreme cases, the ship may need to turn 180° on the wire so you start pulling in the opposite direction from how you initially got the dredge stuck. KEEPING ACCURATE NOTES OF TIME, WIRE OUT, MAX TENSION, SHIP HEADING AND DIRECTION OF TRAVEL OVER THE SEAFLOOR ARE ALL ESSENTIAL TO REMEMBERING THE ACTIONS TAKEN DURING THE OPERATION TO FREE THE DREDGE.

Pulling at tensions that are designed to break the side links or main link to free the dredge should only be done after consultation with the ship's Captain, the Chief Engineer, and the Chief Scientist. THE FANTAIL OF THE SHIP SHOULD BE CLEARED AND NO ONE SHOULD BE ALLOWED ON DECK WHEN THE DREDGE IS HUNG UP OR IF BREAKING TENSIONS ARE BEING APPLIED.

7. Removing rocks from the dredge on deck

The ship's Bosun and the ResTechs will assist with recovering the dredge and securing it so that samples can be recovered. It is important that the deck be clean and washed after the last dredge so that no contamination takes place between the two dredges. All scientists involved in recovering rocks from the dredge should wear life jackets, hard hats and closed toed shoes, and be wearing gloves so you hands are not cut. Seafloor volcanic rocks often contain glass rinds and the glass is VERY sharp and can cut easily. Rocks should be collected in buckets and care should be taken to determine if there are animals in and amongst the rocks – these will be curated by the biologists on board. Rocks from a dredge should all be labeled and put in one location so that no confusion ensues in terms of what rocks are from what dredge.

Sometimes rocks can be easily picked from the dredge netting. Be sure to wear a hard hat and have someone hold the dredge bucket so it does not move. It should be secured with lines. Sometimes additional encouragement is needed to free large rocks from the dredge (right photo).

7. Dredge Sample Repositories and On-line Information

National Geophysical Data Center - SIO Dredge Respository Online Archive
http://www.ngdc.noaa.gov/mgg/curator/sio.html

Scripps Dredging Repository Online Archive
http://collections.ucsd.edu/dr/index.cfm

Lamont-Doherty Repository Online Archive
http://www.ldeo.columbia.edu/res/fac/CORE_REPOSITORY/RHP5.html

WHOI Repository Online Archive
http://vishnu.whoi.edu/corelab/publications/corelab_pub.html